

TTK-10-45  
IPPP/10/61  
DCPT/10/122  
FR-PHENO-2010-026  
SFB/PPP-10-65  
arXiv:1007.5414 [hep-ph]

September 28, 2010

# Threshold resummation for pair production of coloured heavy (s)particles at hadron colliders

M. BENEKE<sup>a</sup>, P. FALGARI<sup>b</sup>, C. SCHWINN<sup>c</sup>

<sup>a</sup>*Institute für Theoretische Teilchenphysik und Kosmologie,  
D-52056 Aachen, Germany*

<sup>b</sup>*IPPP, Department of Physics, University of Durham,  
Durham DH1 3LE, England*

<sup>c</sup>*Albert-Ludwigs Universität Freiburg, Physikalisches Institut,  
D-79104 Freiburg, Germany*

## Abstract

We derive a factorization formula for the production of pairs of heavy coloured particles in hadronic collisions near the production threshold that establishes factorization of soft and Coulomb effects. This forms the basis for a combined resummation of Coulomb and soft corrections, including the non-trivial interference of the two effects. We develop a resummation formalism valid at NNLL accuracy using the momentum-space approach to soft gluon resummation. We present numerical results for the NLL resummed squark-antisquark production cross section at the LHC and Tevatron, including also the contribution of squark-antisquark bound states below threshold. The total correction on top of the next-to-leading order approximation is found to be sizeable, and amounts to (4–20)% in the squark mass region 200 GeV – 3 TeV at the 14 TeV LHC. The scale dependence of the total cross section is also reduced.

# 1 Introduction

In perturbative calculations of partonic cross sections at hadron colliders there often arise terms that are kinematically enhanced in certain regions in phase space. In the Drell-Yan process, for instance, Sudakov logarithms of the form  $[\alpha_s \ln^2(1-z)]^n$  arise, where  $z = Q^2/\hat{s}$ , and  $Q^2$  and  $\hat{s}$  represent the invariant mass squared of the lepton pair and the partonic centre-of-mass (cms) energy, respectively. In the threshold region  $z \rightarrow 1$ , these terms are large, and spoil the convergence of the perturbative expansion in the QCD coupling  $\alpha_s$ . If the dominant contribution to the hadronic cross sections originates from the partonic threshold region, which is certainly the case when  $Q^2$  approaches the cms energy  $s$ , these logarithms need to be resummed to all orders in perturbation theory to attain a reliable theoretical description. This was accomplished in [1, 2] for the inclusive Drell-Yan cross section by solving evolution equations in Mellin space. In production processes of pairs of heavy coloured particles such as top quarks or coloured particles in extensions of the standard model, e.g. squarks and gluinos in supersymmetric extensions, the partonic cross section contains terms of the form  $(\alpha_s \log^2 \beta)^n$  (“threshold logarithms”), where  $\beta = (1 - 4M^2/\hat{s})^{1/2}$  is the heavy particle velocity, and  $(\alpha_s/\beta)^n$  (“Coulomb singularities”), which are also enhanced near the partonic threshold  $\hat{s} \approx 4M^2$ . Resummation of threshold logarithms for heavy-particle and di-jet production has also been implemented in Mellin space [3–9] up to now, and has been used for improved predictions of the top-pair production cross section at hadron colliders [10–16]. Recently the resummation of threshold logarithms for production processes of supersymmetric coloured particles [17–20] and colour octet scalars [21, 22] has been studied as well. The resummation of multiple exchanges of Coulomb gluons and bound-state effects has been studied for the total top-antitop cross section [10, 23] and the invariant mass distribution of top quarks and gluinos [24–26].

The theoretical basis for resummation is a factorization of the partonic cross section  $\hat{\sigma}$  in the partonic threshold region into hard and soft contributions of the schematic form

$$\hat{\sigma} = H \otimes S \tag{1.1}$$

with a hard function  $H$  and a soft function  $S$  both of which are matrices in colour space. If the invariant mass  $Q^2 = (p_1 + p_2)^2$  of the heavy-particle pair  $H(p_1)H'(p_2)$  is held fixed, the “partonic threshold” is then defined more generally as the kinematical region where  $Q^2$  is close to the partonic centre-of-mass energy  $\hat{s}$ . Arguments from perturbative QCD [27], the properties of Wilson lines [28, 29], or effective theories [30–33] can then be used to demonstrate exponentiation of the enhanced contributions by solving evolution equations for the functions  $S$  and  $H$ . Traditionally this resummation is performed in Mellin space which requires a numerical transformation of the resummed result back to momentum space. A resummation method directly in momentum space was proposed in [31] and has been applied subsequently e.g. to Drell-Yan or Higgs production [33–35] and recently to the top-quark invariant mass distribution [36].

In this paper we consider the production of a pair of heavy coloured particles  $H, H'$  with masses  $m_H$  and  $m_{H'}$ , respectively, in the collision of hadrons  $N_1$  and  $N_2$ ,

$$N_1(P_1)N_2(P_2) \rightarrow H(p_1)H'(p_2) + X \tag{1.2}$$

and concentrate on the resummation of the total cross section. In this case, after integration over the invariant mass of  $HH'$ , the enhanced logarithms appear when

$$\hat{s} \approx (m_H + m_{H'})^2. \quad (1.3)$$

In this limit, the factorization of soft gluons is complicated by the fact that the non-relativistic energy of the heavy particles is of the same order as the momenta of the soft gluons, in contrast to the assumptions made in the derivation of the usual factorization formula (1.1). We show that in this kinematical regime the partonic cross sections factorizes into three contributions,

$$\hat{\sigma} = H \otimes W \otimes J, \quad (1.4)$$

where  $H$  is determined by hard fluctuations,  $W$  by soft fluctuations and  $J$  accounts for the propagation of the heavy-particle pair including Coulomb-gluon exchange. The short-hand  $W \otimes J$  includes a convolution which accounts for the energy loss of the heavy particles due to soft emissions (the precise form of the factorization formula is given in (2.63) below).

The main points of the present approach are as follows:

- Our approach is largely model-independent and highlights the universal features of soft-gluon and Coulomb resummation: the precise nature of the heavy particles and the physics model enter the factorization formula (1.4) only in the hard function  $H$ ; the soft function and the Coulomb function depend only on the colour and (in the latter case) the spin quantum numbers of the heavy-particle pair. The hard function can be obtained directly from the  $HH'$  production amplitude, expanded near threshold, without any need to perform a full cross section calculation.
- Eq. (1.4) generalizes previous results of the form (1.1) by factorizing the Coulomb effects in addition to those from soft gluons. Multiple exchange of Coulomb gluons associated to corrections  $\sim \alpha_s^n / \beta^m$  can be resummed in the function  $J$  using methods familiar from non-relativistic QCD (NRQCD). The presence of the Coulomb function  $J$  leads to a more complicated colour structure of the soft functions  $W$  compared to previous treatments based on a factorization of the form (1.1). The factorization formula (1.4) allows a combined resummation of soft and Coulomb gluons and justifies earlier treatments [11, 18, 24, 25] where the factorization of Coulomb from soft gluons was put in as an assumption.
- The kinematical structure of the soft function  $W$  simplifies in the threshold region (1.3) compared to the more general situation considered in [7]. This has allowed us to construct a basis in colour space that diagonalizes the soft functions relevant for hadron collider pair production processes of heavy particles in arbitrary representations of the colour gauge group to all orders of perturbation theory [37]. The diagonal colour bases for resummation of threshold logarithms for all production processes of pairs of coloured supersymmetric particles at hadron colliders, i.e. squark-antisquark, squark-squark, squark-gluino and gluino-gluino production have

been provided in [37], extending explicit one-loop results for soft anomalous dimensions at threshold [7, 17, 18, 20]. This result greatly simplifies threshold resummations at NNLL accuracy and has allowed us to extract the two-loop soft anomalous dimension for arbitrary colour representations [37] from results of [38–40], in agreement with an independent two-loop study for top-pair production [41]. The more complicated colour structures in the two-loop soft anomalous dimension for massive particles with generic kinematics [42–44] have been shown not to contribute to the NNLO total production cross section of a heavy-particle pair produced in an  $S$ -wave at threshold [45].

- We use the method of [31, 32] to perform the resummation of threshold logarithms  $\log \beta$  directly in momentum space solving evolution equations for the functions  $H$  and  $W$ . The resummation of the total cross section in the threshold region has been performed previously in Mellin space [9, 11]. Our derivation gives a field theoretical definition of the quantities appearing in that approach and the resummation in momentum space allows an analytical treatment, since no numerical inverse Mellin transform is necessary. The relation between the Mellin-space and momentum-space formalisms has been discussed in [31–33, 37].
- The formalism includes the case of heavy particles with sizeable decay widths. To first approximation finite-width effects enter only in the Coulomb function and can be included by a shift of the non-relativistic energy  $E \rightarrow E + i\Gamma$  as familiar from top-quark pair production at electron-positron colliders. A systematic description of finite width effects beyond leading order can be achieved in the effective theory approach [46–49].

In this paper we focus on establishing the factorization of soft and Coulomb gluons and demonstrate the new features arising in a combined resummation by presenting numerical results for the example of squark-antisquark production. While we set up a method suitable for resummation at NNLL accuracy, in our initial application we restrict ourselves to NLL accuracy since the required colour separated hard production coefficients for squark-antisquark production are currently unknown. We also do not include finite squark decay widths which are small in typical supersymmetry (SUSY) scenarios and would introduce a dependence on the SUSY parameters but, as mentioned above, could easily be included in our approach. Note that, since in the present work we are concerned with the total cross section, there are no sizable finite-width corrections as long as  $\Gamma \ll M$ , unlike the case of the invariant mass distribution near threshold.

The paper is organized as follows. In section 2 we derive the factorization formula (1.4) using effective field theory methods. We compare to previous treatments of combined soft and Coulomb corrections and extend the diagrammatic argument of [45] on the absence of corrections from subleading couplings of soft gluons to non-relativistic particles at NNLL to all orders in the strong coupling using the effective theory approach. In section 3 we discuss the process-independent ingredients in the factorization formula, the soft function  $W$  and the Coulomb function  $J$ , collect their explicit results and perform the summation of

threshold logarithms using evolution equations in momentum space. We also give a simple prescription for how to obtain the hard-function  $H$ , the only process-dependent ingredient in the resummation formalism, from a standard fixed-order calculation. In section 4 we perform the combined soft-Coulomb resummation at NLL accuracy for squark-antisquark production and present numerical results for the Tevatron and the LHC.<sup>1</sup> A number of additional results concerning parton densities, the Coulomb potential in various colour representations and the resummed and expanded cross section are collected in the appendix.

## 2 Factorization for coloured heavy-particle pair production near the partonic threshold

In this section we derive a factorization formula of the form (1.4) for the process (1.2) near the partonic threshold. The heavy particles are assumed to transform under representations  $R$  and  $R'$  of the colour gauge group  $SU(3)_C$ . The inclusive production cross section is described by the factorization formula

$$\sigma = \sum_{p,p'} \int dx_1 dx_2 f_{p/N_1}(x_1, \mu) f_{p'/N_2}(x_2, \mu) \hat{\sigma}_{pp'}(x_1 x_2 s, \mu), \quad (2.1)$$

where  $\hat{\sigma}_{pp'}$  are the hard-scattering cross sections for the partonic subprocesses

$$p(k_1)p'(k_2) \rightarrow H(p_1)H'(p_2) + X \quad (2.2)$$

and  $pp' \in \{qq, q\bar{q}, \bar{q}q, gg, gq, g\bar{q}\}$ . As usual the nucleon masses are neglected and parton momenta  $k_{1,2}$  are related to the incoming nucleon momenta by

$$k_1 = x_1 P_1, \quad k_2 = x_2 P_2. \quad (2.3)$$

The partonic cms energy is given by

$$\hat{s} \equiv (k_1 + k_2)^2 = x_1 x_2 s. \quad (2.4)$$

At hadron colliders  $\hat{s}$  is not a fixed quantity but one may argue that the steep rise of the parton distribution functions with decreasing  $x$  leads to an enhanced contribution to the total production cross section from the *partonic* threshold region

$$z \equiv \frac{4M^2}{\hat{s}} \sim 1, \quad (2.5)$$

$M = (m_H + m_{H'})/2$  denoting the average heavy-particle mass. According to a recent study of threshold effects in the Drell-Yan process [33] this dynamical enhancement of the partonic threshold region remains effective for values  $4M^2/s = zx_1x_2 \gtrsim 0.2$ . Therefore we expect the resummation of threshold logarithms to be relevant for particles with masses

---

<sup>1</sup>Preliminary results have appeared in [50, 51].

$M \gtrsim 3$  TeV (1.6, 2.2 TeV) at the LHC at 14 TeV (7, 10 TeV) and  $M \gtrsim 450$  GeV at the Tevatron which are at the border of the estimated reach for coloured SUSY particles at the LHC [52, 53] and the exclusion limits obtained at the Tevatron [54, 55]. However, experience with the NLO corrections to top-quark production suggests that also for smaller masses there is a sizable contribution to the total cross section from those terms in the partonic cross section that are enhanced for  $z \rightarrow 1$  so that resummation can serve as an estimate of higher-order effects. In addition, expansions of resummed cross sections can also be used to predict the threshold-enhanced terms in higher-order perturbative calculations [12, 45, 56].

The heavy particles produced near threshold are non-relativistic. In terms of dimensionless variables the partonic threshold is characterized by the smallness of

$$\beta = \sqrt{1 - \frac{4M^2}{\hat{s}}} = \sqrt{1 - z}, \quad (2.6)$$

which for equal masses also corresponds to the non-relativistic velocity of the heavy particles in the partonic cms. The aim of this paper is to perform a resummation of threshold logarithms  $\log \beta$  and Coulomb corrections  $1/\beta$ . In order to discuss the systematics of the combined resummations of the two corrections we count both  $\alpha_s \ln \beta$  and  $\alpha_s/\beta$  as quantities of order one and introduce a parametric representation of the expansion of the cross section of the form [37]

$$\begin{aligned} \hat{\sigma}_{pp'} &\propto \hat{\sigma}_{pp'}^{(0)} \sum_{k=0} \left( \frac{\alpha_s}{\beta} \right)^k \exp \left[ \underbrace{\ln \beta g_0(\alpha_s \ln \beta)}_{\text{(LL)}} + \underbrace{g_1(\alpha_s \ln \beta)}_{\text{(NLL)}} + \underbrace{\alpha_s g_2(\alpha_s \ln \beta)}_{\text{(NNLL)}} + \dots \right] \\ &\times \left\{ 1 \text{ (LL, NLL)}; \alpha_s, \beta \text{ (NNLL)}; \alpha_s^2, \alpha_s \beta, \beta^2 \text{ (NNNLL)}; \dots \right\}. \end{aligned} \quad (2.7)$$

With this counting, the resummed cross section at LL accuracy includes all terms of order  $1/\beta^k \times \alpha_s^{n+k} \ln^{2n} \beta$  relative to the Born cross section near threshold. Next-to-leading summation includes in addition all terms of order  $\alpha_s \ln \beta$ ;  $\alpha_s^2 \{1/\beta \times \ln \beta, \ln^3 \beta\}$ ;  $\dots$ , while furthermore all terms  $\alpha_s$ ;  $\alpha_s^2 \{1/\beta, \ln^{2,1} \beta\}$ ;  $\dots$  are included in NNLL approximation.<sup>2</sup>

In the threshold region, the cross section of the process (2.2) receives contributions from hard, potential, soft and two collinear momentum regions defined by

$$\begin{aligned} \text{hard } (h) : & \quad k \sim M \\ \text{potential } (p) : & \quad k_0 \sim M\lambda, \quad \vec{k} \sim M\sqrt{\lambda} \\ \text{soft } (s) : & \quad k_0 \sim \vec{k} \sim M\lambda \\ n\text{-collinear } (c) : & \quad k_- \sim M, \quad k_+ \sim M\lambda, \quad k_\perp \sim M\sqrt{\lambda} \\ \bar{n}\text{-collinear } (\bar{c}) : & \quad k_+ \sim M, \quad k_- \sim M\lambda, \quad k_\perp \sim M\sqrt{\lambda}, \end{aligned} \quad (2.8)$$

---

<sup>2</sup>The NNLL terms odd in  $\beta$  at order  $\alpha_s$  and  $\alpha_s^2$ ,  $\alpha_s \beta \ln^{2,1} \beta$ ;  $\alpha_s^2 \beta \ln^{4,3} \beta$ , vanish due to rotational invariance for the total cross section when the heavy-particle pair is dominantly produced in an  $S$ -wave state at tree level [37, 45]. See also below in section 2.5.

assuming equal heavy-particle masses for simplicity. Here we introduced the generic power counting parameter  $\lambda \sim 1 - z = \beta^2 \ll 1$ . For the collinear momentum we employ the light-cone decomposition

$$p^\mu = \frac{p_-}{2} n^\mu + \frac{p_+}{2} \bar{n}^\mu + p_\perp^\mu \quad (2.9)$$

with two light-like vectors  $n$  and  $\bar{n}$  satisfying  $n \cdot \bar{n} = 2$ . Due to the threshold kinematics  $(k_1 + k_2)^2 \sim 4M^2$ , no collinear modes can appear in the final state so that the particles denoted by  $X$  in (1.2) are entirely given by soft modes.

In order to achieve the separation of the effects corresponding to the different regions (2.8) it is useful to describe the heavy-pair production process in the framework of effective field theories. The relevant effective Lagrangian contains elements of non-relativistic QCD (NRQCD), describing the interaction of potential and soft modes, and soft-collinear effective theory (SCET) [57–60] describing the interaction of soft and collinear modes. Hard modes with virtuality of order  $M^2$  are integrated out and are not part of the effective Lagrangian. This effective theory is similar to that used in [48, 49, 61] to describe  $W$ -pair production near threshold in  $e^+e^-$  collisions and the construction of the effective Lagrangian proceeds along similar lines. As in the discussion of the Drell-Yan process in [33] the following considerations will be adequate to establish factorization of the partonic cross section; the discussion of the hadronic cross section requires to include additional modes with a scaling given by powers of  $\Lambda_{\text{QCD}}/M$  [32]. We also note the existence of an additional region with scaling  $k \sim M\sqrt{\lambda}$ , usually referred to as “soft” in the NRQCD literature. It is related to potential forces between the heavy particles, and will not be relevant for the following discussion of the leading Coulomb corrections.

In the EFT framework, the factorization formula is derived by a series of steps involving first a matching calculation from QCD (or another “full theory” such as the MSSM) to the EFT followed by field redefinitions that decouple soft gluons from collinear [58, 62] and potential [63] fields. These will be described in the remainder of this section.<sup>3</sup> We also show that, up to NNLL accuracy, corrections from subleading interactions to the effective Lagrangians not included in the derivation of the factorization formula either vanish or can be straightforwardly incorporated.

## 2.1 Matching to SCET and NRQCD

The first step in the derivation of the factorization formula consists of representing the scattering amplitude for the process (1.2) in terms of effective theory matrix elements of production operators  $\mathcal{O}_{\{a;\alpha\}}^{(\ell)}$  corresponding to the partonic sub-processes  $p(k_1)p'(k_2) \rightarrow H(p_1)H'(p_2)X$ , multiplied by coefficient functions that contain the hard part of the amplitude. After this step the partonic scattering amplitude is given by

$$\mathcal{A}(pp' \rightarrow HH'X) = \sum_{\ell} C_{\{a;\alpha\}}^{(\ell)}(\mu) \langle HH'X | \mathcal{O}_{\{a;\alpha\}}^{(\ell)}(\mu) | pp' \rangle_{\text{EFT}}. \quad (2.10)$$

---

<sup>3</sup>The corresponding discussion of factorization of electromagnetic effects and resummation for the  $W$ -pair production cross section at  $e^+e^-$  colliders has been given in [64].

The subscript ‘‘EFT’’ means that the matrix element is evaluated with the effective Lagrangian discussed below. We now explain the definition of the operators and the calculation of the coefficient functions.

The hard production subprocess corresponds to the  $2 \rightarrow 2$  process  $p(k_1)p'(k_2) \rightarrow H(p_1)H'(p_2)$ . Near the partonic threshold, kinematics forbids additional massive or energetic particles in the production operator, while additional soft fields connected directly to the hard process imply additional highly off-shell propagators and therefore lead to operators power-suppressed in  $\lambda \sim 1 - z$  relative to the leading four-particle operators. The required four-particle operators take the form

$$\mathcal{O}_{\{a;\alpha\}}^{(0)}(\mu) = \left[ \phi_{c;a_1\alpha_1} \phi_{\bar{c};a_2\alpha_2} \psi_{a_3\alpha_3}^\dagger \psi'_{a_4\alpha_4}{}^\dagger \right](\mu). \quad (2.11)$$

The form of the production operators is thus similar to those describing the production of non-relativistic  $W$ -pairs in  $e^+e^-$  collisions discussed in [48, 49]. Several remarks on the notation are in order:

(1) The fields  $\psi^\dagger$  and  $\psi'^\dagger$  are non-relativistic fields which create the heavy particles  $H$  and  $H'$  with momenta

$$p_1^\mu = m_H w^\mu + \tilde{p}_1^\mu \quad , \quad p_2^\mu = m_{H'} w^\mu + \tilde{p}_2^\mu \quad (2.12)$$

with the cms velocity  $w^\mu$  ( $w^2 = 1$ ) and small residual momenta  $\tilde{p}_{1/2}$  in the potential region (2.8). In the partonic cms frame  $w = (1, \vec{0})$  and  $\tilde{p}_1 = -\tilde{p}_2 \equiv \tilde{p}$  for the spatial components of  $\tilde{p}_{1,2}$ . The fields  $\phi_c$  ( $\phi_{\bar{c}}$ ) are collinear (anticollinear) fields that destroy the initial state partons  $p$  and  $p'$  with momenta

$$k_1^\mu \approx M n^\mu \quad , \quad k_2^\mu \approx M \bar{n}^\mu, \quad (2.13)$$

respectively.<sup>4</sup> We provide more details on the definition of these fields and their effective Lagrangians in the following subsection.

(2) Greek indices  $\alpha_i$  denote the spin (or Lorentz group representation) index of the field. Where convenient we use the multi-index notation  $\{\alpha\} = \alpha_1\alpha_2\alpha_3\alpha_4$ . Repeated multi-indices are summed by summing over all four components. A similar convention is used for colour indices, which we denote by Latin letters  $\{a\} = a_1 \dots a_4$ . We employ creation fields for the heavy final state particles and destruction fields for the initial state. If, for example,  $H'$  is the antiparticle of  $H$ , then this convention implies that  $\psi'$  transforms in the complex conjugate SU(3) representation of  $\psi$ . Similarly, an initial-state antiquark transforms in the antifundamental representation. In effective-theory calculations it is conventional to decompose operators into a complete basis in spin and colour, making operators and coefficient functions ‘‘scalars’’. Here we prefer to work with operators and coefficient functions that carry open spin and colour indices, see (2.11). This turns out to

---

<sup>4</sup>We do not have to consider operators where the  $\phi_c$  destroy particles different from  $p$  and  $p'$ . These would arise from a splitting of a collinear gluon into a collinear and a soft quark or of a collinear quark into a soft quark and a collinear gluon, but these interactions are present only in the power-suppressed part of the SCET Lagrangian [59].



be convenient for the spin indices, since the soft gluon contributions are spin-independent, as well as the Coulomb contributions needed at NLL accuracy. Thus, it is more direct to perform the spin summations on the square of the amplitude as in standard unpolarized cross section calculations instead of decomposing the amplitude. At NNLL accuracy the spin-dependence of the potential corrections has to be taken into account in order to obtain all terms of the order  $\alpha_s^2 \ln \beta$ . For this purpose a spin decomposition of the potential function is introduced in section 2.4. As concerns colour, given the representations  $r, r'$  and  $R, R'$  of the initial and final state particles, we can introduce a set of independent colour matrices  $c^{(i)}$  that form an orthonormal basis of invariant tensors in the representation  $r \otimes r' \otimes \bar{R} \otimes \bar{R}'$ . The colour structure of the Wilson coefficients can be decomposed in this basis according to

$$C_{\{a;\alpha\}}^{(\ell)} = \sum_i c_{\{a\}}^{(i)} C_{\{\alpha\}}^{(\ell,i)} \quad (2.14)$$

This allows us to write

$$C_{\{a;\alpha\}}^{(\ell)}(\mu) \mathcal{O}_{\{a;\alpha\}}^{(\ell)}(\mu) = \sum_i C_{\{\alpha\}}^{(\ell,i)}(\mu) \left[ c_{\{a\}}^{(i)} \mathcal{O}_{\{a;\alpha\}}^{(\ell)}(\mu) \right] \equiv \sum_i C_{\{\alpha\}}^{(\ell,i)}(\mu) \mathcal{O}_{\{\alpha\}}^{(\ell,i)}(\mu) \quad (2.15)$$

in (2.10). For example, in a  $3 + \bar{3} \rightarrow 3 + \bar{3}$  scattering process (such as  $q\bar{q} \rightarrow t\bar{t}$  and squark-antisquark production), a convenient colour basis is [7]

$$\begin{aligned} c_{\{a\}}^{(1)} &= \frac{1}{N_c} \delta_{a_2 a_1} \delta_{a_3 a_4} \\ c_{\{a\}}^{(2)} &= \frac{2}{\sqrt{D_A}} T_{a_2 a_1}^b T_{a_3 a_4}^b, \end{aligned} \quad (2.16)$$

with  $D_A = N_c^2 - 1$ , expressing colour conservation and the fact that the initial and final states can be in a colour-singlet or a colour-octet state. Suitable colour bases for the different colour scattering processes have been constructed in [37] where also more details on the properties of the basis tensors can be found.

(3) In (2.10) the argument  $\mu$  denotes the factorization scale dependence of the operators and hard functions. We drop this in the following, but note that exploiting the invariance of the physical amplitude under changes of the factorization scale will be a key element in deriving the resummation formula. The superscript  $\ell$  stands for higher order terms in the expansion of the amplitude, which correspond to operators of the form (2.11) with derivatives acting on the fields, as discussed below.

(4) Fields without space-time arguments are at  $x = 0$ . In general, the SCET representation of a scattering amplitude involves a convolution of the Wilson coefficient with collinear fields evaluated at different positions along the light ray [59], instead of a product with a local bilinear operator  $\phi_{c;a_1\alpha_1} \phi_{\bar{c};a_2\alpha_2}$  as in (2.10). However, since here there is only one collinear field of a given type in the operator, translation invariance may be used to rewrite the operator in a local form [59, 65]. Applying the translation operators on the initial state turns the convolution integrals with the coefficient function into the Fourier-transform of the position-space coefficient functions to momentum-space coefficient

functions. These then depend on the large momentum components of the partons, and are the natural objects to work with. The hard functions  $C_{\{a;\alpha\}}^{(\ell)}$  in (2.10) refer to the momentum-space quantities.

Despite the somewhat complicated formalism and notation, there is a straightforward general prescription for the computation of the matching coefficients  $C_{\{a;\alpha\}}^{(\ell)}$  in the expression (2.10). One simply calculates the renormalized scattering amplitude for the partonic process  $p(k_1)p'(k_2) \rightarrow H(p_1)H'(p_2)$  without any averages or sums over colour and spin states, and expands it in  $\tilde{p}_{1,2}$  defined by (2.12) around the production threshold  $(k_1 + k_2)^2 = (m_H + m_{H'})^2$ . Beyond tree level, the matching coefficients can be extracted directly by expanding the loop integrand under the assumption that all loop momenta are hard [66] and by performing the loop integration of the expanded integrand in dimensional regularization. As a special case, the leading term in the kinematical expansion is found by calculating the full amplitude directly at threshold. In this case the loop corrections to the effective theory matrix element evaluated directly at threshold vanish since they are given by scaleless integrals. Therefore only tree diagrams have to be considered on the effective theory side of the matching calculation and the hard function is determined from

$$\mathcal{A}(pp' \rightarrow HH')|_{\hat{s}=4M^2} = \sum_i C_{\{a;\alpha\}}^{(0)} \langle HH' | \mathcal{O}_{\{a;\alpha\}}^{(0)} | pp' \rangle_{\text{EFT tree}}. \quad (2.17)$$

Since the matrix element on the right-hand side is simply a product of spinors (polarization vectors) and the operator renormalization factor, the  $\overline{\text{MS}}$  scheme coefficient function  $C_{\{a;\alpha\}}^{(0)}$  equals the scattering amplitude at threshold with the spinors (polarization vectors) stripped off, and all  $1/\epsilon$  poles set to zero. The Born-level matching required for squark-antisquark production is discussed explicitly in section 4.

The leading term in the kinematical expansion describes the production of  $HH'$  in an  $S$ -wave state. The next term is related to the terms linear in  $\tilde{p}_{1,2}$ , more precisely their components orthogonal to  $w^\mu$ , denoted by the symbol  $\Upsilon$ , since the other component is of higher order in the potential region. The  $P$ -wave production operators corresponding to this term are of the form (2.11) with the replacement

$$\psi_{a_3\alpha_3}^\dagger \psi'_{a_4\alpha_4} \rightarrow \psi_{a_3\alpha_3}^\dagger \left( -\frac{i}{2} \overleftrightarrow{D}_\Upsilon^\mu \right) \psi'_{a_4\alpha_4} \equiv -\frac{i}{2} \left( \psi_{a_3\alpha_3}^\dagger [\overrightarrow{D}_\Upsilon^\mu \psi'_{a_4\alpha_4}] - [\psi_{a_3\alpha_3}^\dagger \overleftarrow{D}_\Upsilon^\mu] \psi'_{a_4\alpha_4} \right) \quad (2.18)$$

in the non-relativistic part of the operator, with the covariant derivative  $D^\mu$  in the appropriate colour representation. The series in  $\ell$  in (2.10) accounts for the threshold expansion in powers of  $\lambda$ . In the following, we will mostly consider only the leading term  $\ell = 0$ . In particular, the factorization formula we derive is valid only for the case that the Born cross section is dominated by  $S$ -wave production.

## 2.2 Effective Lagrangians

### 2.2.1 Non-relativistic

The propagation and interactions of the non-relativistic fields  $\psi$  and  $\psi'$  are described by the potential NRQCD Lagrangian [67–70]. That is, we assume that the modes with momentum  $k \sim M\sqrt{\lambda}$  and potential gluons have already been integrated out. At leading order, in the partonic cms frame, the effective Lagrangian, including the decay widths of the heavy particles, is given by

$$\begin{aligned} \mathcal{L}_{\text{PNRQCD}} = & \psi^\dagger \left( iD_s^0 + \frac{\vec{\partial}^2}{2m_H} + \frac{i\Gamma_H}{2} \right) \psi + \psi'^\dagger \left( iD_s^0 + \frac{\vec{\partial}^2}{2m_{H'}} + \frac{i\Gamma_{H'}}{2} \right) \psi' \\ & + \int d^3\vec{r} \left[ \psi^\dagger \mathbf{T}^{(R)a} \psi \right](\vec{r}) \left( \frac{\alpha_s}{r} \right) \left[ \psi'^\dagger \mathbf{T}^{(R')a} \psi' \right](0). \end{aligned} \quad (2.19)$$

Here  $\mathbf{T}^{(R)}$  are the  $SU(3)$  generators in the appropriate representation of the heavy particle. In this convention  $\psi'$  transforms in the antifundamental representation, if  $H'$  is an antiparticle in the fundamental representation. This deviates from the standard NRQCD notation for quark-antiquark production that employs a field  $\chi$  that creates an antiquark and transforms in the fundamental representation. Our notation is convenient since it accommodates the case where the heavy particles produced are not particle-antiparticle pairs. This convention leads to a different sign of the potential term compared to the conventional formulation.

The only relevant interactions in (2.19) are the exchange of Coulomb (potential) gluons, rewritten as an instantaneous, but spatially non-local operator in the second line, and an interaction with the zero component (that is,  $w \cdot A_s$ , in a general frame) of the soft gluon field in the soft covariant derivative  $iD_s^0 \psi(x) = (i\partial^0 + g_s \mathbf{T}^{(R)a} A^{a0}(x_0)) \psi(x)$ , and the analogous expression for  $\psi'$  with the generator in the representation  $R'$ . Using the canonically normalized NRQCD Lagrangian (2.19), one has to take into account a normalization factor  $\sqrt{2E_H} \equiv (2m_H(1 + \vec{p}^2/m_H^2))^{1/2} = \sqrt{2m_H} + \mathcal{O}(\lambda^2)$  in the definition of the state  $|H\rangle$  (similarly for  $|H'\rangle$ ) on the NRQCD side of the matching relation.<sup>5</sup>

The NRQCD Lagrangian (2.19) is invariant under soft gauge transformations in the appropriate representation:

$$\psi(x) \rightarrow U_s^{(R)}(x_0) \psi(x) \quad , \quad \psi'(x) \rightarrow U_s^{(R')}(x_0) \psi'(x). \quad (2.20)$$

The soft gauge transformation depends only on  $x_0$  since soft fields have to be multipole expanded when multiplied with potential fields in order to maintain a uniform power counting [70–72]. The invariance of the Coulomb potential for arbitrary representations follows from the property

$$U^{(R)\dagger} \mathbf{T}^{(R)a} U^{(R)} = U_{ab}^{(8)} \mathbf{T}^{(R)b} \quad (2.21)$$

---

<sup>5</sup>For  $\Gamma_H = 0$ . See [47] for the general case.

where  $U^{(R)}$  is a  $SU(3)$  transformation in the representation  $R$  and “8” denotes the adjoint. Therefore under a soft gauge transformation:

$$[\psi^\dagger \mathbf{T}^{(R)a} \psi](x + \vec{r}) \Rightarrow [\psi^\dagger \mathbf{T}^{(R)b} \psi](x + \vec{r}) U_{s,ab}^{(8)}(x_0) \quad (2.22)$$

and analogously for the  $\psi'$  fields. The gauge invariance of the Coulomb potential term follows then from the fact that the transformations in the adjoint representation are real so that  $U_{ab}^{(8)} U_{ac}^{(8)} = (U^{(8)\dagger} U^{(8)})_{bc} = \delta_{bc}$ . For this is essential that only the time component enters the soft gauge transformation since the  $\psi$  fields and the  $\psi'$  fields in the Coulomb potential are defined at different points in space but at the same time.

### 2.2.2 Soft-collinear

The propagation and interactions of quark and gluon collinear modes with large momentum proportional to  $n^\mu$  is described by the SCET Lagrangian [57]. At leading order, in the position-space formalism of SCET [59, 60] it is given by

$$\mathcal{L}_c = \bar{\xi}_c \left( in \cdot D + i \not{D}_{\perp c} \frac{1}{i \bar{n} \cdot D_c} i \not{D}_{\perp c} \right) \frac{\not{n}}{2} \xi_c - \frac{1}{2} \text{tr} (F_c^{\mu\nu} F_{\mu\nu}^c) . \quad (2.23)$$

Here  $\xi_c$  denotes the  $n$ -collinear quark field, which satisfies  $\not{n} \xi_c = 0$  and the projection identity  $(\not{n} \not{\bar{n}}/4) \xi_c = \xi_c$ . The covariant derivatives are defined as  $iD_c = i\partial + g_s A_c$  with  $A_c$  the matrix-valued gluon field in the fundamental representation. The covariant derivative  $D$  without subscript, however, contains both the collinear and soft gluon field. The quantity  $F_{\mu\nu}^c$  is the field-strength tensor built from the collinear gauge field in the usual way, except that  $n_- \cdot D$  rather than  $n_- \cdot D_c$  appears [60]. The collinear and soft fields are evaluated at  $x$ , but in products of soft and collinear fields the soft fields are evaluated at  $x_+^\mu = (\bar{n} \cdot x/2) n^\mu \equiv x_- n^\mu$ , according to the multipole expansion. In this notation  $x_-$  is a scalar, while  $x_+^\mu$  is a vector. The  $\bar{n}$ -collinear fields are described by an identical Lagrangian with the roles of  $n$  and  $\bar{n}$  interchanged. The corresponding quark field satisfies  $\not{\bar{n}} \xi_{\bar{c}} = 0$  and  $(\not{\bar{n}} \not{n}/4) \xi_{\bar{c}} = \xi_{\bar{c}}$ . The two collinear sectors couple only via soft gluon interactions.

It is convenient to express the collinear part of the operators (2.11) in terms of fields that are invariant under the collinear gauge transformation as defined in [60]. Let  $W_c$  be the collinear Wilson line in the  $\bar{n}$  direction,

$$W_c(x) = \text{P exp} \left[ ig_s \int_{-\infty}^0 dt \bar{n} \cdot A_c(x + \bar{n}t) \right] . \quad (2.24)$$

Then  $\phi_c$  in (2.11) is given by the combinations

$$W_c^\dagger \xi_c(x) , \quad \bar{\xi}_c W_c(x) \quad (2.25)$$

for the quark and antiquark initial state, respectively. Note that our conventions imply that the conjugate fields  $\phi_c^\dagger$  are  $\xi_c^\dagger W_c = \bar{\xi}_c \gamma^0 W_c$  for the quark and  $W_c^\dagger \gamma^0 \xi_c$  for the antiquark

initial state. For the gluon initial state we use the following definition that is invariant under the collinear gauge transformations [73]:

$$\mathcal{A}_c^{\perp\mu}(x) = g_s^{-1}(W_c^\dagger[iD_c^{\mu\perp}W_c])(x) = \int_{-\infty}^0 ds \bar{n}_\nu (W_c^\dagger F_c^{\nu\mu\perp} W_c)(x + s\bar{n}). \quad (2.26)$$

The anticollinear fields are defined similarly with  $\bar{n}$  replaced by  $n$ . These collinear operators transform under the soft gauge symmetry of the SCET Lagrangian [60] according to

$$\begin{aligned} (W_c^\dagger \xi_c)(x) &\rightarrow U_s^{(3)}(x_-)(W_c^\dagger \xi_c)(x) \\ \mathcal{A}_c^a(x)T^a &\rightarrow U_s^{(3)}(x_-)\mathcal{A}_c^a(x)T^a U_s^{(3)\dagger}(x_-) = U_{ab}^{(8)}(x_-)\mathcal{A}_c^b(x)T^a, \end{aligned} \quad (2.27)$$

where  $U_s^{(R)}(x_-)$  is a soft gauge transformation in the representation  $R$  at the point  $x_-n^\mu$ .

## 2.3 Decoupling of soft gluons

Since the collinear fields  $\phi_c$ , anticollinear fields  $\phi_{\bar{c}}$  and the potential fields  $\psi^\dagger$  in the production operators (2.11) interact with each other only via exchange of soft gluons, an essential step in deriving a factorization of the hadronic cross section is the decoupling of soft gluons from the collinear and potential degrees of freedom. In SCET it is well known that the soft gluons can be decoupled from the collinear fields at leading power by performing field redefinitions involving Wilson lines [58]. Here we will show that an analogous transformation also decouples the soft gluons from the potential fields at leading order in the non-relativistic expansion. As a result, the production operators factorize into products of non-interacting collinear, anticollinear, potential and soft contributions.

In order to decouple the soft gluons from the collinear and anticollinear fields, the required redefinitions are familiar from the derivation of factorization formulas in SCET [58, 62]

$$\begin{aligned} \xi_c(x) &= S_n^{(3)}(x_-)\xi_c^{(0)}(x) \\ \bar{\xi}_{\bar{c}}(x) &= \bar{\xi}_{\bar{c}}^{(0)}(x)S_n^{(3)\dagger}(x_-) = \bar{\xi}_{\bar{c}}^{(0)}(x)S_n^{(3)T}(x_-) \\ A_c^{a,\mu}(x) &= S_{n,ab}^{(8)}(x_-)A_c^{(0)b,\mu} \end{aligned} \quad (2.28)$$

with the soft Wilson lines  $S_n^{(R)}$  for a particle in the representation  $R$  of  $SU(3)$  given by

$$S_n^{(R)}(x) = \text{P exp} \left[ ig_s \int_{-\infty}^0 dt n \cdot A_s^c(x + nt) \mathbf{T}^{(R)c} \right] \quad (2.29)$$

and similarly for particles collinear to  $\bar{n}$ . Consistent with our treatment of incoming antiparticles as particles in the complex conjugate representations, we have rewritten the transformation of the conjugate collinear spinor as a transformation in the antifundamental representation with the generators  $\mathbf{T}^{(\bar{3})} = -T^T$ .

These transformations induce analogous transformations on the collinear fields  $\phi_c \in \{W_c^\dagger \xi_c, \bar{\xi}_c W_c, \mathcal{A}_c^\perp\}$  entering the production operators:

$$\phi_{c;a\alpha}(x) = S_{n,ab}^{(r)}(x_-) \phi_{c;b\alpha}^{(0)}(x) \quad (2.30)$$

as follows from the transformation

$$W_c(x) \rightarrow S_n^{(3)}(x_-) W_c^{(0)}(x) S_n^{(3)\dagger}(x_-) \quad (2.31)$$

of the collinear Wilson line. For the incoming parton in the anticollinear direction we exchange  $n$  by  $\bar{n}$ ,  $x_-$  by  $x_+$  in the argument of the Wilson lines, and the representation  $r$  by  $r'$ . In the expressions with the superscript (0) all collinear fields are replaced by the decoupled fields  $A_c^{(0)}$  and  $\xi_c^{(0)}$  and the soft gluon fields are set to zero.

Turning to the non-relativistic sector, we first note that from the diagrammatic perspective the coupling between the non-relativistic and soft fields is non-trivial, since the non-relativistic energy of the heavy fields and the energy of soft gluons is of the same order  $M\lambda \sim M\beta^2$ . Thus, soft gluons can attach to the non-relativistic lines, to and in between the Coulomb ladder rungs, leaving potential lines in the potential region. However, a redefinition of the non-relativistic fields by a time-like Wilson line decouples the soft gluons also from the potential fields at leading order in the non-relativistic expansion. Namely, the interaction with soft gluons in the PNRQCD Lagrangian given in (2.19) can be eliminated through

$$\psi_a(x) = S_{w,ab}^{(R)}(x_0) \psi_b^{(0)}(x) \quad (2.32)$$

$$\psi_a^\dagger(x) = \psi_b^{(0)\dagger}(x) S_{w,ba}^{(R)\dagger}(x_0), \quad (2.33)$$

where the soft Wilson lines  $S_w^{(R)}$  are defined as<sup>6</sup>

$$S_w^{(R)}(x) = \bar{\text{P}} \exp \left[ -ig_s \int_0^\infty dt w \cdot A_s^c(x+wt) \mathbf{T}^{(R)c} \right] \quad (2.34)$$

$$S_w^{(R)\dagger}(x) = \text{P} \exp \left[ ig_s \int_0^\infty dt w \cdot A_s^c(x+wt) \mathbf{T}^{(R)c} \right] \quad (2.35)$$

and analogously for the primed field transforming under the representation  $R'$ . This transformation eliminates the interaction contained in the soft covariant derivative  $D_s^0$  in (2.19), since

$$S_w^{(R)\dagger} iD_s^0 S_w^{(R)} = i\partial^0, \quad (2.36)$$

---

<sup>6</sup> Note that in contrast to (2.30) we do not use a field redefinition of the non-relativistic annihilation fields  $\psi$  with Wilson lines extending from  $-\infty$  to  $x_0$  but (2.32), since the former definition would obscure the decoupling of the soft gluons in the PNRQCD Lagrangian. As discussed in [74], the two different forms of the redefinition are equivalent if one takes an appropriate phase for external non-relativistic in-states into account. Since we encounter only external outgoing non-relativistic particles, this subtlety is irrelevant in the present context.

but at first sight introduces the soft Wilson lines into the Coulomb potential interaction. However, since the identity (2.21) also holds if the group elements  $U$  are the Wilson lines  $S_w$  [37], and since the  $S_w$  in the transformations (2.32), (2.33) only depends on the time coordinate, the soft gluon Wilson lines drop out from the Coulomb potential term expressed in terms of the redefined fields. In other words, in terms of the redefined fields the PNRQCD Lagrangian takes exactly the same form as (2.19) except that  $D_s^0 \rightarrow \partial^0$ , so that the Lagrangian is independent of the soft-gluon field. At the next order in the velocity expansion, the PNRQCD Lagrangian contains an interaction involving the gauge invariant chromoelectric operator  $\vec{x} \cdot \vec{E}_s(t, 0)$  [67, 75] that is not removed by the above transformation so the decoupling of soft and potential modes is only valid at leading order in the non-relativistic expansion.<sup>7</sup> We demonstrate in section 2.5 that the corrections to the total cross section from a single insertion of this operator vanish to all orders.

Assembling the different contributions shows that the operators (2.11) for  $S$ -wave production ( $\ell = 0$ ) factorize into an expression of the form

$$\mathcal{O}_{\{a;\alpha\}}^{(0,i)}(x, \mu) = \mathcal{S}_{\{j\}}^{(i)}(x) \left[ \phi_{c;j_1\alpha_1}^{(0)} \phi_{\bar{c};j_2\alpha_2}^{(0)} \psi_{j_3\alpha_3}^{(0)\dagger} \psi_{j_4\alpha_4}^{\prime(0)\dagger} \right](x, \mu), \quad (2.37)$$

with the universal soft contribution

$$\mathcal{S}_{\{j\}}^{(i)}(x) = c_{\{a\}}^{(i)} S_{n,a_1j_1}(x_-) S_{\bar{n},a_2j_2}(x_+) S_{w,j_3a_3}^\dagger(x_0) S_{w,j_4a_4}^\dagger(x_0). \quad (2.38)$$

Here and in the following we suppress the representation labels on the soft Wilson lines, and take it as understood that the Wilson lines always are in the representations appropriate for the respective particles. The decoupled fields  $\psi^{(0)\dagger}$ ,  $\phi_c^{(0)}$  and  $\phi_{\bar{c}}^{(0)}$  in (2.37) do not interact with the soft Wilson lines and with each other at leading power in SCET and at leading order in the non-relativistic expansion.

Near the partonic threshold only soft radiation can occur in the final state so the state  $|X\rangle$  is free of collinear radiation. Therefore the Fock space is a direct product of potential, soft, collinear and anticollinear contributions,

$$|pp'\rangle = |p\rangle_c \otimes |p'\rangle_{\bar{c}} \otimes |0\rangle_s \otimes |0\rangle_p, \quad |HH'X\rangle = |0\rangle_c \otimes |0\rangle_{\bar{c}} \otimes |X\rangle_s \otimes |HH'\rangle_p, \quad (2.39)$$

and we obtain the scattering amplitude in the factorized form:

$$\begin{aligned} \mathcal{A}(pp' \rightarrow HH'X) &= \sum_i C_{\{\alpha\}}^{(0,i)}(\mu) \langle X | \mathcal{S}_{\{j\}}^{(i)}(0) | 0 \rangle \langle HH' | \psi_{j_3\alpha_3}^{(0)\dagger} \psi_{j_4\alpha_4}^{\prime(0)\dagger} | 0 \rangle \\ &\quad \times \langle 0 | \phi_{c;j_1\alpha_1}^{(0)} | p \rangle \langle 0 | \phi_{\bar{c};j_2\alpha_2}^{(0)} | p' \rangle. \end{aligned} \quad (2.40)$$

As remarked above, soft-potential and soft-collinear factorization is only valid at leading order in the non-relativistic and collinear expansion. Similarly for a  $P$ -wave production operator (2.18) the field redefinitions (2.33) do not eliminate the soft gluons in the covariant derivative.

---

<sup>7</sup>In order to achieve factorization of soft gluons in a kinematical regime where relativistic corrections become important one can describe the heavy fields by two copies of heavy quark effective theory with different velocities  $w_1$  and  $w_2$ , see also [36]. Performing separate field redefinitions for  $H$  and  $H'$  with Wilson lines defined in terms of the two velocities decouples the soft gluons up to corrections of the order  $1/m_H, 1/m_{H'}$ .

## 2.4 Factorization formula for the cross section near threshold

We now show that the total partonic cross section for the production of a heavy-particle pair near the production threshold factorizes into hard, potential and soft contributions as sketched in (1.4). To this end, we consider the cross section for the production of a heavy-particle pair near threshold in an  $S$ -wave from the partonic process (2.2) for on-shell, massless initial state partons  $p$  and  $p'$  with zero transverse momentum. In this case only the hard, soft, collinear and anticollinear modes (2.8) contribute to the cross section since no smaller scale related to  $\Lambda_{\text{QCD}}$ , parton masses or off-shellness is introduced and the modes included in the effective theory introduced in section 2.1 are sufficient. We can therefore use the expression for the amplitude (2.40) in terms of decoupled collinear and potential fields and soft Wilson lines to compute the cross section as usual by squaring the scattering amplitude, averaging over initial state and summing over final state polarizations and colours, and integrating over the final-state phase space:

$$\sigma_{pp'}(s) = \frac{1}{2s} \int d\Phi_1 d\Phi_2 d\Phi_X \sum_{\text{pol}} \sum_{\text{colour}} |\mathcal{A}(pp' \rightarrow HH'X)|^2 (2\pi)^4 \delta^{(4)}(p_1 + p_2 + P_X - P) \quad (2.41)$$

Here  $P$  is the total incoming momentum and  $P_X$  is the total momentum of the hadronic state  $X$ . We suppress the normalization factors for the initial-state averages. We do not aim here at a proof of the factorization of the hadronic cross section, that would also require the treatment of modes related to the QCD scale, as in the case of deep inelastic scattering for  $x \rightarrow 1$  in [32]. Rather, we are concerned with the dimensionally regularized partonic cross section (2.41) and its short-distance counterpart with the initial-state infrared divergences subtracted.

The factorized form (2.40) of the scattering amplitude holds if the expectation value of the EFT operator is evaluated with the leading order PNRQCD and SCET Lagrangians. This is a priori appropriate for NLL accuracy in the counting (2.7). Since according to (2.7) the NNLL approximation includes  $\mathcal{O}(\beta)$  corrections, subleading soft interactions in the effective Lagrangian that are not removed by the decoupling transformations could contribute to the cross section starting from NNLL. At fixed-order NNLO accuracy it was shown in [45] that these corrections do not, in fact, contribute to the total cross section and the only corrections not generated by the leading order effective Lagrangian are the one-loop hard function and NLO Coulomb and non-Coulomb potentials. These considerations will be elaborated on in section 2.5 and extended to all orders in the coupling expansion. Therefore the derivation of the simple factorization of the form (1.4) given in the following holds at NNLL accuracy for production processes dominated by  $S$ -wave production.

As for the hadronic cross section (2.1), standard QCD factorization implies that the cross section for the parton initial states factorizes according to

$$\sigma_{pp'}(s) = \sum_{\tilde{p}, \tilde{p}'} \int dx_1 dx_2 f_{p/\tilde{p}}(x_1, \mu) f_{p'/\tilde{p}'}(x_2, \mu) \hat{\sigma}_{\tilde{p}\tilde{p}'}(x_1 x_2 s, \mu), \quad (2.42)$$

where the parton distribution functions of parton  $\tilde{p}$  in parton  $p$ ,  $f_{p/\tilde{p}}(x, \mu)$ , contain the collinear modes. We will consider this cross section near the production threshold,  $s \approx$



$4M^2$ , and show that the short-distance cross section  $\hat{\sigma}_{\tilde{p}\tilde{p}'}$  itself factorizes into hard, soft and potential contributions as sketched in (1.4). At threshold, the PDFs in (2.42) necessarily appear in the limit  $x \rightarrow 1$ , where the flavour off-diagonal PDFs are suppressed, so it is sufficient to consider the case  $p = \tilde{p}$ ,  $p' = \tilde{p}'$ . This is consistent with the fact that, at leading power, we only have to consider EFT matrix elements in (2.10) where the collinear (antcollinear) field  $\phi_c$  ( $\phi_{\bar{c}}$ ) annihilates the state  $|p\rangle$  ( $|p'\rangle$ ). According to QCD factorization,  $\hat{\sigma}_{\tilde{p}\tilde{p}'}$  is independent of the initial states  $p$ ,  $p'$  so it is identical to the hard-scattering cross section to be used in the hadronic cross section (2.1). Therefore the factorized form of the short-distance cross section (1.4) derived in this way can be used in the hadronic cross section in the *partonic* threshold region where  $x_1 x_2 s \sim 4M^2$ . As discussed above, this region is expected to give a sizable contribution to the total cross section for heavy-particle masses  $4M^2 \sim 0.2s$ . For values of  $x_{1,2}$  outside the partonic threshold region, the factorized formula is not necessarily a good approximation to the cross section and the resummed cross section should be matched to the fixed-order expansion as discussed further in section 3.6.

We now proceed with the derivation of the factorization formula which follows similar steps as that for the Drell-Yan process in [33]. The new ingredients here are the presence of the potential fields and additional Wilson lines for the heavy coloured particles, resulting in a more involved colour and spin structure. After inserting the factorized matrix element (2.40) into the standard expression for the cross section (2.41), we use an integral representation of the  $\delta$  function,

$$(2\pi)^4 \delta^{(4)}(p_1 + p_2 + P_X - P) = \int d^4 z e^{-iz \cdot (p_1 + p_2 + P_X - P)}. \quad (2.43)$$

Rewriting the exponential in terms of the momentum operator acting on the external states, we can translate the collinear, potential and soft operators in the conjugate matrix element to  $z$ , e.g.  $e^{iz \cdot k_1} \langle p(k_1) | \phi_c^{(0)\dagger}(0) | 0 \rangle = \langle p(k_1) | e^{iz \cdot \hat{P}} \phi_c^{(0)\dagger}(0) e^{-iz \cdot \hat{P}} | 0 \rangle = \langle p(k_1) | \phi_c^{(0)\dagger}(z) | 0 \rangle$ . We then obtain for the cross section:

$$\begin{aligned} \sigma_{pp'}(s) &= \frac{1}{2s} \sum_{\text{pol}} \sum_{\text{colour}} \sum_{i,i'} C_{\{\alpha\}}^{(0,i)} C_{\{\beta\}}^{(0,i')*} \int d^4 z e^{-2iMw \cdot z} J_{k_3 k_4 j_3 j_4}^{\beta_3 \beta_4 \alpha_3 \alpha_4}(z) \\ &\times \langle p | \phi_{c;k_1 \beta_1}^{(0)\dagger}(z) | 0 \rangle \langle p' | \phi_{\bar{c};k_2 \beta_2}^{(0)\dagger}(z) | 0 \rangle \langle 0 | \phi_{c;j_1 \alpha_1}^{(0)}(0) | p \rangle \langle 0 | \phi_{\bar{c};j_2 \alpha_2}^{(0)}(0) | p' \rangle \\ &\times \int d\Phi_X \langle 0 | \mathcal{S}_{\{k\}}^{(i')*}(z) | X \rangle \langle X | \mathcal{S}_{\{j\}}^{(i)}(0) | 0 \rangle. \end{aligned} \quad (2.44)$$

Here we introduced the definition of the *potential function* in terms of the PNRQCD matrix elements:

$$J_{\{a\}}^{\{\alpha\}}(z) = \int d\Phi_1 d\Phi_2 \sum_{\text{pol,colour}} \langle 0 | [\psi_{a_2 \alpha_2}'^{(0)} \psi_{a_1 \alpha_1}^{(0)}](z) | HH' \rangle \langle HH' | [\psi_{a_3 \alpha_3}^{(0)\dagger} \psi_{a_4 \alpha_4}'^{(0)\dagger}](0) | 0 \rangle. \quad (2.45)$$

The factor  $e^{-2iMw \cdot z} = e^{-i(m_H + m_{H'})w \cdot z}$  arises because, by definition, the non-relativistic fields depend only on the residual momentum so that  $\psi(z) = e^{iz \cdot \hat{P}} \psi(0) e^{-iz \cdot \hat{P}} = e^{-iz \cdot \tilde{p}} \psi(0)$ . We

can introduce a colour basis for the potential function  $J$  by introducing projectors  $P^{R_\alpha}$  onto the irreducible representations  $R_\alpha$  appearing in the decomposition of the final-state representations,  $R \otimes R' = \sum_{R_\alpha} R_\alpha$ :

$$J_{\{a\}}^{\{\alpha\}} = \sum_{R_\alpha} P_{\{a\}}^{R_\alpha} J_{R_\alpha}^{\{\alpha\}}. \quad (2.46)$$

A systematic procedure for the construction of the projectors for arbitrary representations out of Clebsch-Gordan coefficients for the coupling  $R \otimes R' \rightarrow R_\alpha$  is reviewed in [37] where the projectors needed for all production processes of pairs of coloured SUSY particles are collected and further properties of the projectors can be found.

Since the leading order PNRQCD Lagrangian is spin independent, the spin structure of the leading order potential function (resumming multiple Coulomb exchange) is trivial:

$$J_{R_\alpha}^{\{\alpha\}}(x) = \delta_{\alpha_1\alpha_3} \delta_{\alpha_2\alpha_4} J_{R_\alpha}(x). \quad (2.47)$$

However, as mentioned above, spin-dependent non-Coulomb potentials become relevant starting from NNLL accuracy in the combined counting in  $\alpha_s \ln \beta$  and  $\alpha_s/\beta$  defined in (2.7). Therefore we introduce a decomposition of the potential function into different spin states:

$$J_{R_\alpha}^{\{\alpha\}}(x) = \sum_{S=|s-s'|}^{s+s'} \Pi_S^{\{\alpha\}} J_{R_\alpha}^S(x). \quad (2.48)$$

Here  $s$  ( $s'$ ) is the spin of the heavy particle  $P$  ( $P'$ ). The projectors  $\Pi_S$  project on the  $HH'$  state with total spin  $S$ . They satisfy the completeness relation

$$\sum_{S=|s-s'|}^{s+s'} \Pi_{\{\alpha\}}^S = \delta_{\alpha_1\alpha_3} \delta_{\alpha_2\alpha_4}. \quad (2.49)$$

As an example, for two spin  $\frac{1}{2}$  particles, the projectors on singlet and triplet states read in the cms frame:

$$\begin{aligned} \Pi_0^{\{\alpha\}} &= \frac{1}{2} \delta_{\alpha_2\alpha_1} \delta_{\alpha_3\alpha_4}, \\ \Pi_1^{\{\alpha\}} &= \frac{1}{2} \sigma_{\alpha_2\alpha_1}^i \sigma_{\alpha_3\alpha_4}^i. \end{aligned} \quad (2.50)$$

The explicit expression for the function  $J$  is given in section 3.3.

In order to bring (2.44) into the form of the standard factorization formula (2.42) we have to identify the collinear matrix elements with the PDFs which requires to combine the products of the matrix elements of the collinear fields into a single expectation value (the same discussion applies for the anticollinear fields). This can be achieved by recalling that due to the threshold kinematics collinear radiation from the initial state is inhibited. We can therefore formally sum over the states of the collinear final state Fock space  $|C\rangle$  since

the only contribution comes from the vacuum. After subsequent use of the completeness relation we can simplify the product of collinear matrix elements to

$$\begin{aligned} \langle p | \phi_c^{(0)\dagger}(z) | 0 \rangle \langle 0 | \phi_c^{(0)}(0) | p \rangle &\Rightarrow \sum_C \int d\Phi_C \langle p | \phi_c^{(0)\dagger}(z) | C \rangle \langle C | \phi_c^{(0)}(0) | p \rangle \\ &= \langle p | \phi_c^{(0)\dagger}(z) \phi_c^{(0)}(0) | p \rangle . \end{aligned} \quad (2.51)$$

The same result for the collinear matrix element is obtained in the standard collinear factorization away from threshold where the final state contains collinear radiation and the sum over the collinear Fock space is present from the beginning. We therefore define

$$\langle p(P_1) | \phi_{c;k_1\beta_1}^{(0)\dagger}(z) \phi_{c;j_1\alpha_1}^{(0)}(0) | p(P_1) \rangle |_{\text{avg.}} = \delta_{k_1 j_1} \int_0^1 \frac{dx_1}{x_1} e^{ix_1(z \cdot P_1)} N_{\alpha_1 \beta_1}^p(x_1 P_1) f_{p/\tilde{p}}(x_1, \mu), \quad (2.52)$$

where  $\tilde{p}$  is the parton annihilated by the field  $\phi$  and the average refers to colour and polarization. We show in appendix A that the so defined functions  $f_{p/\tilde{p}}(x_1, \mu)$  coincide with the standard definition of the quark, antiquark and gluon parton distribution functions. Since the momentum of the external state is  $P_1^\mu = \bar{n} \cdot P_1 n^\mu / 2$ , the matrix element depends on  $z$  only through  $z_+ = n \cdot z \propto z \cdot P_1$  since  $z \cdot P_1 = (n \cdot z)(\bar{n} \cdot P_1) / 2$ , which has been used to represent it as a one-dimensional Fourier transform. This also allows us to replace  $z^\mu$  by  $(n \cdot z) \bar{n}^\mu / 2$  on the left-hand side. For all parton species, the prefactor is given by the helicity average of the polarization wave functions  $\chi_\alpha$  of the SCET fields

$$N_{\alpha\beta}^p(x_1 P_1) = \frac{1}{n_s D_r} \sum_\lambda \chi_\alpha^\lambda(x_1 P_1) \chi_\beta^{\lambda*}(x_1 P_1), \quad (2.53)$$

where the sum extends over the physical polarization states.  $D_r$  denotes the dimension of the SU(3) colour representation of the initial state parton  $p$  and the number of spin-degrees of freedom is  $n_s = 2$  for all relevant cases. Note that the polarization wave functions are evaluated for a particle with momentum  $x_1 P_1$ , which corresponds to the standard rule for calculating parton scattering cross sections. At the same time the factors  $1/x_1$  (and  $1/x_2$  for the other parton) from the definition (2.52) combine with the prefactor  $1/(2s)$  in (2.44) to yield the standard flux factor  $1/(2\hat{s})$  for partonic scattering.

The soft matrix elements in the cross section (2.44) can be collected in the *soft function*

$$\hat{W}_{ii'}^{R_\alpha}(z, \mu) = \sum_X \int d\Phi_X \langle 0 | \mathcal{S}_{\{j_1 j_2 k_1 k_2\}}^{(i')*}(z) | X \rangle P_{\{k\}}^{R_\alpha} \langle X | \mathcal{S}_{\{j_1 j_2 k_3 k_4\}}^{(i)}(0) | 0 \rangle, \quad (2.54)$$

which is a matrix in the colour basis given by the  $c_{\{a\}}^{(i)}$ . Since the collinear matrix elements are diagonal in colour and due to the colour decomposition of the potential function (2.46), the initial-state colour indices  $j_1, j_2$  are summed over and the final state indices are projected on the irreducible representations  $R_\alpha$ . Since we are concerned with the total cross section, the soft matrix elements can be combined in a correlation function by summing

over the hadronic final state and using the completeness relation

$$\sum_X \int d\Phi_X |X\rangle \langle X| = I \quad (2.55)$$

of the soft Hilbert space. The soft function can then be written as

$$\hat{W}_{ii'}^{R_\alpha}(z, \mu) = P_{\{k\}}^{R_\alpha} c_{\{a\}}^{(i)} \hat{W}_{\{ab\}}^{\{k\}}(z, \mu) c_{\{b\}}^{(i')*} \quad (2.56)$$

with the correlation function of soft Wilson lines

$$\hat{W}_{\{a,b\}}^{\{k\}}(z, \mu) = \langle 0 | \overline{\text{T}}[S_{w,b_4k_2} S_{w,b_3k_1} S_{\bar{n},jb_2}^\dagger S_{n,ib_1}^\dagger](z) \text{T}[S_{n,a_1i} S_{\bar{n},a_2j} S_{w,k_3a_3}^\dagger S_{w,k_4a_4}^\dagger](0) | 0 \rangle. \quad (2.57)$$

In combining the soft matrix elements into a correlation function we have introduced time- and anti-time-ordering symbols as discussed in [33]. In evaluating this correlation function, a soft gluon propagator connecting fields in the time-ordered and anti-time-ordered products is given by a cut propagator, therefore this prescription reproduces the usual rules for the real soft corrections. A colour basis that diagonalizes the soft matrices  $W_{ii'}^{R_\alpha}$  to all orders in perturbation theory has been constructed in [37] as reviewed in section 3.1 below.

Inserting these definitions, the cross section becomes a convolution of the PDFs with the potential and soft functions:

$$\begin{aligned} \sigma_{pp'} &= \int dx_1 dx_2 f_{p/\bar{p}}(x_1, \mu) f_{p'/\bar{p}'}(x_2, \mu) \sum_{i,i'} \sum_{S=|s-s'|}^{s+s'} H_{ii'}^S(\mu) \\ &\times \int \frac{d^4 q}{(2\pi)^4} J_{R_\alpha}^S(q) \int d^4 z e^{i(x_1 P_1 + x_2 P_2 - 2Mw - q) \cdot z} \hat{W}_{ii'}^{R_\alpha}(z, \mu), \end{aligned} \quad (2.58)$$

where we have introduced the Fourier transform of the potential function

$$J_{R_\alpha}^S(q) = \int d^4 z e^{iq \cdot z} J_{R_\alpha}^S(z) \quad (2.59)$$

and the spin and colour dependent *hard functions* defined in terms of the short-distance coefficients averaged over the initial state spins and projected on the spin state of the heavy-particle system:

$$\begin{aligned} H_{ii'}^S(\mu) &= \frac{1}{2\hat{s}} \left[ N_{\alpha_1\beta_1}^{p'}(x_1 P_1) N_{\alpha_2\beta_2}^{p'}(x_2 P_2) C_{\{\alpha\}}^{(0,i)}(\mu) \Pi_S^{\beta_3\beta_4\alpha_3\alpha_4} C_{\{\beta\}}^{(0,i')*}(\mu) \right] \\ &= \frac{1}{2\hat{s}} \frac{1}{4D_r D_{r'}} \sum_{\lambda_1\lambda_2} (C_{\{\alpha\}}^{(0,i)}(\mu) \chi_{\alpha_1}^{\lambda_1} \chi_{\alpha_2}^{\lambda_2}) \Pi_S^{\beta_3\beta_4\alpha_3\alpha_4} (C_{\{\beta\}}^{(0,i')*}(\mu) \chi_{\beta_1}^{\lambda_1} \chi_{\beta_2}^{\lambda_2})^*. \end{aligned} \quad (2.60)$$

In the second line we have inserted the prefactors (2.53) (omitting the momentum argument of the polarization wave functions).<sup>8</sup> Summing over the spin states and using the

---

<sup>8</sup>In (2.60) we could replace  $\hat{s}$  by  $4M^2$  to make the hard function energy-independent. However, in the numerical evaluation it is trivial to keep the kinematic factor  $1/(2\hat{s})$  and this is the convention we adopt in Section 4.

completeness relation of the spin projectors we obtain the spin-averaged hard function that is sufficient for NLL resummations:

$$H_{ii'}(\mu) = \sum_{S=|s-s'|}^{s+s'} H_{ii'}^S(\mu) = \frac{1}{2\hat{s}} \left[ N_{\alpha_1\beta_1}^p(x_1P_1) N_{\alpha_2\beta_2}^{p'}(x_2P_2) C_{\alpha_1\alpha_2\gamma\delta}^{(0,i)}(\mu) C_{\beta_1\beta_2\gamma\delta}^{(0,i')*}(\mu) \right] \quad (2.61)$$

A simple prescription for the computation of the hard functions directly from the scattering amplitudes will be given in section 3.2.

Comparing (2.58) to the factorization formula (2.42) we obtain the factorized expression for the short-distance cross section by stripping off the integrals with the parton distribution functions. The remaining expression can be further simplified in the threshold region. For notational simplicity, we will perform these manipulations in the partonic cms frame where  $w = (1, \vec{0})$ . We first shift the  $q$  integral by introducing the new integration variable  $q' = (x_1P_1 + x_2P_2 - 2Mw - q) = (\sqrt{\hat{s}} - 2M)w - q$  and obtain

$$\hat{\sigma}_{pp'}(\hat{s}, \mu) = \sum_{i,i'} \sum_{S=|s-s'|}^{s+s'} H_{ii'}^S(\mu) \int \frac{d^4q'}{(2\pi)^4} J_{R_\alpha}^S(Ew - q') \int d^4z e^{iq'\cdot z} \hat{W}_{ii'}^{R_\alpha}(z, \mu). \quad (2.62)$$

Here we defined the partonic centre-of-mass energy measured from threshold,  $E = \sqrt{\hat{s}} - 2M = M(1 - z) + \mathcal{O}(\lambda^2)$ . The function  $\hat{W}$  contains soft fields that, by definition, vary significantly only on distances  $z \sim 1/\lambda$ . Hence, only soft momenta ( $q' \sim \lambda$ ) contribute to the  $q'$  integration. On the other hand the function  $J$ , which is defined in terms of potential fields alone, is a function of  $q = (\sqrt{\hat{s}} - 2M)w - q'$ . In the partonic centre of mass frame we have by assumption  $x_1P_1 + x_2P_2 = \sqrt{\hat{s}}w = p_1 + p_2 + k_s = 2Mw + k'_s$  with soft momenta  $k_s, k'_s$ , therefore  $q$  is also soft. Since potential fields with scalings  $(k_0, \vec{k}) \sim (\lambda, \sqrt{\lambda})$  can depend on soft momenta only through their small time-like components,  $J$  is a function of  $q_0 = \sqrt{\hat{s}} - 2M - q'_0$  alone. This enables us to perform the  $\vec{q}$  integration in (2.62) which sets  $\vec{z} = 0$  in the argument of the soft function. We then obtain the final expression for the factorized short-distance cross sections:

$$\hat{\sigma}_{pp'}(\hat{s}, \mu) = \sum_{S=|s-s'|}^{s+s'} \sum_{i,i'} H_{ii'}^S(\mu) \int d\omega \sum_{R_\alpha} J_{R_\alpha}^S(E - \frac{\omega}{2}) W_{ii'}^{R_\alpha}(\omega, \mu). \quad (2.63)$$

Here we defined the Fourier transform of the soft function

$$W_{ii'}^{R_\alpha}(\omega, \mu) = \int \frac{dz_0}{4\pi} e^{i\omega z_0/2} \hat{W}_{ii'}^{R_\alpha}(z_0, \vec{0}, \mu). \quad (2.64)$$

The formula (2.42), with the partonic cross section (2.63), establishes the factorization into collinear (the parton distribution functions), potential (the function  $J$ ) and soft (the soft function  $W$ ) contributions for heavy particles produced in an  $S$ -wave, and constitutes the main theoretical result of this work. Some further comments on the structure and validity range of the factorization formula as well as a comparison to previous results are given in section 2.5 below. The simplification of the colour sum over  $i, i'$  due to the existence of a diagonal basis [37] is reviewed in section 3.1.

## 2.5 Some comments on the factorization formula

### 2.5.1 Gauge invariance

Let us briefly comment on the gauge invariance of the ingredients in the factorization formula. The hard function is defined in terms of on-shell fixed-order scattering amplitudes projected on a given colour and spin state. The gauge invariance of the hard function then follows from the gauge invariance of the on-shell scattering amplitude and the linear independence of the elements of the colour and spin bases. The effective-theory Lagrangian is invariant under the collinear gauge transformations of SCET [60] and the soft gauge transformations (2.27) and (2.20). Collinear gauge invariance is built into the formalism since the operators are constructed from the invariant fields  $\phi_c$ . The invariance of the components of the soft function (2.64) under soft gauge transformations follows since the elements of the colour basis are invariant tensors satisfying

$$c_{\{a\}}^{(i)} = U_{a_3 b_3}^{(R)\dagger} U_{a_4 b_4}^{(R')\dagger} c_{\{b\}}^{(i)} U_{b_1 a_1}^{(r)} U_{b_2 a_2}^{(r')}. \quad (2.65)$$

Note that for this it is essential that only the soft function with vanishing spatial argument,  $W_{ii'}^{R\alpha}(x_0, \vec{0}, \mu)$ , enters the final factorization formula since for the soft function at arbitrary  $x$  the gauge transformations of the collinear, anticollinear and potential fields appear with different arguments  $x_-$ ,  $x_+$  and  $x_0$ . Finally the collinear matrix elements and the potential function are defined in terms of the decoupled fields that transform trivially under soft gauge transformations.

### 2.5.2 Subleading corrections to the cross section

In our derivation of the factorization formula we relied on field redefinitions that decouple the soft gluons from the leading SCET and PNRQCD Lagrangians. The subleading effective Lagrangians include higher-order potentials, but also interactions of the soft gluons to the potential fields via the  $\vec{x} \cdot \vec{E}$  interaction mentioned above and analogous couplings to the collinear fields. These terms cannot be eliminated using the decoupling transformations. However, being sub-leading, these interactions can be treated as perturbations in  $\beta$  and, since the soft gluons decouple from the leading effective Lagrangian, the cross section can be written to all orders in the non-relativistic and SCET expansions in the schematic form

$$\hat{\sigma} = \sum_a H^a [W^a \otimes J^a], \quad (2.66)$$

with higher-order hard, soft and potential functions labeled by the index  $a$ . At NNLL accuracy, several effects could be relevant that are not included in the leading term  $a = 0$  in (2.66) considered so far in this work. We now discuss these effects and show that they either do not contribute at NNLL or are incorporated in a straightforward way without spoiling the factorization.

It is worth mentioning at this point that in standard situations of soft gluon resummation not requiring the consideration of Coulomb singularities, the expansion in powers

of  $1 - z$  and  $\alpha_s$  can be considered separately. Thus the discussion of power-suppressed interactions is not necessary to any order in  $\alpha_s$  as long as one drops subleading terms in  $1 - z$ . In joint soft-gluon and Coulomb resummations the two expansions are linked by the counting  $\alpha_s/\beta \sim 1$ , so that  $\mathcal{O}(\beta)$  suppressed terms that would normally be referred to as power corrections now appear at the same NNLL order as  $\alpha_s$  terms, see (2.7). This is a complication characteristic of perturbative non-relativistic systems that have kinematic singularities which are stronger than logarithmic.

*Hard effects.* Higher-order production operators such as the  $P$ -wave operator (2.18) can appear at  $\mathcal{O}(\beta)$ , which according to (2.7) corresponds to a NNLL effect. These can include interactions with soft gluons through a spatial covariant derivative that are not removed by the decoupling transformation. However, since there is no interference between  $S$ - and  $P$ -wave production for the total cross section, these corrections are at least  $\mathcal{O}(\beta^2)$ , beyond NNLL accuracy.

*Potential effects.* Beyond the leading-order Coulomb potential in (2.19), subleading effects lead to further potential interactions of the form

$$\int d^3\vec{r} [\psi_a^\dagger \psi_b](\vec{r}) \delta V_{abcd}(r) [\psi_c^\dagger \psi_d'](0). \quad (2.67)$$

The running of the strength of the Coulomb potential causes a NLL correction beginning with  $\alpha_s^2/\beta \times \log \beta$ , which is accounted for by evaluating the coupling in the leading-order Coulomb potential at a scale of order  $m_{\text{red}}\beta$ , where  $m_{\text{red}}$  denotes the reduced mass of the heavy-particle system, or by an explicit logarithmic correction to  $\delta V_{abcd}(r)$ . Genuine loop corrections to the colour Coulomb potential lead to the substitution

$$\frac{\alpha_s(1/r)}{r} \rightarrow \frac{\alpha_s(1/r)}{r} \left( 1 + \hat{a}_1 \frac{\alpha_s}{4\pi} + \dots \right) \quad (2.68)$$

in the Lagrangian (2.19). Only the one-loop correction  $\hat{a}_1$  is needed at NNLL, and contributes terms beginning with  $\alpha_s^2/\beta$ . In addition there exist the spin-dependent and independent non-Coulomb potentials of form  $\alpha_s^2/r^2$  and (summarily)  $\alpha_s/r^3$ , see e.g. [76], leading to NNLL terms beginning with  $\alpha_s^2 \log \beta$ . Here the logarithm arises from non-relativistic factorization and is related to the fact that the short-distance functions  $H_{ii'}^S(\mu)$  have potential infrared divergences in addition to the familiar soft and collinear divergences. These additional potential terms in the PNRQCD Lagrangian do not involve soft gluon fields and the decoupling transformation can be applied as for the leading potential. Therefore these terms can be included in the evaluation of the potential function  $J$ , as was done in [45] to compute all  $\log \beta$  and  $1/\beta$  enhanced terms of the  $t\bar{t}$ -production cross section at  $\mathcal{O}(\alpha_s^4)$ .

*Subleading potential-soft interactions.* We next discuss possible contributions to subleading terms in (2.66) arising from the higher-order couplings of soft gluons to collinear and potential fields that are not decoupled by the field redefinition. In a diagrammatic language, these arise from the interference of subleading soft gluons coupling to the initial or final state with potential gluon exchange, that could contribute NNLL terms beginning with

$\alpha_s/\beta \times \alpha_s \beta \log^{2,1} \beta$ . As shown in [45] using power-counting and rotational invariance, the fixed-order NNLO corrections of this form vanish for the total cross section. We will now use the effective theory language to show that the NNLL corrections arising from the subleading SCET and PNRQCD Lagrangians vanish to all orders in the strong coupling, so that the leading factorization formula (2.63) does not require modification at NNLL.

We begin with the  $\mathcal{O}(\beta)$  suppressed interactions in the subleading PNRQCD Lagrangian [67, 70, 75],

$$\begin{aligned} \mathcal{L}_{\text{PNRQCD}}^{(1)} &= -g_s \left[ \psi^\dagger(x) \vec{x} \cdot \vec{E}_s(x^0, \vec{0}) \psi(x) + \psi'^\dagger(x) \vec{x} \cdot \vec{E}_s(x^0, \vec{0}) \psi'(x) \right] \\ &\equiv -g_s \vec{x} \cdot \vec{E}_s^a(x^0, \vec{0}) \mathcal{J}^a(x) \end{aligned} \quad (2.69)$$

with the bilinear product of potential fields

$$\mathcal{J}^a = \psi^\dagger \mathbf{T}^{(R)a} \psi + \psi'^\dagger \mathbf{T}^{(R')a} \psi'. \quad (2.70)$$

We treat the chromoelectric vertex perturbatively, i.e. we consider contributions to the cross section where one of the matrix elements contains an insertion of the vertex  $\vec{x} \cdot \vec{E}$  and evaluate these matrix elements with the LO PNRQCD Lagrangian. The first-order correction to (2.10) from the interaction (2.69) is given by

$$\Delta \mathcal{A}^{(1)}(pp' \rightarrow HH'X) = C_{\{a;\alpha\}}^{(0)}(\mu) \int d^4x \langle HH'X | \text{T}[\mathcal{L}_{\text{PNRQCD}}^{(1)}(x) \mathcal{O}_{\{a;\alpha\}}^{(0)}(\mu)] | pp' \rangle_{\text{EFT}}. \quad (2.71)$$

The expectation value is evaluated with the leading-order effective-theory Lagrangian, so the soft, collinear and potential fields decouple after the field redefinition. Under this redefinition, the chromoelectric interaction is transformed into

$$\psi^\dagger(x) \vec{x} \cdot \vec{E}_s(x_0, \vec{0}) \psi(x) = \psi^{\dagger(0)}(x) \vec{x} \cdot \vec{\mathcal{E}}_s(x_0, \vec{0}) \psi^{(0)}(x) \quad (2.72)$$

with  $\mathcal{E}_s = S_w^\dagger E_s S_w$ . Independent of the colour representation of the heavy particles, due to the identity (2.21), which also holds for the Wilson lines, the components of the redefined chromoelectric fields are given by

$$\vec{\mathcal{E}}_s^a(x_0) = S_{w,ab}^{(8)} \vec{E}_s^b(x_0). \quad (2.73)$$

In analogy to (2.40), the effective theory matrix element factorizes and the correction to the scattering amplitude can be written as

$$\begin{aligned} \Delta \mathcal{A}^{(1)}(pp' \rightarrow HH'X) &= \sum_i C_{\{\alpha\}}^{(0,i)}(\mu) \langle 0 | \phi_{c;j_1\alpha_1}^{(0)} | p \rangle \langle 0 | \phi_{\bar{c};j_2\alpha_2}^{(0)} | p' \rangle \\ &\times \int d^4x \vec{x} \langle X | \text{T}[\vec{\mathcal{E}}_s^a(x_0, \vec{0}) \mathcal{S}_{\{j\}}^{(i)}(0)] | 0 \rangle \langle HH' | \text{T}[\mathcal{J}^{a(0)}(x) \psi_{j_3\alpha_3}^{(0)\dagger} \psi_{j_4\alpha_4}^{(0)\dagger}] | 0 \rangle. \end{aligned} \quad (2.74)$$

Repeating the steps leading to the factorization formula (2.62) and the subsequent discussion, we obtain an analogous formula with the replacement



$$\begin{aligned}
& \int \frac{dq^0}{(2\pi)} J_{R_\alpha}(E - q^0) \int dz^0 e^{iq^0 z^0} \hat{W}_{ii'}^{R_\alpha}(z^0, \mu) \\
\Rightarrow & \int \frac{dq^0}{(2\pi)} \int \frac{d^4 k}{(2\pi)^4} J_{R_\alpha}^{a(1)}(E - q^0, k) \int dz^0 e^{iq^0 z^0} \int d^4 x e^{-ik \cdot x} \vec{x} \cdot \vec{W}_{ii'}^{a, R_\alpha(1)}(z^0, x^0, \mu) + \text{c.c.}
\end{aligned} \tag{2.75}$$

Here we have defined the subleading soft function with an insertion of the chromoelectric field according to

$$\vec{W}_{ii'}^{a, R_\alpha(1)}(z^0, x^0, \mu) = P_{\{k\}}^{R_\alpha} \langle 0 | \bar{\text{T}}[\mathcal{S}_{\{ijk_1 k_2\}}^{(i')*}(z^0)] \text{T}[\vec{\mathcal{E}}_s^a(x^0) \mathcal{S}_{\{ijk_3 k_4\}}^{(i)}(0)] | 0 \rangle \tag{2.76}$$

as well as a subleading potential function with an insertion of the bilinear (2.70):

$$J_{\{\alpha\}R_\alpha}^{a(1)}(q, k) = P_{\{a\}}^{R_\alpha} \int d^4 z e^{iq \cdot z} \int d^4 x e^{ik \cdot x} \langle 0 | [\psi_{\alpha_1 a_1}^{(0)} \psi'_{\alpha_2 a_2}{}^{(0)}](z) \text{T}[\mathcal{J}^{a(0)}(x) [\psi_{\alpha_3 a_3}^{(0)\dagger} \psi'_{\alpha_4 a_4}{}^{(0)\dagger}](0)] | 0 \rangle . \tag{2.77}$$

Since the matrix elements are evaluated with the spin-independent leading order PNRQCD Lagrangian, the spin dependence simplifies in analogy to (2.47) as was used in (2.75). In the terms denoted by “c.c.” in (2.75) the operator  $\mathcal{E}_s$  is inserted in the anti-time-ordered product in the subleading soft function and the potential function is defined with the insertion of  $\mathcal{J}^{(0)}$  in an anti-time-ordered product with the annihilation fields.

Because the subleading soft function does not depend on  $\vec{x}$ , we can perform the integral over the spatial components of  $x$  in (2.75) and obtain the expression

$$\int \frac{d^4 k}{(2\pi)^4} \delta^{(3)}(\vec{k}) \frac{\partial}{\partial \vec{k}} J_{R_\alpha}^{a(1)}(E - q^0, k) = 0, \tag{2.78}$$

which vanishes since (in the partonic cms frame) there is no three-momentum left that the integral over  $J_{R_\alpha}^{(1)}$  can depend on. Hence we conclude that the correction to the cross section due to a single insertion of the NLO potential Lagrangian vanishes to all orders in the strong coupling constant. Similar to the diagrammatic argument in [45], an essential ingredient in the argument was the multipole expansion of soft fields when multiplying potential fields. Because of this, only  $\vec{E}(x^0)$  appears in the subleading PNRQCD interaction and, as a consequence, the subleading soft function depends only on  $x^0$  which allowed to perform the simplification in the last step. The second ingredient is rotational invariance in combination with the independence of the potential function on any external three-momentum.

*Subleading collinear-soft interactions.* The effects potentially relevant at NNLL arise from the effective Lagrangians at the next-to-leading order in the kinematic expansion. For the SCET Lagrangian of collinear quarks, the relevant interactions are given by [59, 60]

$$\mathcal{L}_\xi^{(1)} = \bar{\xi} (x_\perp^\mu n^\nu W_c g F_{\mu\nu}^s W_c^\dagger) \frac{\not{n}}{2} \xi, \tag{2.79}$$

for  $n$ -collinear modes and similar terms involving transverse derivatives or factors of  $x_\perp$  for the couplings to collinear gluons, and an interaction

$$\mathcal{L}_{\xi q}^{(1)} = \bar{\xi} i \not{D}_\perp W_c q_s + \bar{q}_s W_c^\dagger i \not{D}_\perp \xi \tag{2.80}$$

involving soft quarks but only collinear gluons. As argued already in [45], these vertices with transverse derivatives or  $x_{\perp}^{\mu}$  cannot contribute to the total cross section since the initial-state momenta can be chosen to have zero transverse momentum. Then loop integrals with transverse momentum factors vanish by rotational invariance in the plane transverse to the beam axis. Eq. (2.80) contains a vertex that describes the collinear splitting of a quark into a gluon and a soft quark, which is also an  $\mathcal{O}(\beta)$  term. However, a non-vanishing contribution to the squared amplitude requires two such vertices to contract the soft quark field, hence there is again no contribution at NNLL. Note that insertions of power-suppressed interaction Lagrangians lead to collinear matrix elements that do not take the form of the standard parton densities. At this point it appears that one must distinguish the collinear expansion in powers of  $k_{\perp} \sim M\sqrt{\lambda} \sim M\beta$  from the standard collinear expansion in  $k_{\perp} \sim \Lambda_{\text{QCD}}$ . However, as mentioned above, this issue is not relevant for NLL and NNLL resummations.

To summarize, the factorization formula (2.63) is valid at NNLL accuracy provided subleading Coulomb and non-Coulomb potentials are included in the computation of the potential function and the hard and soft functions are computed at NLO.

### 2.5.3 Comparison to factorization at fixed invariant mass

The result (2.63) can be compared to the analogous formula (1.1) given in [7] for the pair production of relativistic coloured particles with different four-velocity vectors  $w_1, w_2$ , where potential degrees of freedom do not appear. In this case the potential function is absent in the factorization formula and the soft function is given by (taking into account our convention for the antiparticles):

$$\hat{S}_{\{ab\}}(z) = \langle 0 | \overline{\text{T}}[S_{n,ib_1}^{\dagger} S_{\bar{n},jb_2}^{\dagger} S_{w_2,b_4l} S_{w_1,b_3k}](z) \text{T}[S_{\bar{n},a_2j} S_{n,a_1i} S_{w_1,ka_3}^{\dagger} S_{w_2,la_4}^{\dagger}](0) | 0 \rangle. \quad (2.81)$$

In our case the extraction of the potential function  $J$  leads to a more complicated colour structure of the soft function  $W$ , but to a simpler kinematical structure due to the equal four-velocities of the heavy particles. Using the completeness relation of the projectors and the definition of the components of the soft function (2.56), the limit of (2.81) for the case of equal four velocities,  $w_1 = w_2 = w$ , is formally related to the sum of the soft functions for the different final-state representations:

$$S_{ii'}|_{w_1=w_2} = \sum_{R_{\alpha}} W_{ii'}^{R_{\alpha}}. \quad (2.82)$$

The resummation coefficients used in the Mellin space approach to threshold resummation have been calculated at the one-loop level for various colour representations [7, 17, 20] from the threshold limit of the soft function  $S$ . This amounts to taking the threshold limit after extracting the  $1/\epsilon$  poles of the eikonal diagrams contributing to  $S$ . Applying this approach at the two-loop level [42] one encounters three-parton colour correlations proportional to  $\log \beta$  that arise from an interference of soft and potential divergences, and lead to off-diagonal contributions in the colour basis constructed in [37] that diagonalizes the soft

functions  $W^{R_\alpha}$ . In contrast, the effective theory approach constructs an expansion in  $\beta$  before taking the  $\epsilon \rightarrow 0$  limit, resulting in the tower of higher dimensional hard, soft and potential functions (2.66). In this approach, the  $\log \beta$ -dependent divergences are attributed to higher-dimensional soft and potential functions due to the subleading  $\vec{x} \cdot \vec{E}$  vertex in the PNRQCD Lagrangian and subleading potentials, while the leading soft function (2.56) is diagonal to all orders. In order to resum all terms that are enhanced by powers of  $\log \beta$  and inverse powers of  $\beta$  at a given accuracy one should use the formula (2.66), while (1.1) is appropriate for partonic thresholds where the relative velocities of the final state particles are relativistic, as considered e.g. in the recent resummation of the invariant mass distribution of top-quark pairs in [36].

#### 2.5.4 Soft-Coulomb factorization in Mellin moment space

The enhancement due to single-Coulomb exchange has been included in the Mellin moment space approach to resummation as part of the hard function [11], which implicitly assumes the factorization of soft and potential gluons. We now briefly discuss the relation of our factorization formula (2.63) to the Mellin space formalism and show that the convolution of the soft and potential function factorizes in Mellin space in the large  $N$  limit, which justifies the earlier treatment. We recall that the Mellin moments of the cross section in the variable  $z = 4M^2/\hat{s}$  are defined as:

$$\hat{\sigma}(N, \mu) = \int_0^1 dz z^{N-1} \hat{\sigma}(\hat{s}, \mu). \quad (2.83)$$

In order to Mellin-transform the factorized cross section (2.63), we approximate  $E = \sqrt{\hat{s}} - 2M \approx M(1 - z)$  and make the transformation of variables  $\omega = 2M(1 - w)$ . For stable particles and neglecting bound-state contributions, the potential function is non-vanishing only for  $E - \omega/2 \approx M(w - z) > 0$  so we can write

$$\hat{\sigma}_{pp'}(\hat{s}, \mu) \approx 2M \sum_{S, i, i'} H_{ii'}^S \int_z^1 \frac{dw}{w} \sum_{R_\alpha} J_{R_\alpha}^S(M(1 - \frac{z}{w})) W_{ii'}^{R_\alpha}(2M(1 - w), \mu). \quad (2.84)$$

Here we have used  $z < w \lesssim 1$  so that  $E - \omega/2 \approx M(w - z) \approx M(1 - z/w)$  and introduced a factor  $\frac{1}{w} \approx 1$ . Since a convolution of the form  $\int \frac{dw}{w} f(w)g(z/w)$  factorizes under a Mellin transform, we conclude that, up to power suppressed terms, our factorization formula implies multiplicative soft-Coulomb factorization of the cross section in Mellin space:

$$\hat{\sigma}_{pp'}(N, \mu) \approx \sum_{S, i, i'} H_{ii'}^S \sum_{R_\alpha} J_{R_\alpha}^S(N) S_{ii'}^{R_\alpha}(N, \mu), \quad (2.85)$$

where the soft function in Mellin space is given by

$$S_{ii'}^{R_\alpha}(N, \mu) = 2M \int_0^1 dz z^{N-1} W_{ii'}^{R_\alpha}(2M(1 - z), \mu) = \int_0^\infty d\omega e^{-\frac{N}{2M}\omega} W_{ii'}^{R_\alpha}(\omega, \mu) + \mathcal{O}(N^{-1}), \quad (2.86)$$

and

$$J_{R_\alpha}^S(N) = \int_0^1 dz z^{N-1} J_{R_\alpha}^S(M(1-z)). \quad (2.87)$$

This shows that previous treatments that put the one-loop Coulomb corrections into the hard function [11] can be extended to include the higher-order Coulomb corrections as well.

### 2.5.5 Invariant mass distribution near threshold

The combination of soft and Coulomb effects for the invariant mass distribution of top-quark and gluino pairs near threshold has been performed in several approximations *assuming* soft-Coulomb factorization [24–26]. We now show that a factorization formula for the differential cross section  $d\sigma/dM_{HH'}$  with  $M_{HH'}^2 = (p_1 + p_2)^2$ , valid for  $M_{HH'}$  near  $2M$ , can be derived from our main result (2.63).

We first introduce the parton luminosity

$$L_{pp'}(\tau, \mu) = \int_0^1 dx_1 dx_2 \delta(x_1 x_2 - \tau) f_{p/N_1}(x_1, \mu) f_{p'/N_2}(x_2, \mu) \quad (2.88)$$

to express the hadron scattering cross section as

$$\sigma_{N_1 N_2 \rightarrow HH' X} = \sum_{p,p'=q,\bar{q},g} \int_{4M^2/s}^1 d\tau L_{pp'}(\tau, \mu) \hat{\sigma}_{pp'}(\tau s, \mu), \quad (2.89)$$

with  $\hat{\sigma}_{pp'}(\tau s, \mu)$  given by (2.63). Next we observe that the argument  $E - \omega/2 = \sqrt{\tau s} - 2M - \omega/2$  of the Coulomb function  $J_{R_\alpha}^S$  in that equation corresponds to the non-relativistic energy of the  $HH'$  pair in the partonic cms frame. In this frame the three momentum of the pair is soft and therefore makes a negligible contribution to the invariant mass, so the relation

$$M_{HH'} = 2M + E - \frac{\omega}{2} + \mathcal{O}(M\beta^4) = \sqrt{\tau s} - \omega/2 + \mathcal{O}(M\beta^4) \quad (2.90)$$

applies. We now change variables from  $\omega$  to  $M_{HH'}$  in (2.63) and interchange the  $\tau$  and (implicit)  $\omega$  integration in (2.89) using

$$\int_{4M^2/s}^1 d\tau \int_0^{2E} d\omega = 2 \int_{2M}^{\sqrt{s}} dM_{HH'} \int_{M_{HH'}^2/s}^1 d\tau \quad (2.91)$$

and the fact that for stable particles, and neglecting bound-state contributions, the Coulomb function has support only for positive values of its argument, which fixes the upper limit  $2E$ . This results in

$$\begin{aligned} \frac{d\sigma_{N_1 N_2 \rightarrow HH' X}}{dM_{HH'}} &= \sum_{p,p'=q,\bar{q},g} \int_{M_{HH'}^2/s}^1 d\tau L_{pp'}(\tau, \mu) \frac{d\hat{\sigma}_{pp'}(\tau s, \mu)}{dM_{HH'}} \\ &= \sum_{p,p'=q,\bar{q},g} \sum_{S=|s-s'|}^{s+s'} \sum_{i,i'} 2H_{ii'}^S(\mu) \sum_{R_\alpha} J_{R_\alpha}^S(M_{HH'} - 2M) \end{aligned}$$

$$\times \int_{M_{HH'}^2/s}^1 d\tau L_{pp'}(\tau, \mu) W_{ii'}^{R_\alpha}(2(\sqrt{\tau s} - M_{HH'}), \mu) \quad (2.92)$$

with

$$\frac{d\hat{\sigma}_{pp'}(\hat{s}, \mu)}{dM_{HH'}} = \sum_{S=|s-s'|}^{s+s'} \sum_{i,i'} 2H_{ii'}^S(\mu) \sum_{R_\alpha} J_{R_\alpha}^S(M_{HH'} - 2M) W_{ii'}^{R_\alpha}(2(\sqrt{\hat{s}} - M_{HH'}), \mu), \quad (2.93)$$

which is the desired result. This shows that Coulomb and soft effects factorize multiplicatively in the invariant mass distribution near threshold, as assumed in [24–26]. Note that in the hadronic cross section only the soft function is averaged with the parton luminosity. Eqs. (2.92), (2.93) apply unmodified to bound-state contributions, in which case the invariant mass distribution extends below the nominal threshold  $2M$ , and unstable particles, where in addition the Coulomb function is evaluated at complex argument  $M_{HH'} - 2M + i(\Gamma_H + \Gamma_{H'})/2$ .

### 3 Resummation of soft and Coulomb gluons

The factorization formula (2.63) provides the basis for resummation of soft and Coulomb gluon effects in the soft function  $W$  and the potential function  $J$ , respectively. The soft gluon resummation is performed by solving evolution equations for the soft and hard functions [27–31], while the resummation of potential effects can be performed using results obtained for top-quark production in electron-positron collisions [76–78]. In this section we provide the explicit results for the resummed soft and potential functions. In section 3.1 we recall the colour basis constructed in [37] that diagonalizes the soft function to all orders in the strong coupling constant and quote the result for the one-loop soft function. In section 3.2 we relate the hard function to the colour- and spin decomposed Born cross section and the colour decomposed one-loop amplitudes at threshold to demonstrate that the implementation of the resummation formula requires only a standard calculation in fixed-order perturbation theory. In section 3.3 we provide the leading order potential function summing up multiple Coulomb gluon exchange, as required for the NLL resummation performed in section 4. In section 3.4 we obtain evolution equations for the short-distance coefficients  $C$  and the soft function  $W$  that allow to resum soft-gluon effects. The anomalous dimensions required up to NNLL have already been collected in [37]. The final result for the resummed cross section using the momentum-space formalism of [31–33] is presented in section 3.5 with the explicit expression of the resummation exponent up to NLL relegated to appendix C. Expansions of the resummed result to order  $\alpha_s$ , as required for the matching to a fixed-order calculation, are given in appendix D.

#### 3.1 The soft function

In the factorization formula (2.63), the hard- and soft function are matrices in colour space in the basis of the tensors  $c^{(i)}$  introduced in (2.14). The soft function can be diagonalized

to all orders in the strong coupling for an arbitrary heavy coloured particle production process using the colour basis constructed in [37]. In this basis, the components of the soft function (2.56) can be expressed in terms of the soft function for a single heavy final state particle in the irreducible colour representation  $R_\alpha$ . This gives a precise meaning to the picture of soft gluon radiation resolving only the total colour charge of a heavy-particle pair at rest [11]. We review this construction here and quote the result of the one-loop soft function.

It is useful to perform a decomposition of the product of the representations of the initial state and final state particles into irreducible representations:

$$r \otimes r' = \sum_{\alpha} r_{\alpha}, \quad R \otimes R' = \sum_{R_{\alpha}} R_{\alpha}. \quad (3.1)$$

It is intuitively clear that a final state pair in an irreducible colour representation  $R_\alpha$  can only be produced from an initial state system in an equivalent representation. In order to implement this picture formally, one forms pairs  $P_i = (r_\alpha, R_\beta)$  of equivalent initial and final state representations  $r_\alpha$  and  $R_\beta$ , treating multiple occurrences of equivalent representations in the decomposition as distinct, e.g. in the case of a symmetric or antisymmetric coupling of  $8 \otimes 8 \rightarrow 8$ . It has been shown in [37] that a basis respecting colour conservation (2.65) can always be chosen by forming for every pair  $P_i$  of equivalent representations the associated basis element

$$c_{\{a\}}^{(i)} = \frac{1}{\sqrt{\dim(r_\alpha)}} C_{\alpha a_1 a_2}^{r_\alpha} C_{\alpha a_3 a_4}^{R_\beta^*}, \quad (3.2)$$

where the  $C_{\alpha a_1 a_2}^{R_\alpha}$  are Clebsch-Gordan coefficients implementing a unitary basis transformation from the basis vectors of the tensor product space  $R \otimes R'$  to basis vectors of the irreducible representations  $R_\alpha$ , and analogously for the initial state representations. The Clebsch-Gordan coefficients, basis elements and projectors for all squark and gluino production processes at hadron colliders have been provided in appendix B of [37]. For squark-antisquark production from quark-antiquark annihilation, the allowed pairs of representations are

$$P_i \in \{(1, 1), (8, 8)\} \quad (3.3)$$

and the basis has been given already in (2.16). For the gluon fusion channel the allowed pairs of representations are

$$P_i \in \{(1, 1), (8_S, 8), (8_R, 8)\} \quad (3.4)$$

and the basis is given in (4.13) below.

Using properties of Wilson lines and the Clebsch-Gordan coefficients it was shown in [37] that the components of the soft function (2.56) in the basis (3.2) can be obtained from the soft function for the production of a *single particle* in the representation  $R_\alpha$

$$\hat{W}_{\{a\alpha, b\beta\}}^{R_\alpha}(z, \mu) \equiv \langle 0 | \overline{\text{T}}[S_{w, \beta\kappa}^{R_\alpha} S_{\bar{n}, j b_2}^\dagger S_{n, i b_1}^\dagger](z) \text{T}[S_{n, a_1 i} S_{\bar{n}, a_2 j} S_{w, \kappa\alpha}^{R_\alpha \dagger}](0) | 0 \rangle \quad (3.5)$$

by contracting with appropriate Clebsch-Gordan coefficients

$$W_{ii'}^{R_\alpha}(\omega, \mu) = \frac{1}{\sqrt{\dim(r_\alpha)\dim(r_{\alpha'})}} \delta_{R_\alpha R_{\beta'}} \delta_{R_\alpha R_\beta} C_{\{a\alpha\}}^{r_\alpha} W_{\{a\alpha, b\beta\}}^{R_\alpha}(\omega, \mu) C_{\{b\beta\}}^{r_{\alpha'}^*}. \quad (3.6)$$

As indicated, the elements are non-vanishing only if the irreducible representation  $R_\alpha$  is identical to both final state representations  $R_\beta$  and  $R_{\beta'}$  in the pairs  $P_i = (r_\alpha, R_\beta)$  and  $P_{i'} = (r_{\alpha'}, R_{\beta'})$  that define the tensors  $c^{(i)}$ ,  $c^{(i')}$ . This is intuitively plausible since we project on a specific final state representation so only production from initial states in an equivalent representation is possible. This shows that the soft function is automatically block diagonal in the basis (3.2) where off-diagonal elements are only possible if several initial state representations  $r_\alpha$  are equivalent. For initial state quarks, antiquarks and gluons this only happens for two gluons in the initial state that can be combined into a symmetric and antisymmetric octet, see (3.4). Using Bose symmetry it is furthermore possible to show that the symmetric and antisymmetric octet production channels do not interfere so the soft function is diagonal, i.e.

$$W_{ii'}^{R_\alpha}(\omega, \mu) = W_i^{R_\alpha}(\omega, \mu) \delta_{ii'} \delta_{R_\alpha R_\beta}. \quad (3.7)$$

The one-loop term in the loop expansion of the soft function,

$$W_i^{R_\alpha}(\omega, \mu) = \sum_{n=0}^{\infty} \left( \frac{\alpha_s(\mu)}{4\pi} \right)^n W_i^{(n)R_\alpha}(\omega, \mu), \quad (3.8)$$

was calculated in [37] and depends only on the quadratic Casimir operators  $C_R$  of the representations of the initial state particles and the final state pair, in agreement with calculations for specific colour representations [7, 17, 20]. The result in position space can be written in terms of the variable  $L = 2 \ln \left( \frac{iz_0 \mu e^{\gamma_E}}{2} \right)$  and is given by

$$\hat{W}_i^{(1)R_\alpha}(L, \mu) = (C_r + C_{r'}) \left( \frac{2}{\epsilon^2} + \frac{2}{\epsilon} L + L^2 + \frac{\pi^2}{6} \right) + 2C_{R_\alpha} \left( \frac{1}{\epsilon} + L + 2 \right), \quad (3.9)$$

where the normalization is such that  $\hat{W}_i^{(0)R_\alpha}(L, \mu) = 1$ . For a final state singlet and a quark-antiquark initial state this agrees with the Drell-Yan Wilson line [29], for a colour octet final state the result agrees with [21]. The Fourier transform of this result enters the factorization formula (2.63) and has been computed in [37]. Since in the momentum space formalism the solution of the renormalization group equation for the soft function is obtained using the Laplace transform of the momentum space soft function that can be obtained from the position space result by a simple replacement rule, the momentum space expression is not explicitly needed in this paper.

### 3.2 The hard function

In order to simplify the application of the factorization formula (2.63) we show how to bypass the matching to the effective theory used in our derivation and express the hard

function (2.60) directly in terms of hard-scattering amplitudes for the production of the heavy-particle pair. The potential and soft functions are universal functions, depending only on the colour quantum numbers. The only process dependent input for NLL resummation are then the colour-separated leading-order production cross sections for the process of interest. For NNLL resummation, in addition the tree cross sections for individual spin states of the heavy-particle pair and the colour separated NLO amplitudes at threshold are required. We work in the colour basis that diagonalizes the soft function and denote the diagonal elements of the hard function by  $H_i^S$ .

We recall that the  $S$ -wave matching coefficients  $C_{\{\alpha\}}^{(0,i)}$  are simply given by the scattering amplitudes at threshold, with polarization vectors removed and projected on a specific colour channel according to  $\mathcal{A}_{\{\alpha\}} = \sum_i c_{\{\alpha\}}^{(i)} \mathcal{A}^{(i)}$ . Thus the scattering amplitude for a given colour configuration and fixed helicities and spins  $\lambda_i$  can be written as

$$\mathcal{A}^{(i)}(p^{\lambda_1} p'^{\lambda_2} \rightarrow H^{\lambda_3} H'^{\lambda_4}) = 2\sqrt{m_H m_{H'}} C_{\{\alpha\}}^{(0,i)}(\mu) \chi_{\alpha_1}^{\lambda_1} \chi_{\alpha_2}^{\lambda_2} \xi_{\alpha_3}^{\lambda_3*} \xi_{\alpha_4}^{\lambda_4*}, \quad (3.10)$$

where we have accounted for the normalization factors  $\sqrt{2m_H}$  in the definition of the non-relativistic states. Here the  $\xi$  are the polarization spinors or vectors of the non-relativistic particles satisfying the completeness relation

$$\sum_{\lambda} \xi_{\alpha}^{\lambda} \xi_{\beta}^{\lambda*} = \delta_{\alpha\beta}. \quad (3.11)$$

Computing the spin averaged partonic tree cross section for the production of a heavy-particle pair in a fixed colour state using the expression of the amplitude in the effective theory (3.10) we obtain

$$\begin{aligned} \hat{\sigma}_{pp'}^{(0,i)}(\hat{s}) &= \frac{1}{2\hat{s}} \frac{\lambda^{1/2}(\hat{s}, m_H^2, m_{H'}^2)}{8\pi\hat{s}} \frac{1}{4D_r D_{r'}} \sum_{\text{pol}} |\mathcal{A}_{\text{Born}}^{(i)}(pp' \rightarrow HH')|^2 \\ &\underset{\hat{s} \rightarrow 4M^2}{\approx} \frac{(m_H m_{H'})^{3/2}}{M} \frac{\beta}{4\pi\hat{s}} \frac{1}{4D_r D_{r'}} \sum_{\lambda_i} (C_{\{\alpha\}}^{(0,i)}(\mu) \chi_{\alpha_1}^{\lambda_1} \chi_{\alpha_2}^{\lambda_2}) \delta_{\alpha_3\beta_3} \delta_{\alpha_4\beta_4} (C_{\{\beta\}}^{(0,i)}(\mu) \chi_{\beta_1}^{\lambda_1} \chi_{\beta_2}^{\lambda_2})^*. \end{aligned} \quad (3.12)$$

In the second line we have approximated the prefactor using  $\lambda(\hat{s}, m_H^2, m_{H'}^2) = (\hat{s} - 4M^2)(\hat{s} - (m_H - m_{H'})^2) \approx (\hat{s} - 4M^2)4m_H m_{H'}$  and the  $C_{\{\alpha\}}^{(0,i)}(\mu)$  should be computed in the tree approximation. Comparing to the definition of the hard function (2.60), we obtain a simple relation between the leading order hard functions and the spin averaged total cross section for a given colour channel:

$$\hat{\sigma}_{pp'}^{(0,i)}(\hat{s}) \underset{\hat{s} \rightarrow 4M^2}{\approx} \frac{(m_H m_{H'})^{3/2}}{M} \frac{\beta}{2\pi} H_{ii}^{(0)}. \quad (3.13)$$

The tree-level hard functions can therefore be obtained from the threshold limit of the Born cross sections in a specific colour channel. With the aim of extending the validity of the resummed expressions one may consider defining an improved hard function by using



full tree-level cross section instead of its threshold limit. In this way, some higher order terms in  $\beta$  are included, though not systematically.

At NNLL spin-dependent hard functions are required in the tree approximation, which can be obtained by a formula analogous to (3.13) from the cross section for a fixed colour and spin channel. In the framework of a standard computation of the leading order cross section, the projection on the final-state spin can be performed introducing scattering amplitudes for a fixed final state spin  $S$  that can be obtained from the helicity amplitudes for the production of the  $HH'$  pair according to

$$\mathcal{A}^{(i)}(p^{\lambda_1} p'^{\lambda_2} \rightarrow (HH')^{S,\lambda}) = \sum_{\lambda_3 \lambda_4} N_S(\lambda|\lambda_3 \lambda_4) \mathcal{A}^{(i)}(p^{\lambda_1} p'^{\lambda_2} \rightarrow H^{\lambda_3} H'^{\lambda_4}). \quad (3.14)$$

The  $N_S(\lambda|\lambda_3 \lambda_4)$  are Clebsch-Gordan coefficients that can be found for the case of spin one-half particles, e.g. in [79].

Furthermore, at NNLL accuracy also the one-loop hard function is required. Since the spin-dependence of the potential function is already an  $\mathcal{O}(\alpha_s^2)$  effect, one may use the spin summed one-loop hard functions  $H_i^{(1)}$  at NNLL without formal loss of accuracy. The one-loop hard function is given by the interference of the Born and the one-loop amplitudes for a given colour channel, evaluated directly at threshold:

$$\begin{aligned} H_i^{(1)}(\mu) &= \frac{1}{2\hat{s}} \left[ N_{\alpha_1 \beta_1}^p N_{\alpha_2 \beta_2}^{p'} 2\text{Re} (C_{\alpha_1 \alpha_2 \gamma \delta}^{(0,i)1\text{-loop}}(\mu) C_{\beta_1 \beta_2 \gamma \delta}^{(0,i)\text{tree}*}(\mu)) \right] \\ &= \frac{1}{8m_H m_{H'} \hat{s}} \frac{1}{4D_r D_{r'}} \sum_{\text{pol}} 2\text{Re} \left( \mathcal{A}_{\text{Born}}^{(i)*}(pp' \rightarrow HH') \mathcal{A}_{\text{NLO}}^{(i)}(pp' \rightarrow HH') \right). \end{aligned} \quad (3.15)$$

Here  $\mathcal{A}_{\text{NLO}}$  is the UV-renormalized one-loop amplitude evaluated directly at threshold with IR singularities regularized dimensionally and subtracted in the  $\overline{\text{MS}}$ -scheme. This is therefore the only process independent input required for NNLL resummations and is far simpler to compute than the full NLO cross section. Alternatively, the hard function can be extracted from the threshold expansion of the NLO partonic cross sections in each colour channel [45]. These are available for  $t\bar{t}$  production at hadron colliders [80] but not yet for the production of squarks or gluinos.

### 3.3 The potential function

We now discuss the relation of the potential function  $J$  to the Coulomb Green function familiar from PNRQCD. The momentum-space potential function (2.59) can be written in terms of the correlation function

$$\begin{aligned} J_{\{a\}}^{\{\alpha\}}(q) &= \int d^4 z e^{iq \cdot z} \int d\Phi_1 d\Phi_2 \sum_{\text{pol, colour}} \langle 0 | [\psi_{a_2 \alpha_2}'^{(0)} \psi_{a_1 \alpha_1}^{(0)}](z) | HH' \rangle \langle HH' | [\psi_{a_3 \alpha_3}^{(0)\dagger} \psi_{a_4 \alpha_2}'^{(0)\dagger}](0) | 0 \rangle \\ &= \int d^4 z e^{iq \cdot z} \langle 0 | [\psi_{a_2 \alpha_2}'^{(0)} \psi_{a_1 \alpha_1}^{(0)}](z) [\psi_{a_3 \alpha_3}^{(0)\dagger} \psi_{a_4 \alpha_2}'^{(0)\dagger}](0) | 0 \rangle, \end{aligned} \quad (3.16)$$

where the matrix elements are evaluated with the leading order PNRQCD Lagrangian.<sup>9</sup> In the second line we used that in this approximation the soft gluon fields are decoupled from the fields  $\psi^{(0)}$  so we can replace the sum over the two-particle Hilbert space by a sum over the full Hilbert space and use the completeness relation. The definition of  $J$  given here is sufficient for  $S$ -wave production of the heavy particles; for  $P$ -wave production also expectation values of fields with derivatives have to be considered. As explained in section 2.5.2, effects of the  $\vec{x} \cdot \vec{E}$  vertex in the sub-leading PNRQCD Lagrangian are not included in the calculation of the potential function  $J$  at higher orders but lead to additional contributions to the factorization formula with generalized soft and potential functions, to be calculated with the leading effective Lagrangians. As shown in section 2.5.2 these terms are only relevant for the total cross section beyond the NNLL order.

Defining a tensor product notation for the decoupled potential fields,

$$(\psi \otimes \psi')_{a_1 a_2}(t, \vec{r}, \vec{R}) = \psi_{a_1}^{(0)}(t, \vec{R} + \frac{\vec{r}}{2}) \psi_{a_2}'^{(0)}(t, \vec{R} - \frac{\vec{r}}{2}), \quad (3.17)$$

with the relative coordinates  $r$  and the cms coordinates  $R$  and using the projectors onto the irreducible representations  $R_\alpha$  introduced in (2.46), we can perform the colour decomposition

$$(\psi \otimes \psi')_{a_1 a_2} = \sum_{R_\alpha} P_{\{a\}}^{R_\alpha} (\psi \otimes \psi')_{a_3 a_4} \equiv \sum_{R_\alpha} (\psi \otimes \psi')_{a_1 a_2}^{R_\alpha}. \quad (3.18)$$

This is analogous to the singlet-octet decomposition discussed in [67] (see also [81], in particular eq. (48)). With this notation, the colour structure of the Coulomb potential simplifies to

$$\begin{aligned} [\psi^{(0)\dagger} \mathbf{T}^{(R)a} \psi^{(0)}] [\psi'^{(0)\dagger} \mathbf{T}^{(R')a} \psi'^{(0)}] &= \sum_{R_\alpha, R_\beta} (\psi'^{\dagger} \otimes \psi^{\dagger})_{b_4 b_3} P_{\{b\}}^{R_\beta} \mathbf{T}_{b_1 a_1}^{(R)b} \mathbf{T}_{b_2 a_2}^{(R')b} P_{\{a\}}^{R_\alpha} (\psi \otimes \psi')_{a_3 a_4} \\ &= \sum_{R_\alpha} (\psi \otimes \psi')^{R_\alpha \dagger} D_{R_\alpha} (\psi \otimes \psi')^{R_\alpha}. \end{aligned} \quad (3.19)$$

Here the coefficients of the Coulomb potential are defined by the relation

$$\mathbf{T}_{a_1 c_1}^{(R)b} \mathbf{T}_{a_2 c_2}^{(R')b} P_{c_1 c_2 a_3 a_4}^{R_\alpha} = D_{R_\alpha} P_{\{a\}}^{R_\alpha} \quad (3.20)$$

and we have used the projection property

$$P_{a_1 a_2 b_1 b_2}^{R_\alpha} P_{b_1 b_2 c_1 c_2}^{R_\beta} = \delta_{R_\alpha R_\beta} P_{a_1 a_2 c_1 c_2}^{R_\alpha}. \quad (3.21)$$

Using the simplification of the Coulomb potential, the leading order PNRQCD Lagrangian for the decoupled fields can be written in the tensor-product notation as a sum

---

<sup>9</sup>As discussed in section 2.5, to reach NNLL accuracy, the LO Lagrangian is to be supplemented by NLO Coulomb and the leading non-Coulomb potentials.

over the irreducible colour representations,

$$\begin{aligned} \mathcal{L}_{\text{PNRQCD}} = \sum_{R_\alpha} \left\{ (\psi \otimes \psi')^{R_\alpha \dagger} \left( i\partial_s^0 + \frac{\vec{\partial}_r^2}{2m_{\text{red}}^2} + \frac{\vec{\partial}_R^2}{2(2M)^2} \right) (\psi \otimes \psi')^{R_\alpha} \right. \\ \left. + \int d^3\vec{r} [(\psi \otimes \psi')^{R_\alpha \dagger}(t, -\vec{r}/2, 0)] \left( \frac{\alpha_s D_{R_\alpha}}{r} \right) [(\psi \otimes \psi')^{R_\alpha}(t, \vec{r}/2, 0)] \right\}, \end{aligned} \quad (3.22)$$

with the reduced mass  $m_{\text{red}} = m_H m_{H'}/(m_H + m_{H'})$ . The kinetic term can be written in terms of the tensor field as shown here after a projection on the two-particle sector of the theory [67, 81].

For top-antitop and squark-antisquark production the irreducible representations are given by  $3 \otimes \bar{3} = 1 \oplus 8$  and the coefficients are familiar from quarkonium physics (recall our sign convention for the Coulomb potential):

$$\begin{aligned} D_1 = -C_F = -\frac{N_C^2 - 1}{2N_C} \quad (\text{attractive}), \\ D_8 = -\left[ C_F - \frac{C_A}{2} \right] = \frac{1}{2N_C} \quad (\text{repulsive}). \end{aligned} \quad (3.23)$$

The explicit values of the coefficients for all remaining representations relevant for the production of coloured SUSY particles are collected in appendix B.

Since the Lagrangian is now diagonal in colour and spin, the leading-order Coulomb Green function is of the form

$$J_{\{a\}}^{\{\alpha\}}(q) = \sum_{R_\alpha} P_{\{a\}}^{R_\alpha} \delta_{\alpha_1 \alpha_3} \delta_{\alpha_2 \alpha_4} J^{R_\alpha}(q) \quad (3.24)$$

with the correlation function

$$J^{R_\alpha}(q) = \int d^4z e^{iq \cdot z} \langle 0 | [\psi'^{(0)} \psi^{(0)}](z) [\psi^{(0)\dagger} \psi'^{(0)\dagger}](0) | 0 \rangle. \quad (3.25)$$

In this expression the fields carry no colour and spin indices any more and the correlation functions are to be calculated with the term in (3.22) corresponding to the representation  $R_\alpha$  with Coulomb potential  $\alpha_s D_{R_\alpha}/r$ . Since the annihilation fields  $\psi$  annihilate the vacuum, we can replace  $(\psi \psi')(z) (\psi^\dagger \psi'^\dagger)(0) = [(\psi \psi')(z), (\psi^\dagger \psi'^\dagger)(0)]$  in the vacuum expectation value and express the correlation function in terms of the imaginary part of a time ordered product

$$\begin{aligned} J^{R_\alpha}(q) &= \int d^4z e^{iq \cdot z} 2 \text{Im} \langle 0 | \text{T}[\psi'^{(0)} \psi^{(0)}](z) [\psi^{(0)\dagger} \psi'^{(0)\dagger}](0) | 0 \rangle \\ &= 2 \text{Im} G_C^{R_\alpha(0)}(0, 0; E). \end{aligned} \quad (3.26)$$

Here we introduced the zero-distance Coulomb Green function of the Schrödinger operator  $-\vec{\nabla}^2/(2m_{\text{red}}) - (-D_{R_\alpha})\alpha_s/r$ , i.e. the Green function  $G_C^{R_\alpha(0)}(\vec{r}_1, \vec{r}_2; E)$  evaluated at  $\vec{r}_1 = \vec{r}_2 = 0$ .

Using the representation of the Green function given in [82], the  $\overline{\text{MS}}$ -subtracted zero-distance Coulomb Green function including all-order gluon exchange, reads as follows [70]:

$$G_C^{R_\alpha(0)}(0, 0; E) = -\frac{(2m_{\text{red}})^2}{4\pi} \left\{ \sqrt{-\frac{E}{2m_{\text{red}}}} + (-D_{R_\alpha})\alpha_s \left[ \frac{1}{2} \ln \left( -\frac{8m_{\text{red}}E}{\mu^2} \right) - \frac{1}{2} + \gamma_E + \psi \left( 1 - \frac{(-D_{R_\alpha})\alpha_s}{2\sqrt{-E/(2m_{\text{red}})}} \right) \right] \right\}. \quad (3.27)$$

Here  $\gamma_E$  is the Euler-Mascheroni constant and one should apply the prescription  $E \rightarrow E + i\delta$  for stable heavy particles and  $E \rightarrow E + i(\Gamma_H + \Gamma_{H'})/2$  for unstable ones.

For positive values of  $E$  the potential function evaluates to the Sommerfeld factor

$$J_{R_\alpha}(E) = \frac{(2m_{\text{red}})^2 \pi D_{R_\alpha} \alpha_s}{2\pi} \left( e^{\pi D_{R_\alpha} \alpha_s \sqrt{\frac{2m_{\text{red}}}{E}}} - 1 \right)^{-1} \quad E > 0. \quad (3.28)$$

If the potential is attractive,  $D_{R_\alpha} < 0$ , there is a sum of bound states below threshold given by

$$J_{R_\alpha}^{\text{bound}}(E) = 2 \sum_{n=1}^{\infty} \delta(E - E_n) \left( \frac{2m_{\text{red}}(-D_{R_\alpha})\alpha_s}{2n} \right)^3 \quad E < 0 \quad (3.29)$$

with bound-state energies

$$E_n = -\frac{2m_{\text{red}}\alpha_s^2 D_{R_\alpha}^2}{4n^2}. \quad (3.30)$$

A series representation of the imaginary part of the Coulomb Green function for finite widths and arbitrary energies can be found in [23].

The above results suffice for resummation with NLL accuracy as performed in section 4. For NNLL accuracy in the counting (2.7) one has to resum in addition all  $\alpha_s \times (\alpha_s/\beta)^n$  corrections as well as the non-relativistic logarithms of the form  $\alpha_s^2 \ln \beta$ ,  $\alpha_s^3 \ln^2 \beta$ ,  $\dots$ . The fixed-order NNLO corrections of this form have been obtained in [45]. An analytical result resumming all  $\alpha_s \times (\alpha_s/\beta)^n$  terms was obtained in [76] and is quoted e.g. in [25]. Resummation of the non-relativistic logarithms requires the generalization of results for top-quark pair production obtained e.g. in [83, 84] to arbitrary colour representations.

### 3.4 Evolution equations of hard and soft functions

In the momentum-space approach to threshold resummation one calculates the short-distance coefficients  $C^{(i)}(\mu)$  at a hard scale  $\mu_h \sim 2M$  and the soft function  $W(\omega, \mu)$  at a soft scale of the order of  $\mu_s \sim M\beta^2$ . Threshold logarithms  $\log \beta$  are resummed by using evolution equations to evolve both functions to an intermediate factorization scale  $\mu_f$ . In this subsection we will provide these evolution equations in the colour basis (3.2) that diagonalizes the soft function. In this case the structure of the evolution equations is similar to those in the Drell-Yan process [33, 35] and the complications of matrix-valued anomalous

dimensions depending on the kinematics [7, 36] are avoided. The resummed cross section obtained from solving the equations is given in 3.5.

The evolution equation of the hard coefficients has been obtained in [37] from the results of [38] for the IR structure of general massive QCD amplitudes:

$$\frac{d}{d \ln \mu} C_{\{\alpha\}}^{(i)}(\mu) = \left( \frac{1}{2} \gamma_{\text{cusp}} \left[ (C_r + C_{r'}) \left( \ln \left( \frac{4M^2}{\mu^2} \right) - i\pi \right) + i\pi C_{R_\alpha} \right] + \gamma_i^V \right) C_{\{\alpha\}}^{(i)}(\mu). \quad (3.31)$$

Here Casimir scaling was used to write the cusp anomalous dimension for a massless parton in the representation  $r$  in the form  $\Gamma_{\text{cusp}}^r = C_r \gamma_{\text{cusp}}$  which holds at least up to the three-loop order. At least up to the two-loop level the anomalous dimension  $\gamma_i^V$  can be written in terms of single-particle anomalous dimensions:

$$\gamma_i^V = \gamma^r + \gamma^{r'} + \gamma_{H,s}^{R_\alpha}. \quad (3.32)$$

The anomalous dimension  $\gamma_{H,s}^{R_\alpha}$  is related to a massive particle in the final state representation  $R_\alpha$  in the pair  $P_i = (r'_\alpha, R_\alpha)$  defining the colour basis element  $c^{(i)}$  with index  $i$ . While the one- and two-loop anomalous-dimension coefficients  $\gamma^r$  of massless quarks and gluons have been available for some time, the two-loop results for the heavy particle soft anomalous dimension  $\gamma_{H,s}^{R_\alpha}$  have become available only recently [37, 41]. The one-loop coefficients of the cusp and soft anomalous dimensions are simply  $\gamma_{\text{cusp}}^{(0)} = 4$  and  $\gamma_{H,s}^{R_\alpha(0)} = -2C_{R_\alpha}$ . The anomalous dimensions  $\gamma^r$  related to the light partons do not obey Casimir scaling already at one loop. The explicit one- and two-loop results for all remaining anomalous dimensions appearing in this section are available in the literature and have been collected in [37]. We observe that, as noted for the production of a colour octet final state particle in [21], the imaginary part in the evolution equation (3.31) can not simply be absorbed in the argument of the logarithm by the continuation  $M^2 \rightarrow -(M^2 + i0)$  which complicates the resummation of “ $\pi^2$ -enhanced” terms compared to colour singlet final states as in Higgs production [34, 35]. We will not consider such a resummation of constant terms here. The evolution equation of the hard-functions is obtained from (3.31) as

$$\frac{d}{d \ln \mu} H_i^S(\mu) = \left( \gamma_{\text{cusp}} (C_r + C_{r'}) \ln \left( \frac{4M^2}{\mu^2} \right) + 2\gamma_i^V \right) H_i^S(\mu). \quad (3.33)$$

As discussed in [37] and section 2.5.2, starting from the two-loop order there are IR divergent contributions to the short-distance coefficients that are related to UV divergences of insertions of the non-Coulomb PNRQCD potentials in the extended factorization formula (2.66). These divergences cause additional scale dependence, not included in (3.33), which is cancelled by a non-trivial scale-dependence of the potential function including the non-Coulomb potential insertions. The factorization scale dependence in the separation of  $H$  and  $J$  is related to additional non-relativistic  $\log \beta$  terms of the NNLL order. Since in this paper we do not consider the resummation of these non-relativistic logarithms, in order to obtain the evolution equation of the soft function, these contributions to the scale

dependence of the hard function have to be dropped as done in (3.33). Beyond NNLL further complications can arise from the structure of the extended factorization formula (2.66) including terms with higher-dimensional soft functions, but the discussion of resummation beyond NNLL is beyond the scope of this paper.

The evolution equation of the soft function can be obtained from that of the hard function using the factorization scale independence of the hadronic cross section. Consistent with our discussion above, we consider the potential function to be scale independent which is appropriate for the NLO potential function quoted in [25]. Scale invariance of the total cross section and the known factorization scale dependence of the PDFs implies the evolution equation of the partonic cross section

$$\frac{d}{d \ln \mu} \hat{\sigma}_{pp'}(z, \mu) = - \sum_{\tilde{p}, \tilde{p}'} \int_z^1 \frac{dx}{x} (P_{p/\tilde{p}}(x) + P_{p'/\tilde{p}'}(x)) \hat{\sigma}_{\tilde{p}\tilde{p}'}(z/x, \mu), \quad (3.34)$$

where  $P_{p/\tilde{p}}(x)$  are the Altarelli-Parisi splitting functions for the splitting of a parton  $p$  into a parton  $\tilde{p}$ . Consistent with the derivation of the factorization formula in section 2 from the on-shell scattering process  $pp' \rightarrow HH'X$  at production threshold, we use the  $x \rightarrow 1$  limit of the splitting functions for a parton  $p$  in the colour representation  $r$ ,

$$P_{p/\tilde{p}}(x) = \left( 2\Gamma_{\text{cusp}}^r(\alpha_s) \frac{1}{[1-x]_+} + 2\gamma^{\phi,r}(\alpha_s) \delta(1-x) \right) \delta_{p\tilde{p}} + \mathcal{O}(1-x). \quad (3.35)$$

As discussed in section 2.5.2, subleading collinear terms could potentially be enhanced by the Coulomb singularity, so care in dropping higher order corrections in equations like this is required. In the present case, however, the corrections to (3.35) are of the order  $1-z = \beta^2$  so they are not relevant at NNLL accuracy. We recall the property of the plus distribution,

$$\int_z^1 dx f(x) \left[ \frac{1}{(1-x)} \right]_+ = \int_z^1 dx \frac{f(x) - f(1)}{(1-x)} - \int_0^z dx \frac{f(1)}{(1-x)}. \quad (3.36)$$

Inserting the factorized form of the partonic cross section into (3.34) and making use of the evolution equation of the short-distance coefficients (3.31) leads to an evolution equation of the soft function. Using the relations  $\hat{s} \approx 4M^2$ ,  $(1-z/x) \approx (1-z) - (1-x)$  valid in the  $x \rightarrow 1$ ,  $z \rightarrow 1$  limits and introducing the variable  $\omega = 4M(1-x)$ , the resulting equation can be written in the same form as the equation found for the Drell-Yan process [33]:

$$\begin{aligned} \frac{d}{d \ln \mu} W_i^{R\alpha}(\omega, \mu) = & -2 \left[ \left( \Gamma_{\text{cusp}}^r + \Gamma_{\text{cusp}}^{r'} \right) \ln \left( \frac{\omega}{\mu} \right) + 2\gamma_{W,i}^{R\alpha} \right] W_i^{R\alpha}(\omega, \mu) \\ & - 2 \left( \Gamma_{\text{cusp}}^r + \Gamma_{\text{cusp}}^{r'} \right) \int_0^\omega d\omega' \frac{W_i^{R\alpha}(\omega', \mu) - W_i^{R\alpha}(\omega, \mu)}{\omega - \omega'}, \end{aligned} \quad (3.37)$$

with the anomalous-dimension coefficient

$$\gamma_{W,i}^{R\alpha} = \gamma_i^V + \gamma^{\phi,r} + \gamma^{\phi,r'}. \quad (3.38)$$

These results hold for the colour basis (3.2) that diagonalizes the soft function to all orders [37], where only the diagonal elements  $W_i = W_{ii}$  of the soft function have to be considered. Analogously to the anomalous dimension  $\gamma_i^V$  of the hard function (3.32), at least up to the two-loop level the anomalous-dimension coefficient of the soft function (3.38) can be written in terms of separate single-particle contributions

$$\gamma_{W,i}^{R_\alpha} = \gamma_{H,s}^{R_\alpha} + \gamma_s^r + \gamma_s^{r'} \quad (3.39)$$

with

$$\gamma_s^r = \gamma^r + \gamma^{\phi,r}. \quad (3.40)$$

The anomalous-dimension coefficients  $\gamma_s^r$  vanish at one-loop level so that  $\gamma_{W,i}^{R_\alpha(0)} = \gamma_{H,s}^{R_\alpha(0)} = -2C_{R_\alpha}$ . Taking the Fourier transform of the evolution equation of the position space soft function given in (3.30) of [37] one obtains the momentum-space evolution equation quoted in (3.37). In order to obtain this result, the logarithmic term multiplied by  $\Gamma_{\text{cusp}}$  has to be treated with care, for instance by writing  $\ln x = \lim_{\epsilon \rightarrow 0} \frac{1}{\epsilon}(1 - x^{-\epsilon})$  (see also [28]).

The terms proportional to the cusp anomalous dimensions in the evolution equations are related to the resummation of double logarithms  $\ln^2 \beta$ , while the coefficients  $\gamma_i^V$  and  $\gamma_{W,i}^{R_\alpha}$  are related to single logarithms. For LL summation one needs the one-loop cusp anomalous dimension while all other quantities enter at LO. For an NLL resummation the required ingredients are the two-loop cusp anomalous dimensions and the one-loop anomalous dimensions  $\gamma_i^V$  and  $\gamma_{W,i}^{R_\alpha}$ . For a NNLL resummation one needs in addition to the three-loop cusp anomalous dimensions and the two-loop anomalous dimensions, the one-loop soft function (3.9) and the one-loop hard function (3.15).

### 3.5 Resummed cross section

As mentioned in the beginning of section 3.4, the resummation of soft-gluon corrections in the approach of [31–33] is performed by calculating the hard and soft functions at scales  $\mu_h$  and  $\mu_s$  that minimize the radiative corrections to these quantities and subsequently using the renormalization group equations (3.33) and (3.37) to evolve to a common scale  $\mu_f$  to compute the partonic cross section (2.63) and perform the convolution with the PDFs evaluated at the same scale (see figure 1).

Since we have determined a colour basis that diagonalizes the soft function to all orders in perturbation theory for all hadron collider processes of interest, the evolution equations have the same form as those for the Drell-Yan process [33]. The resummed hard function solving the evolution equation (3.33) is given by

$$H_i^S(\mu) = \exp[4S(\mu_h, \mu) - 2a_i^V(\mu_h, \mu)] \left( \frac{4M^2}{\mu_h^2} \right)^{-2a_\Gamma(\mu_h, \mu)} H_i^S(\mu_h), \quad (3.41)$$

with the functions  $S$ ,  $a_i^V$  and  $a_\Gamma$  defined as [33]

$$S(\mu_h, \mu) = - \int_{\alpha_s(\mu_h)}^{\alpha_s(\mu)} d\alpha_s \frac{\Gamma_{\text{cusp}}^r(\alpha_s) + \Gamma_{\text{cusp}}^{r'}(\alpha_s)}{2\beta(\alpha_s)} \int_{\alpha_s(\mu_h)}^{\alpha_s} \frac{d\alpha'_s}{\beta(\alpha'_s)},$$

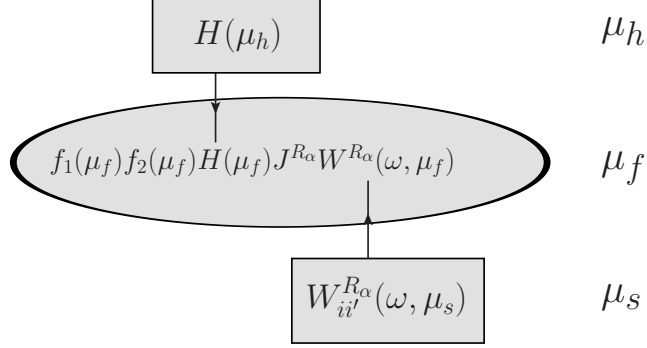


Figure 1: Sketch of the resummation of soft gluon corrections using RGEs.

$$\begin{aligned}
a_\Gamma(\mu_h, \mu) &= - \int_{\alpha_s(\mu_h)}^{\alpha_s(\mu)} d\alpha_s \frac{\Gamma_{\text{cusp}}^r(\alpha_s) + \Gamma_{\text{cusp}}^{r'}(\alpha_s)}{2\beta(\alpha_s)}, \\
a_i^V(\mu_h, \mu) &= - \int_{\alpha_s(\mu_h)}^{\alpha_s(\mu)} d\alpha_s \frac{\gamma_i^V(\alpha_s)}{\beta(\alpha_s)}.
\end{aligned} \tag{3.42}$$

Here  $\alpha_s(\mu)$  represents the QCD coupling in the  $\overline{\text{MS}}$  scheme and  $\beta(\alpha_s)$  the corresponding  $\beta$ -function. Explicit results for the functions  $\beta$ ,  $a_\Gamma$  and the Sudakov exponent  $S$  up to the NLL order as needed for section 4 are collected in appendix C; expressions up to the N<sup>3</sup>LL order can be found in [33].

The evolution equation of the soft function (3.37) can be solved in momentum space [31, 32] by introducing the Laplace-transform with respect to the variable  $s = 1/(e^{\gamma_E} \mu e^{\rho/2})$ ,

$$\tilde{s}_i^{R_\alpha}(\rho, \mu) = \int_{0_-}^{\infty} d\omega e^{-s\omega} \overline{W}_i^{R_\alpha}(\omega, \mu), \tag{3.43}$$

where we have defined the  $\overline{\text{MS}}$ -renormalized soft function  $\overline{W}_i^{R_\alpha}$ . In practice, it is not necessary to perform the Laplace transform explicitly, since the soft function in position space  $\hat{W}_i^{R_\alpha}(z_0, \mu)$  depends on the arguments solely through the combination [28, 29]

$$\frac{iz_0 \mu e^{\gamma_E}}{2} \equiv e^{L/2}. \tag{3.44}$$

It is then easy to see that the function  $\tilde{s}_i^{R_\alpha}(\rho)$  is obtained by simply replacing  $L \rightarrow -\rho$  in the  $\overline{\text{MS}}$ -renormalized result for the soft function in position space. From the results of the tree-level and one-loop soft function in the diagonal basis (3.2) quoted in (3.9) we obtain, discarding the  $1/\epsilon$  poles due to the  $\overline{\text{MS}}$  subtraction,

$$\tilde{s}_i^{(0)R_\alpha}(\rho, \mu) = 1, \tag{3.45}$$

$$\tilde{s}_i^{(1)R_\alpha}(\rho, \mu) = (C_r + C_{r'}) \left( \rho^2 + \frac{\pi^2}{6} \right) - 2C_{R_\alpha}(\rho - 2). \tag{3.46}$$



The resummed soft function can be written in terms of the Laplace transform with the argument  $\rho$  replaced by the derivative with respect to an auxiliary variable  $\eta$  that is set to  $\eta = 2a_\Gamma(\mu_s, \mu)$  after performing the derivatives:

$$W_i^{R_\alpha, \text{res}}(\omega, \mu) = \exp[-4S(\mu_s, \mu) + 2a_{W_i}^{R_\alpha}(\mu_s, \mu)] \tilde{s}_i^{R_\alpha}(\partial_\eta, \mu_s) \frac{1}{\omega} \left(\frac{\omega}{\mu_s}\right)^{2\eta} \theta(\omega) \frac{e^{-2\gamma_E \eta}}{\Gamma(2\eta)}. \quad (3.47)$$

Here the functions  $a_{W_i}^{R_\alpha}$  are defined in analogy to the functions (3.42) with the obvious replacement of the anomalous dimensions  $\gamma_i^V \rightarrow \gamma_{W_i}^{R_\alpha}$ . For  $\eta < 0$  the solution (3.47) should be understood in the distributional sense [32] as will be discussed below. The evolution equation of the soft function (3.37) can also be solved in Mellin moment space [29] and the standard resummation formula in Mellin space is reproduced. The precise relation between the quantities in the momentum space approach to resummation and the Mellin moment space formalism is discussed in [32, 33, 35, 37].

Using the solutions of the RGEs to evolve the hard and soft function in the factorized expression for the partonic cross section (2.63) to the common factorization scale  $\mu_f$  we obtain the result for the resummed cross section

$$\begin{aligned} \hat{\sigma}_{pp'}^{\text{res}}(\hat{s}, \mu_f) &= \sum_{S=|s-s'|}^{s+s'} \sum_i H_i^S(\mu_h) U_i(M, \mu_h, \mu_s, \mu_f) \left(\frac{2M}{\mu_s}\right)^{-2\eta} \\ &\quad \times \tilde{s}_i^{R_\alpha}(\partial_\eta, \mu_s) \frac{e^{-2\gamma_E \eta}}{\Gamma(2\eta)} \int_0^\infty d\omega \frac{J_{R_\alpha}^S(E - \frac{\omega}{2})}{\omega} \left(\frac{\omega}{\mu_s}\right)^{2\eta} \\ &= \sum_{S=|s-s'|}^{s+s'} \sum_i H_i^S(\mu_h) U_i(M, \mu_h, \mu_s, \mu_f) \\ &\quad \times \int_0^\infty d\omega \frac{J_{R_\alpha}^S(E - \frac{\omega}{2})}{\omega} \left(\frac{\omega}{2M}\right)^{2\eta} \tilde{s}_i^{R_\alpha} \left(2 \ln \left(\frac{\omega}{\mu_s}\right) + \partial_\eta, \mu_s\right) \frac{e^{-2\gamma_E \eta}}{\Gamma(2\eta)}, \end{aligned} \quad (3.48)$$

where we have defined the evolution function

$$\begin{aligned} U_i(M, \mu_h, \mu_f, \mu_s) &= \left(\frac{4M^2}{\mu_h^2}\right)^{-2a_\Gamma(\mu_h, \mu_s)} \left(\frac{\mu_h^2}{\mu_s^2}\right)^\eta \times \exp \left[4(S(\mu_h, \mu_f) - S(\mu_s, \mu_f))\right. \\ &\quad \left. - 2a_i^V(\mu_h, \mu_s) + 2a^{\phi, r}(\mu_s, \mu_f) + 2a^{\phi, r'}(\mu_s, \mu_f)\right] \end{aligned} \quad (3.49)$$

and now  $\eta = 2a_\Gamma(\mu_s, \mu_f)$ . The sum over the final state representations  $R_\alpha$  in the factorization formula (2.63) has disappeared in the colour basis (3.2) since there is a unique final state representation for each term in the sum over  $i$  (see the expression (3.7) for the diagonal soft function). The evolution function  $U_i$  has been simplified using the identity

$$a_\Gamma(\mu_h, \mu_f) + a_\Gamma(\mu_f, \mu_s) = a_\Gamma(\mu_h, \mu_s). \quad (3.50)$$

It could be further simplified using the identity [32]

$$S(\mu_h, \mu_f) - S(\mu_s, \mu_f) = S(\mu_h, \mu_s) - a_\Gamma(\mu_s, \mu_f) \ln \frac{\mu_h}{\mu_s} \quad (3.51)$$

to obtain

$$U_i(M, \mu_h, \mu_f, \mu_s) = \left( \frac{4M^2}{\mu_h^2} \right)^{-2a_\Gamma(\mu_h, \mu_s)} \times \exp \left[ 4S(\mu_h, \mu_s) - 2a_i^V(\mu_h, \mu_s) + 2a^{\phi, r}(\mu_s, \mu_f) + 2a^{\phi, r'}(\mu_s, \mu_f) \right], \quad (3.52)$$

which makes it clear that the  $\mu_f$  dependence is related to the parton density functions. Eq. (3.51) is formally satisfied at whatever N<sup>k</sup>LL accuracy employed, but not strictly valid in an expansion in the strong coupling since  $S$  and  $a_\Gamma$  are evaluated at different orders. In the numerical evaluation we do not use this simplification but use (3.49).

A similar convolution of the resummed Coulomb Green function as in (3.48) was encountered in [61] where the mixed Coulomb and one-loop soft corrections to  $W$ -pair production were considered. The formula (3.48) generalizes the result in [61] to QCD and by resumming soft-gluons to all orders. An analogous formula was already used in [64] to resum QED corrections of the form  $\ln(\Gamma_W/M_W)$  for  $W$ -pair production in electron-positron collisions.

At the NLL order only the trivial, LO  $\mathcal{O}(\alpha_s^0)$  soft function, the spin-independent LO potential function and the leading-order hard functions are required so that the resummed cross section is given by

$$\hat{\sigma}_{pp'}^{\text{NLL}}(\hat{s}, \mu_f) = \sum_i H_i^{(0)}(\mu_h) U_i(M, \mu_h, \mu_s, \mu_f) \frac{e^{-2\gamma_E \eta}}{\Gamma(2\eta)} \int_0^\infty d\omega \frac{J_{R_\alpha}(E - \frac{\omega}{2})}{\omega} \left( \frac{\omega}{2M} \right)^{2\eta}. \quad (3.53)$$

As mentioned before, for  $\eta < 0$  the kernel  $\frac{1}{\omega} \left( \frac{\omega}{2M} \right)^{2\eta}$  should be understood in the distribution sense [32]. Neglecting heavy particle decay and bound-state effects, the potential function  $J_{R_\alpha}$  vanishes for  $E < 0$  and the  $\omega$  integral is defined as the star-distribution [32]

$$\int_0^{2E} d\omega f(\omega) \left[ \frac{1}{\omega} \left( \frac{\omega}{2M} \right)^{2\eta} \right]_* = \int_0^{2E} d\omega \frac{f(\omega) - f(0) - \omega f'(0)}{\omega} \left( \frac{\omega}{2M} \right)^{2\eta} + \left[ \frac{f(0)}{2\eta} + \frac{2E}{2\eta + 1} f'(0) \right] \left( \frac{E}{M} \right)^{2\eta}, \quad (3.54)$$

where the double subtraction is sufficient to render the integral convergent for  $\eta > -1$ . The poles of the original integrand at  $\eta = 0$  and  $\eta = -\frac{1}{2}$  show up explicitly in the second line but are cancelled by the overall prefactor  $1/\Gamma(2\eta)$  in (3.48) and (3.53).

Note that the all-order solution (3.48) to the RGEs does not depend on the hard and soft scales  $\mu_h$  and  $\mu_s$ , but truncating the perturbative expansion at a finite order in  $\alpha_s$  introduces a residual dependence on these scales, which is of higher order in  $\alpha_s$ . As pointed out in [32, 33] the standard resummation formula in Mellin space following [1, 2] corresponds to the implicit scale choices  $\mu_h = \mu_f$  and  $\mu_s = M/N$  for the  $N$ -th Mellin moment. The explicit appearance of these scales in the momentum-space formalism allows to use the residual scale dependence of the resummed cross section to estimate the remaining uncertainties from uncalculated higher order corrections. Our choices for these scales and the estimates for the remaining scale uncertainties are discussed in section 4.2.

### 3.6 Matching to the fixed-order NLO calculation

For the implementation of the NLL resummed cross section, we match to the fixed-order NLO calculation valid outside the threshold region. The matched result for the partonic cross section is then given by

$$\begin{aligned}\hat{\sigma}_{pp'}^{\text{matched}}(\hat{s}) &= \left[ \hat{\sigma}_{pp'}^{\text{NLL}}(\hat{s}) - \hat{\sigma}_{pp'}^{\text{NLL}(1)}(\hat{s}) \right] \theta(\Lambda - [\sqrt{\hat{s}} - 2M]) + \hat{\sigma}_{pp'}^{\text{NLO}}(\hat{s}) \\ &\equiv \Delta\hat{\sigma}_{pp'}^{\text{NLL}}(\hat{s}, \Lambda) + \hat{\sigma}_{pp'}^{\text{NLO}}(\hat{s}),\end{aligned}\tag{3.55}$$

where  $\hat{\sigma}_{pp'}^{\text{NLO}}(\hat{s})$  is the fixed-order NLO cross section obtained in standard perturbation theory and  $\hat{\sigma}_{pp'}^{\text{NLL}(1)}$  is the resummed cross section expanded to NLO. The result is given explicitly in (D.1) in appendix D. Since the resummed NLL cross section is expected to be a good approximation to the total cross section only near the threshold, we allowed for a cutoff  $E = \sqrt{\hat{s}} - 2M < \Lambda$  to switch off the resummation outside the threshold region, as was done in [14]. In the calculation of squark-antisquark production we choose, however, not to introduce this cut-off as discussed in section 4.2.

The total hadronic cross section at NLL is then obtained by convoluting (3.55) with the parton luminosity,

$$\sigma_{N_1 N_2 \rightarrow HH'X}^{\text{matched}}(s) = \sum_{p,p'=q,\bar{q},g} \int_{4M^2/s}^1 d\tau L_{pp'}(\tau, \mu_f) \hat{\sigma}_{pp'}^{\text{matched}}(s\tau, \mu_f),\tag{3.56}$$

where the parton luminosity is defined in terms of the PDFs in (2.88).

## 4 NLL resummation for squark-antisquark production

In this section we use the results of section 3 to perform the NLL resummation for squark-antisquark production in proton-proton and proton-antiproton collisions. According to the systematics introduced in (2.7), NLL accuracy requires the combined resummation of Coulomb gluons and soft gluons. Therefore our results extend previous ones on squark-antisquark production at higher order [17–20], that treated soft and Coulomb resummations separately or used a fixed-order expansion. In section 4.1 we perform the matching to the effective theory, and compare the threshold approximation of the LO and NLO cross sections to the full results. In 4.2 we discuss our choices for the hard, soft and Coulomb scales appearing in the resummed cross section and present predictions for squark-antisquark production at the Tevatron and the LHC at cms energies of 7, 10 and 14 TeV. We also compare to results from soft gluon resummation in the Mellin-moment approach [20].

### 4.1 Threshold expansion of the squark-antisquark cross section

In the following we perform the matching from the MSSM to an effective theory containing only (anti-)collinear partons and non-relativistic squarks and antisquarks, and derive the

hard functions for the partonic subprocesses. As discussed in section 3.2, the hard functions required for NLL resummation can be inferred from the leading-order cross sections for the colour-singlet and octet production channels [18, 19]. Therefore the explicit matching to the EFT is not strictly necessary, but is included here in some detail in order to provide an illustration for the somewhat abstract discussion in section 2. We also use the general result for the threshold expansion at NLO (D.3) to reproduce the known threshold behaviour of the NLO cross section [85].

We consider squark-antisquark production at hadron colliders, which at leading order proceeds through quark-antiquark and gluon-induced subprocesses:

$$\begin{aligned} q_i(k_1)\bar{q}_j(k_2) &\rightarrow \tilde{q}_{\sigma_1 k}(p_1)\bar{\tilde{q}}_{\sigma_2 l}(p_2) \\ g(k_1)g(k_2) &\rightarrow \tilde{q}_{\sigma_1 i}(p_1)\bar{\tilde{q}}_{\sigma_2 j}(p_2), \end{aligned} \quad (4.1)$$

where  $i, j, k, l$  denote the quark/squark flavours and  $\sigma_{1,2} = L/R$  label the scalar partners of the left/right-handed quarks. The relevant Feynman diagrams are shown in figure 2. We follow the setup of [85] and take all squarks to be mass degenerate and do not consider top squarks. The first restriction is done for simplicity (and was also used in other recent works on higher-order soft-gluon effects [17–20]) and is not essential in our formalism, since the results in section 3 include the case of different final state masses. The application to top squarks would require an extension of our framework, since in the quark-antiquark production channel they are produced in a  $P$ -wave [86]. Resummation for top squarks was performed recently in [87] assuming that the resummation formalism for  $S$ -wave production can be applied to  $P$ -wave dominated processes. Since, in the present work, we are concerned with the total cross section, there are no sizable corrections from the finite squark width  $\Gamma$  as long as  $\Gamma \ll M$  unlike the case of the invariant mass distribution near threshold. Contributions to the cross section from below the nominal production threshold will be included through the bound-state contribution to the Coulomb Green function. From a recent study of threshold effects in gluino production [26] we expect additional finite-width effects at most of the order of these bound state corrections.

To obtain the leading-order production operators we evaluate the tree-level scattering amplitudes for the processes (4.1) at the production threshold,  $(k_1 + k_2)^2 = 4m_{\tilde{q}}^2$ , and determine the short-distance coefficients from the matching condition (2.17) in order to compute the hard functions (2.60).

#### 4.1.1 Production from quark-antiquark fusion

The tree-level scattering amplitude for quark-antiquark induced squark-antisquark production at threshold is dominated by  $t$ -channel gluino exchange, if quark and squark (and antiquark and antisquark) flavours are identical. Near threshold the full-theory tree-level scattering amplitude for the quark-antiquark channel is

$$i\mathcal{A}_{\{a\}}^{(0)}(q_i\bar{q}_j \rightarrow \tilde{q}_{kL}\bar{\tilde{q}}_{lR}) = -\frac{2ig_s^2 m_{\tilde{g}}}{m_{\tilde{q}}^2 + m_{\tilde{g}}^2} \delta_{ik}\delta_{jl} T_{a_2 a_4}^b T_{a_3 a_1}^b \bar{v}(m_{\tilde{q}}\bar{n}) P_L u(m_{\tilde{q}}n). \quad (4.2)$$

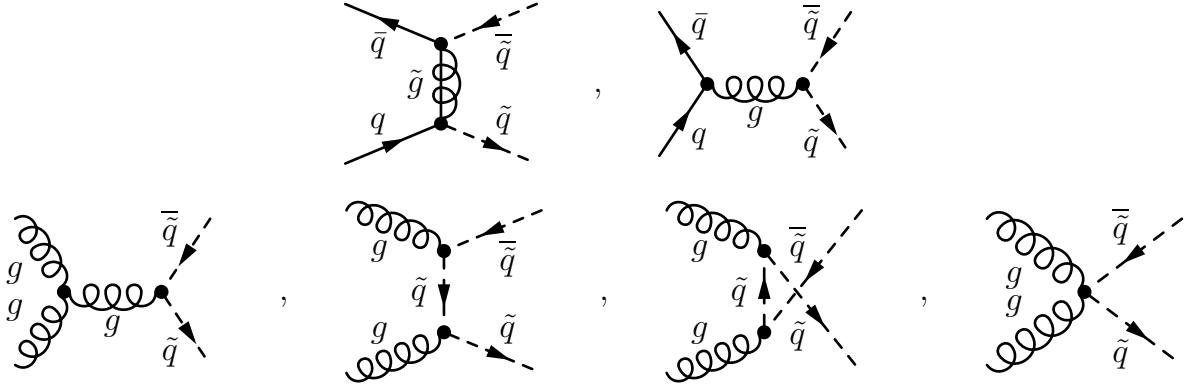


Figure 2: Leading-order Feynman diagrams for the quark-antiquark (top) and gluon-fusion (bottom) induced production of squark-antisquark pairs.

Here we use the usual projectors  $P_{R/L} = (1 \pm \gamma^5)/2$ . There are analogous expressions with left and right labels exchanged.

In the effective theory we introduce fields  $\psi_i$  ( $\psi'_i$ ) that annihilate a left squark (right antisquark) of flavour  $i$ . The quark fields are given by the SCET fields (2.25). We can then match the amplitude onto the effective theory according to the condition (2.17), with the production operator given by (no sum over flavours is implied)

$$\mathcal{O}_{\{a;\alpha\}}^{(0)} = [(\bar{\xi}_{j,\bar{c};\alpha_2} W_{\bar{c}})_{a_2} (W_c^\dagger \xi_{i,c;\alpha_1})_{a_1}] \left( \psi_{i;a_3}^\dagger \psi'_{j;a_4} \right). \quad (4.3)$$

Here  $\xi_{i,c}$  and  $\xi_{i,\bar{c}}$  are the SCET fields describing collinear and anticollinear quarks with flavour  $i$ . From the matching condition (2.17) we can read off the matching coefficient, taking the non-relativistic normalization factor  $2m_{\tilde{q}}$  into account:

$$C_{q\bar{q},\{a;\alpha\}} = -\frac{g_s^2 m_{\tilde{g}}}{m_{\tilde{q}}(m_{\tilde{q}}^2 + m_{\tilde{g}}^2)} T_{a_2 a_4}^b T_{a_3 a_1}^b (P_L)_{\alpha_2 \alpha_1}. \quad (4.4)$$

We now introduce the decomposition of the coefficients into a colour basis (2.14), but leave the spin indices open. For the case at hand, the colour basis has been given already in (2.16). We find for the matching coefficients for the two colour channels:

$$\begin{aligned} C_{q\bar{q},\{\alpha\}}^{(1)} &= (-C_F) \frac{4\pi\alpha_s m_{\tilde{g}}}{m_{\tilde{q}}(m_{\tilde{q}}^2 + m_{\tilde{g}}^2)} (P_L)_{\alpha_2 \alpha_1}, \\ C_{q\bar{q},\{\alpha\}}^{(2)} &= \sqrt{\frac{C_F}{2N_C}} \frac{4\pi\alpha_s m_{\tilde{g}}}{m_{\tilde{q}}(m_{\tilde{q}}^2 + m_{\tilde{g}}^2)} (P_L)_{\alpha_2 \alpha_1}. \end{aligned} \quad (4.5)$$

From the definition (2.60) and the polarization sum (A.7) we obtain the diagonal elements

of the hard function<sup>10</sup>,

$$H_{ii}^{(0)} = \frac{1}{8m_{\tilde{q}}^2} h_i^{(0)} \left( \frac{4\pi\alpha_s m_{\tilde{g}}}{m_{\tilde{q}}(m_{\tilde{q}}^2 + m_{\tilde{g}}^2)} \right)^2 \frac{m_{\tilde{q}}^2}{N_c^2} \text{tr} \left[ \frac{\not{\eta} \not{\bar{\eta}}}{2} P_L \right] = 2h_i^{(0)} \left( \frac{\pi\alpha_s m_{\tilde{g}}}{N_c m_{\tilde{q}}(m_{\tilde{q}}^2 + m_{\tilde{g}}^2)} \right)^2, \quad (4.6)$$

with colour factors

$$h_1^{(0)} = C_F^2, \quad h_2^{(0)} = \frac{C_F}{2N_c} \quad (4.7)$$

for the two colour channels. From (3.13) we obtain the total partonic Born cross section at threshold

$$\hat{\sigma}_{q_i \bar{q}_j \rightarrow \bar{q}_i L \bar{q}_j R}^{(0)} \Big|_{\hat{s}=4m_{\tilde{q}}^2} = \frac{C_F \beta}{2\pi N_c} \left( \frac{\pi\alpha_s m_{\tilde{g}}}{(m_{\tilde{q}}^2 + m_{\tilde{g}}^2)} \right)^2. \quad (4.8)$$

Adding the same expression with left and right squark labels exchanged reproduces the result given e.g. in [85]. In figure 3 we compare the partonic cross section at threshold to the full partonic LO cross section [85], for a squark mass of 1 TeV at the LHC with 14 TeV cms energy. We plot the integrand of the convolution in the formula for the hadronic cross section (2.89), i.e. the product of the partonic cross section and the parton luminosity, as a function of  $\beta$ , taking the Jacobian  $\frac{\partial \tau}{\partial \beta}$  into account:

$$\frac{d\sigma_{q\bar{q} \rightarrow \bar{q}_L \bar{q}_R}^{(0)}}{d\beta} = \frac{8\beta m_{\tilde{q}}^2}{s(1-\beta^2)^2} L_{q\bar{q}}(\beta, \mu_f) \hat{\sigma}_{q\bar{q} \rightarrow \bar{q}_L \bar{q}_R}^{(0)}. \quad (4.9)$$

In the plot we use the MSTW2008LO PDFs [88] with  $\mu_f = m_{\tilde{q}}$ . It can be seen that the threshold approximation is applicable for  $\beta \lesssim 0.3$ , while the main contribution to the cross section comes from the region  $\beta \approx 0.6$ . The results shown here are for a gluino-squark mass ratio of 1.25. For other gluino masses the discrepancies in the region  $\beta > 0.3$  can be somewhat bigger.

An approximation to the NLO cross section can be obtained by expanding the resummed cross section (3.48) to order  $\alpha_s^3$ . The resulting expression can be written in the form  $\Delta\sigma_{pp'}^{(1)} = \sigma_{pp'}^{(0)} \frac{\alpha_s}{4\pi} f_{pp'}^{(1)} + \mathcal{O}(\beta)$ , where the scaling functions  $f_{pp'}^{(1)}$  for an arbitrary colour channel are given explicitly in (D.3). Summing up the two colour channels we obtain the threshold expansion of the scaling function for the quark-antiquark channel

$$f_{q\bar{q}}^{(1)} = \frac{\pi^2(N_c^2 - 2)}{N_c} \frac{1}{\beta} + 8C_F \left[ \ln^2 \left( \frac{8m_{\tilde{q}}\beta^2}{\mu} \right) + 8 - \frac{11\pi^2}{24} \right] - 4 \frac{4N_c^2 - 3}{N_c} \ln \left( \frac{8m_{\tilde{q}}\beta^2}{\mu} \right) + \frac{12}{N_c} + h_{q\bar{q}}^{(1)}(\mu) + \mathcal{O}(\beta). \quad (4.10)$$

The logarithmically enhanced terms and the Coulomb correction agree with the results of [85]. The one-loop hard coefficient  $h^{(1)}$  is currently unknown in analytical form. In the right-hand plot in figure 3 we plot the full NLO corrections to the partonic cross section

<sup>10</sup>For simplicity, in (4.6) and (4.15) we set  $1/(2\hat{s}) \sim 1/(8m_{\tilde{q}}^2)$ . However, in our numerical implementation of the resummed cross section (3.53) this prefactor is kept unexpanded.

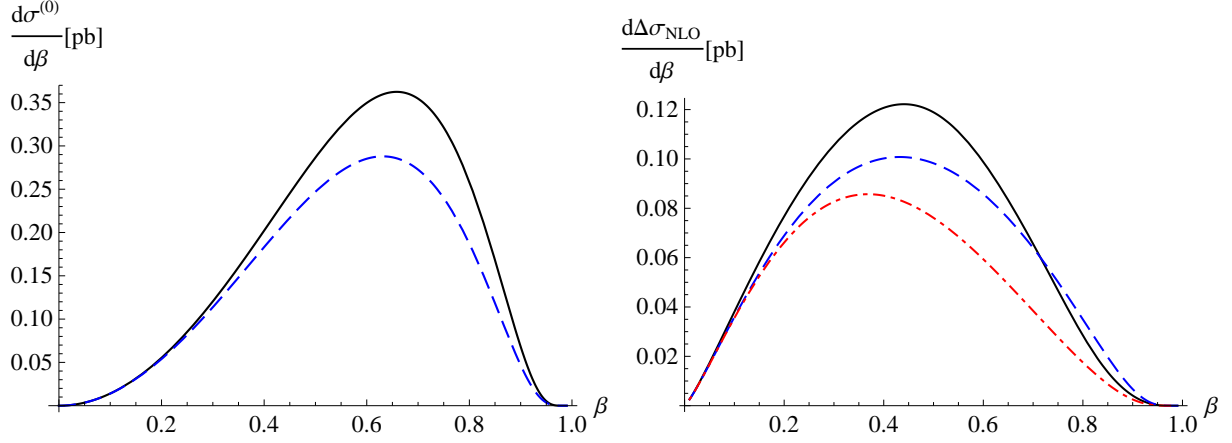


Figure 3: Partonic cross sections for  $q_i \bar{q}_j \rightarrow \tilde{q}_k \bar{\tilde{q}}_b$  multiplied with the quark-antiquark luminosity and summed over quark and squark flavours, for  $m_{\tilde{q}} = 1$  TeV and  $m_{\tilde{g}} = 1.25$  TeV at the 14 TeV LHC. Left panel: exact leading order result (black/solid) and threshold approximation (blue/dashed). Right panel: exact NLO result (black/solid) and the approximation based on (4.10) with  $h_{q\bar{q}}^{(1)}(\mu) = 0$ , using the threshold approximation of the tree (red/dot-dashed) and the full tree (blue/dashed).

obtained from the parameterization given in [19] (solid/black) to the threshold approximation (4.10) with the constant  $h_{q\bar{q}}^{(1)}$  set to zero. In the red/dot-dashed curve we multiply the correction (4.10) with the threshold approximation of the tree, in the blue/dashed curve we use the full tree cross section. It can be seen that the NLO corrections are peaked closer to threshold than the tree cross section, as might be expected. Multiplying the scaling function by the full tree leads to an improved agreement with the full NLO result. Overall the approximation of the full NLO result by the threshold expansion is quite good, in the sense that integrating the approximated partonic cross section captures the bulk part of the exact result.

#### 4.1.2 Production from gluon fusion

For the gluon induced process the  $s$ -channel diagram is again  $P$ -wave suppressed, so the dominant contribution comes from the  $t$ - and  $u$ -channel diagrams and the quartic vertex. These diagrams give

$$i\mathcal{A}_{\{a\}}^{(0)}(gg \rightarrow \tilde{q}_{iR} \bar{\tilde{q}}_{jR}) = ig_s^2 \delta_{ij} \{T^{a_1}, T^{a_2}\}_{a_3 a_4} (\epsilon_1^\mu g_{\mu\nu}^\perp \epsilon_2^\nu), \quad (4.11)$$

with the transverse metric  $g_{\mu\nu}^\perp = g_{\mu\nu} - \frac{1}{2}(n_\mu \bar{n}_\nu + \bar{n}_\mu n_\nu)$ . This form of the scattering amplitude at threshold is reproduced by the matrix element of the effective theory operator (no sum over flavours is implied)

$$O_{\{\mu;a\}}^{(0)} = \mathcal{A}_{c;a_1\mu_1}^\perp \mathcal{A}_{c;a_2\mu_2}^\perp \psi_{i;a_3}^\dagger \psi'_{i;a_4}. \quad (4.12)$$

Here it was used that the polarization vector corresponding to a free SCET gluon fields  $\mathcal{A}^\perp$  is given by  $\epsilon_\perp^\mu = g^{\perp\mu\nu}\epsilon_\nu$ . This can be seen from (2.26) using a Fourier transformation after setting the strong coupling to zero, so that  $W_c = 1$  and the non-abelian terms in the field strength vanish.

To introduce the colour basis, note that the gluon-gluon system admits the decomposition  $8 \otimes 8 = 1 \oplus 8_s \oplus 8_a \oplus 10 \oplus \overline{10} \oplus 27$ . The squark-antisquark pair is again either in a singlet or octet state, but this time the latter can be produced by two different initial colour-octet states. The colour basis obtained for this case from the prescription (3.2) agrees with the one given in [7],

$$\begin{aligned} c_{\{a\}}^{(1)} &= \frac{1}{\sqrt{N_c D_A}} \delta_{a_1 a_2} \delta_{a_3 a_4} \\ c_{\{a\}}^{(2)} &= \frac{1}{\sqrt{2 D_A B_F}} d^{ba_2 a_1} T_{a_3 a_4}^b \\ c_{\{a\}}^{(3)} &= \sqrt{\frac{2}{N_c D_A}} F_{a_2 a_1}^b T_{a_3 a_4}^b, \end{aligned} \quad (4.13)$$

where  $d^{abc}$  are the usual symmetric invariant tensors of  $SU(3)$  and  $F_{a_1 a_2}^b = i f^{a_1 b a_2}$ . We also defined the coefficients  $D_A = N_c^2 - 1$  and  $B_F = \frac{N_c^2 - 4}{4 N_c} = \frac{5}{12}$ . Thus, the matching coefficients for the three colour channels are (including the non-relativistic normalization  $2m_{\bar{q}}$ )

$$\begin{aligned} C_{gg, \{\mu\}}^{(0,1)} &= \sqrt{2 C_F} \frac{2\pi\alpha_s}{m_{\bar{q}}} g_{\mu_1 \mu_2}^\perp, \\ C_{gg, \{\mu\}}^{(0,2)} &= \sqrt{2 D_A B_F} \frac{2\pi\alpha_s}{m_{\bar{q}}} g_{\mu_1 \mu_2}^\perp, \\ C_{gg, \{\mu\}}^{(0,3)} &= 0. \end{aligned} \quad (4.14)$$

The diagonal elements of the hard function are given by

$$H_{ii}^{(0)} = \frac{1}{8m_{\bar{q}}^2} h_i^{(0)} \left( \frac{2\pi\alpha_s}{m_{\bar{q}}} \right)^2 \frac{1}{4D_A^2} g_\mu^\perp{}^\mu = \left( \frac{\pi\alpha_s}{2D_A m_{\bar{q}}^2} \right)^2 h_i^{(0)} \quad (4.15)$$

with the colour factors

$$h_1^{(0)} = 2C_F, \quad h_2^{(0)} = 2D_A B_F, \quad h_3^{(0)} = 0. \quad (4.16)$$

Using  $\sum_i h_i^{(0)} = C_F(N_c^2 - 2)$  gives for the total partonic cross section at threshold

$$\hat{\sigma}_{g\bar{g} \rightarrow \bar{q}_i L \bar{q}_i R}^{(0)} \Big|_{\hat{s}=4m_{\bar{q}}^2} = \frac{\pi\alpha_s^2 \beta}{16m_{\bar{q}}^2} \frac{N_c^2 - 2}{N_c(N_c^2 - 1)}. \quad (4.17)$$

Adding the same expression for left and right squark labels exchanged again reproduces the result of [85]. In figure 4 we compare the partonic cross section at threshold to the full partonic LO cross section [85], for a squark mass of 1 TeV at the LHC with 14 TeV



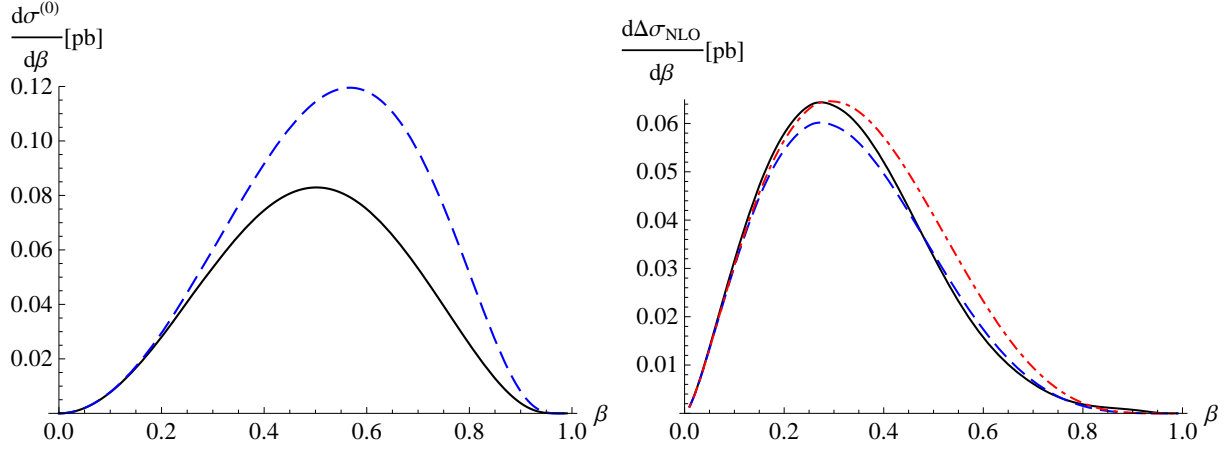


Figure 4: Partonic cross sections for  $gg \rightarrow \tilde{q}\tilde{q}^{\bar{}}$  multiplied with the gluon-gluon luminosity for  $m_{\tilde{q}} = 1$  TeV at the 14 TeV LHC. Left panel: exact leading-order result (black/solid) and threshold approximation (blue/dashed). Right panel: exact NLO result (black/solid) and the approximation (4.18) with  $h_{\tilde{q}\tilde{q}^{\bar{}}}^{(1)}(\mu) = 0$ , using the threshold approximation of the tree (red/dot-dashed) and the full tree (blue/dashed).

cms energy. As for the quark-antiquark induced subprocess we plot the product of the partonic cross section with the parton luminosity and the Jacobian  $\frac{\partial\tau}{\partial\beta}$ . Again the threshold approximation is adequate up to  $\beta \sim 0.3$  while the maximum of the integrand occurs around  $\beta \approx 0.5$ .

For the threshold expansion of the NLO cross section we obtain

$$f_{gg}^{(1)} = \frac{\pi^2(N_c^2 + 2)}{N_c(N_c^2 - 2)} \frac{1}{\beta} + 8N_c \left[ \ln^2 \left( \frac{8m_{\tilde{q}}\beta^2}{\mu} \right) + 8 - \frac{11\pi^2}{24} \right] - 4N_c \frac{9N_c^2 - 20}{N_c^2 - 2} \ln \left( \frac{8m_{\tilde{q}}\beta^2}{\mu} \right) + 12N_c \frac{N_c^2 - 4}{N_c^2 - 2} + h_{gg}^{(1)}(\mu) + \mathcal{O}(\beta). \quad (4.18)$$

The  $\beta$ -dependent terms agree with [85]. Again, the hard corrections  $h_{gg}^{(1)}$  are currently not available analytically. In the right plot of figure 4 we compare the full NLO correction in the parameterization of [19] (black/solid) to the threshold approximation of the NLO correction (4.18) with  $h_{gg}^{(1)} = 0$ , using the threshold approximation of the tree (red/dot-dashed) or the full tree cross section (blue/dashed) as pre-factor. In this case, the threshold approximation gives a better agreement with the full NLO result than for the quark-antiquark initial state. Using the full tree further improves the agreement with the full NLO correction in the full  $\beta$ -range. Once again the integrated threshold approximation provides a very good approximation to the exact NLO correction, especially when multiplying (4.18) by the full Born cross section. This can be compared to the Born cross section itself, for which the leading term in the  $\beta$ -expansion is typically a less reliable approximation.

## 4.2 Results for squark-antisquark production at the LHC and Tevatron

We are now ready to perform the combined soft and Coulomb NLL resummation for squark-antisquark production. We first discuss our choice for the soft, hard and Coulomb scales entering the resummed cross section, and then present numerical results for the LHC and the Tevatron. We also compare to the results of a soft gluon resummation in Mellin space presented in [20].

### 4.2.1 Scale choices

Evaluating the NLL resummed cross section (3.53) requires a choice for the soft, hard and Coulomb scales. As can be seen from the Sudakov logarithm in the evolution equation of the hard function (3.33), the natural scale of the hard corrections is of the order  $\mu_h \sim 2M$ . Therefore we will choose the default value of the hard scale to be  $\tilde{\mu}_h = 2m_{\tilde{q}}$ . Analogously, the form of the approximate NLO corrections (4.10) and (4.18) implies that the scale eliminating large logarithms in the soft corrections to the *partonic* cross section is given by  $\mu_s \sim 8E \approx 8M\beta^2$ . However, it was argued in [32, 33] that this choice leads to similar problems as the inversion of Mellin-space resummation formulae for the partonic cross section [10], i.e. an ill-defined convolution with the parton luminosity. Here we follow [33] and choose a soft scale such that it minimizes the relative fixed-order one-loop soft correction to the *hadronic* cross section. More precisely, we vary the scale in the PDFs and the soft correction and determine the value  $\tilde{\mu}_s$  that minimizes the relative soft corrections:

$$0 = \frac{d}{d\tilde{\mu}_s} \sum_{p,p'} \int_{4m_{\tilde{q}}^2/s}^1 d\tau L_{pp'}(\tau, \tilde{\mu}_s) \frac{\hat{\sigma}_{pp',\text{soft}}^{(1)}(\tau s, \tilde{\mu}_s)}{\sigma_{N_1 N_2}^{(0)}(s, \tilde{\mu}_s)}. \quad (4.19)$$

Here the fixed-order NLO soft correction  $\hat{\sigma}_{pp',\text{soft}}^{(1)}$  is obtained from (4.10) and (4.18), setting the Coulomb correction and the hard corrections  $h_i$  to zero, and we divide by the leading-order hadronic cross section. This procedure results in values

$$\tilde{\mu}_s = 123 - 455 \text{ GeV} \quad \text{for} \quad m_{\tilde{q}} = 200 - 2000 \text{ GeV} \quad (4.20)$$

for the LHC with  $\sqrt{s} = 14 \text{ TeV}$ . The fact that the soft scale is over half of the mass for light squarks, but considerably smaller for larger masses, indicates that the threshold resummation is more important for heavier squarks, as expected. We can approximately fit the numerical results for the soft scale by a function of the form proposed in [33],

$$\tilde{\mu}_s^{\text{LHC}} \approx \frac{m_{\tilde{q}}(1 - \rho)}{\sqrt{3.8 + 149\rho}}, \quad (4.21)$$

with  $\rho = 4m_{\tilde{q}}^2/s$ , which is accurate to better than 5% for  $m_{\tilde{q}} > 450 \text{ GeV}$ . We find that for different cms energies  $\sqrt{s}$  the ratio  $\tilde{\mu}_s^{\text{LHC}}/m_{\tilde{q}}$  is to a good approximation a function of  $\rho$  only, that is, for a squark of mass 500 GeV at 7 TeV cms energy the ratio is approximately

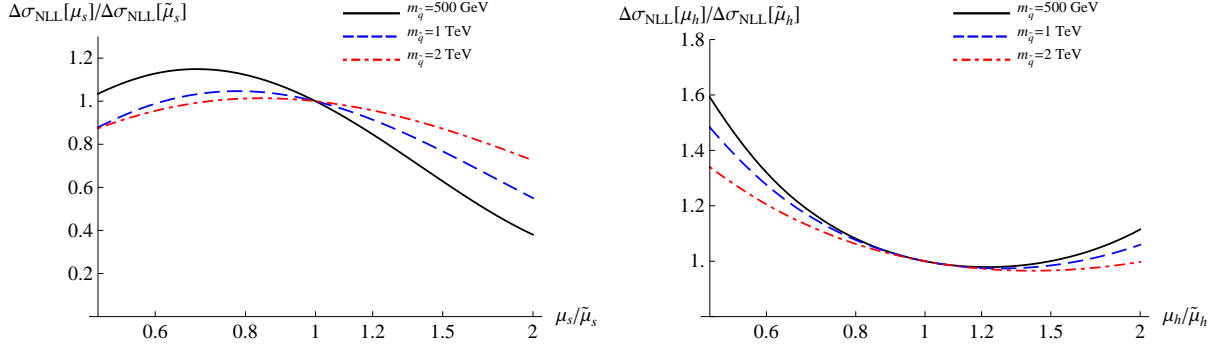


Figure 5: Dependence of the NLL corrections at the 14 TeV LHC on the soft scale (left panel) and the hard scale (right panel), normalized to the corrections at the default scales  $\tilde{\mu}_s$  determined from (4.19) and  $\tilde{\mu}_h = 2m_{\tilde{q}}$ . Black (solid):  $m_{\tilde{q}} = 500$  GeV, blue (dashed):  $m_{\tilde{q}} = 1$  TeV, red (dot-dashed):  $m_{\tilde{q}} = 2$  TeV

the same as for a 1 TeV squark at 14 TeV. In our numerical NLL results, however, we use the numerical values for the soft scale obtained directly by the condition (4.19). At the Tevatron the values for the soft scale can be fitted by the function

$$\tilde{\mu}_s^{\text{TeV}} \approx \frac{m_{\tilde{q}}(1 - \rho)}{\sqrt{1.7 + 81.3\rho}}, \quad (4.22)$$

and representative values for the default soft scale are

$$\tilde{\mu}_s^{\text{TeV}}(200\text{GeV}) = 84\text{GeV}, \quad \tilde{\mu}_s^{\text{TeV}}(400\text{GeV}) = 86\text{GeV}, \quad \tilde{\mu}_s^{\text{TeV}}(600\text{GeV}) = 65\text{GeV}. \quad (4.23)$$

Note that the soft scale begins to decrease above a certain value of  $\rho$ .

Figure 5 shows the dependence of the NLL corrections to the hadronic cross section at the LHC with 14 TeV on the soft and hard scales, varied around the default values  $\tilde{\mu}_s$  and  $\tilde{\mu}_h = 2m_{\tilde{q}}$ . Here by ‘‘NLL corrections’’ we mean the convolution of the expression  $\Delta\hat{\sigma}_{pp'}^{\text{NLL}}(\hat{s}, \Lambda)$  in (3.55) with the parton luminosity, i.e. the corrections on top of the exact NLO cross section due to the higher-order soft-gluon and Coulomb terms (bound-state corrections are not included in these curves, and we set the cutoff  $\Lambda$  to the maximum possible value). In the left panel, the hard scale is fixed to the default value  $\mu_h = \tilde{\mu}_h$  and we vary the soft scale in the interval  $0.5\tilde{\mu}_s \dots 2\tilde{\mu}_s$ . Analogously, in the right panel the soft scale is fixed to the default value and we vary the hard scale in the interval  $m_{\tilde{q}} \dots 4m_{\tilde{q}}$ . The ambiguity due to the choice of the soft scale becomes smaller for larger masses, in agreement with the expectation that soft-gluon resummation is better justified for larger masses, where the contribution from the threshold region to the total cross section is more important.

We now address the choice of the scale used for the strong coupling constant in the Coulomb Green function. The only scale dependence of the imaginary part of the leading-

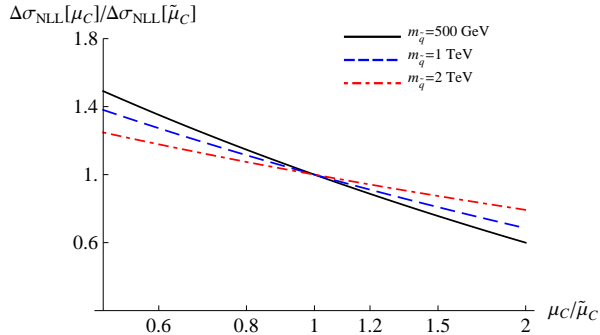


Figure 6: Dependence of the NLL corrections at the 14 TeV LHC on the Coulomb scale, normalized to the corrections at the default scale  $\tilde{\mu}_C = \max\{2\tilde{m}_q\beta, \mu_B\}$ . Black (solid):  $m_{\tilde{q}} = 500$  GeV, blue (dashed):  $m_{\tilde{q}} = 1$  TeV, red (dot-dashed):  $m_{\tilde{q}} = 2$  TeV

order Coulomb Green function (3.27) enters through the coupling constant of the leading-order Coulomb potential, so the potential function is separately renormalization-group invariant at NLL, and the coupling constant can be evaluated at a scale  $\mu_C$  different from the factorization scale. Since the necessary truncation of the perturbative series for the running coupling constant introduces a residual higher-order scale dependence, the scale  $\mu_C$  should be chosen such that higher-order corrections are minimized. Since the Coulomb corrections are related to the exchange of potential gluons with momentum transfer  $|\vec{k}| \sim M\sqrt{\lambda}$ , a natural scale choice  $\mu_C$  is expected to be of the order

$$\mu_C \sim M\sqrt{\lambda} = M\beta \sim M\alpha_s, \quad (4.24)$$

where we have used the NRQCD counting  $\beta \sim \alpha_s$ . Indeed, as mentioned in section 2.5.2, the effect of the scale-dependent strength of the Coulomb potential can be incorporated using the choice  $\mu_C = 2m_{\tilde{q}}\beta$ . The choice  $\mu_C \sim \mathcal{O}(M\beta)$  is in fact required to sum correctly all NLL terms, since  $\mu_C \sim M$  would miss terms such as  $\alpha_s^2/\beta \times \ln \beta$ , which arise in part from the small virtuality of Coulomb gluons. However, very small values of  $\beta$  are integrated over in the convolution of the partonic cross section with the PDFs, and with the choice  $\mu_C \propto \beta$  the strong coupling  $\alpha_s(\mu_C)$  would hit the Landau pole. On the other hand, the relevant scale for bound-state effects is set by the inverse Bohr radius of the first  $HH'$  bound state,  $1/r_B = C_F m_{\tilde{q}} \alpha_s / 2 \equiv \mu_B / 2$ . Therefore, as our default scale choice for the Coulomb Green function we use

$$\tilde{\mu}_C = \max\{2m_{\tilde{q}}\beta, \mu_B\}, \quad (4.25)$$

where we solve the equation  $\mu_B = C_F m_{\tilde{q}} \alpha_s(\mu_B)$  iteratively. The Bohr scale was used in recent studies of threshold effects in top-pair or gluino production [24–26], while in the recent calculation [18] of squark-antisquark and gluino production the Coulomb scale was set equal to the factorization scale. The dependence of the NLL corrections at the LHC

with 14 TeV cms energy on the Coulomb scale (with all other scales fixed to their default values) is shown in Figure 6, where we vary the Coulomb scale in the interval  $0.5\tilde{\mu}_C \dots 2\tilde{\mu}_C$ . The scale dependence is of a similar magnitude as for the soft and hard scales, and again improves for larger masses. In the results given below, we estimate the uncertainty due to the scale choices by varying all scales  $\mu_f$ ,  $\mu_s$ ,  $\mu_h$  and  $\mu_C$  from one-half to twice their default value and add the uncertainties in quadrature.

## 4.2.2 Results

Having fixed the default scale values, we present numerical results<sup>11</sup> for the combined NLL resummation of soft and Coulomb effects obtained by inserting the potential function (3.28) into the cross section (3.53). We use the MSTW2008 PDF set [88] and the associated value of the strong coupling. The results for the fixed-order NLO cross section are obtained using the program PROSPINO, which is based on the calculation of [85]. In contrast to the default setting of PROSPINO, we include contributions from initial-state bottom quarks using  $b$ -quark PDFs. Unless stated otherwise, we use the squark-gluino mass ratio of  $m_{\tilde{g}} = 1.25m_{\tilde{q}}$ . As discussed in section 4.1, we consider the squarks to be mass-degenerate and do not include top squark final states. Our default value for the factorization scale is  $\tilde{\mu}_f = m_{\tilde{q}}$ .

In table 1 we compare the PROSPINO NLO predictions obtained using the MSTW08 and the CTEQ6.6M [89] PDF set for the Tevatron and the LHC at 14 TeV. While we find good agreement for small squark masses, the differences between the two sets grow to over 10% for large masses. Since we expect very similar effects for the results including NLL resummation, we present our predictions using the MSTW PDFs below, but the uncertainties due to differences between current PDF sets at large  $x$  should be taken into account in interpreting our results.

In figure 7 we show the NLL corrections to the partonic cross sections multiplied by the parton luminosities and the Jacobian  $\frac{\partial\sigma}{\partial\beta}$ . It can be seen that the dominant contributions arise from the threshold region  $\beta \leq 0.2$ , and that there is only a small difference between using the hard function obtained from the tree at threshold, as determined in section 4.1, or from the full tree, as mentioned in section 3.2. Thus, in the results presented below we use the hard functions determined from the tree at threshold, and set the cutoff  $\Lambda$  in the matching formula (2.17) to the maximal value, so that the resummed correction is applied in the full phase space. Another plausible choice is to switch off the NLL corrections at the point where they turn negative [14]. In the example shown in figure 7 this occurs at  $\beta \approx 0.4$ , where the validity of the threshold approximation is not immediately clear. Since the integrated contributions from the region  $\beta > 0.4$  are moderate and negative, our procedure gives a conservative estimate of the NLL corrections. We stress that this choice depends on a study of the behaviour of the resummed corrections at larger values of  $\beta$  and that other choices might be required for other processes.

---

<sup>11</sup>There are some differences to preliminary results presented in [50,51] due to a different choice of hard scale ( $\mu_h = m_{\tilde{q}}$ ) in the NLL results, and because the  $qg$  initiated subprocess was not included in the NLO cross section.

$\sigma(p\bar{p} \rightarrow \tilde{q}\tilde{q})(\text{pb}), \sqrt{s} = 1.96 \text{ TeV}$		
$m_{\tilde{q}}[\text{GeV}]$	NLO <sub>MSTW</sub>	NLO <sub>CTEQ</sub>
200	$11.6^{+1.7}_{-1.8}$	$11.6^{+1.2}_{-1.7}$
300	$6.68^{+1.19}_{-1.16} \times 10^{-1}$	$6.93^{+1.19}_{-1.18} \times 10^{-2}$
400	$4.31^{+0.94}_{-0.85} \times 10^{-2}$	$4.64^{+0.98}_{-0.90} \times 10^{-2}$
500	$2.39^{+0.63}_{-0.53} \times 10^{-3}$	$2.73^{+0.69}_{-0.59} \times 10^{-3}$

$\sigma(pp \rightarrow \tilde{q}\tilde{q})(\text{pb}), \sqrt{s} = 14 \text{ TeV}$		
$m_{\tilde{q}}[\text{GeV}]$	NLO <sub>MSTW</sub>	NLO <sub>CTEQ</sub>
500	$14.4^{+1.5}_{-1.6}$	$13.7^{+1.4}_{-1.5}$
1000	$2.58^{+0.29}_{-0.31} \times 10^{-1}$	$2.49^{+0.27}_{-0.29} \times 10^{-1}$
1500	$1.35^{+0.17}_{-0.18} \times 10^{-2}$	$1.38^{+0.16}_{-0.20} \times 10^{-2}$
2000	$9.97^{+1.43}_{-1.44} \times 10^{-4}$	$1.13^{+0.15}_{-0.16} \times 10^{-3}$

Table 1: NLO results for the squark-antisquark production cross section at the Tevatron and the LHC at  $\sqrt{s} = 14 \text{ TeV}$  for  $m_{\tilde{g}} = 1.25m_{\tilde{q}}$  obtained with PROSPINO, using MSTW08NLO and CTEQ6.6M PDFs. The error estimate is obtained by varying the factorization scale in the interval  $m_{\tilde{q}}/2 \leq \mu_f \leq 2m_{\tilde{q}}$

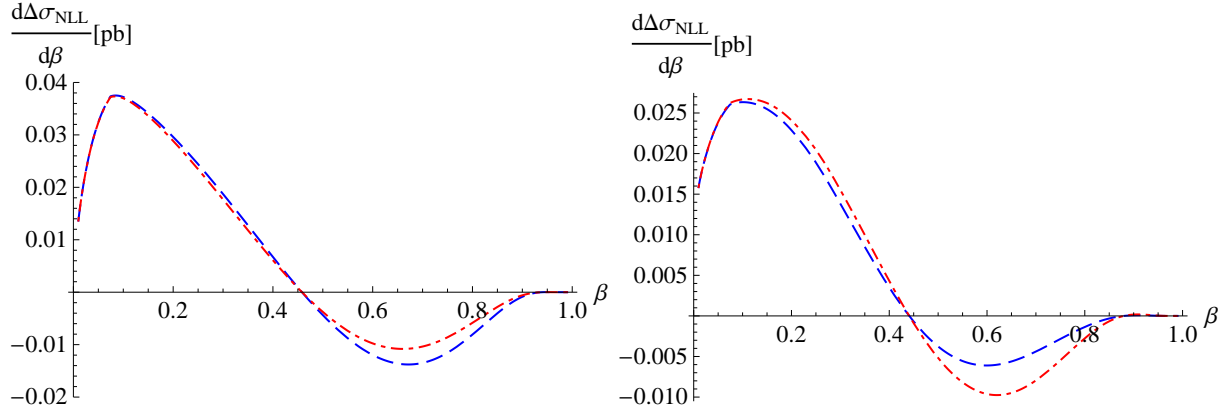


Figure 7: NLL corrections to the partonic cross sections, multiplied with the parton luminosity, for  $q_i \bar{q}_j \rightarrow \tilde{q}_k \bar{q}_l$  (left) and  $gg \rightarrow \tilde{q}_k \bar{q}_l$  at the 14 TeV LHC for  $m_{\tilde{q}} = 1 \text{ TeV}$  and  $m_{\tilde{g}} = 1.25 \text{ TeV}$ , using the threshold approximation of the tree (red, dot-dashed) and the full tree (blue/dashed).

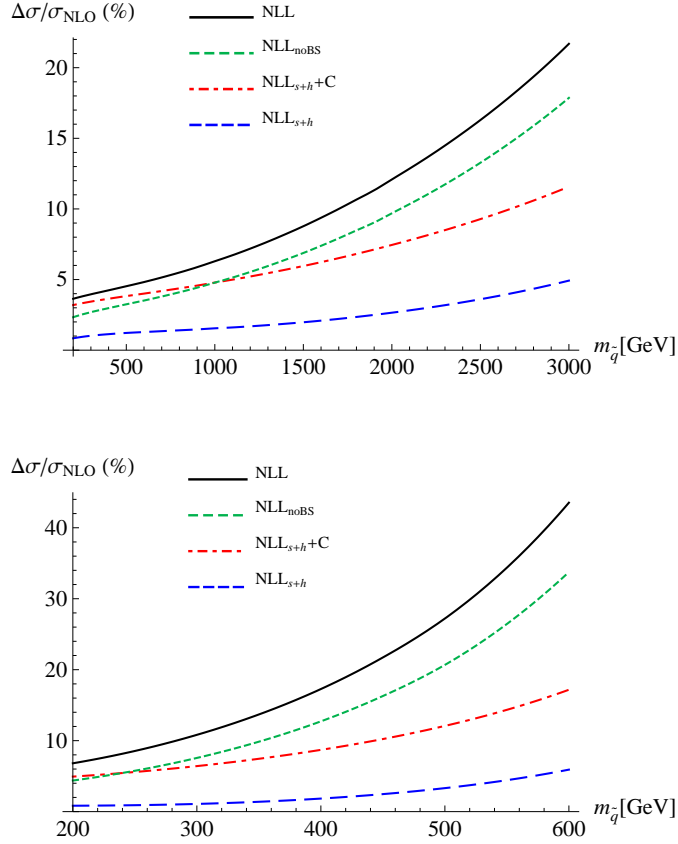


Figure 8: NLL corrections to the squark-antisquark cross section at the LHC with  $\sqrt{s} = 14$  TeV (above) and the Tevatron (below) relative to the NLO cross sections in various approximations. For explanations see text.

In figure 8 we plot the  $K$ -factor relative to the NLO corrections,

$$\Delta K_{\text{NLL}} = \frac{\sigma_{\text{NLL}} - \sigma_{\text{NLO}}}{\sigma_{\text{NLO}}}, \quad (4.26)$$

for the  $\sqrt{s} = 14$  TeV LHC and for the Tevatron, as a function of the squark mass, and consider various approximations to our NLL result to study the effect of the Coulomb and soft corrections separately. The different curves in the figure are defined as follows:

**NLL** (black, solid): Results for the full NLL soft and Coulomb resummation using the resummed cross section (3.53) in the matching formula (3.55), including bound-state effects obtained from the potential function below threshold (3.30).

**NLL<sub>noBS</sub>** (green, dashed): Bound-state effects are omitted from the full NLL result.

**NLL<sub>s+h</sub>** (blue, dashed): NLL resummation without Coulomb corrections, i.e. the cross section (3.53) with the trivial potential function  $J^{(0)}(E) = \frac{m_{\bar{q}}^2}{2\pi} \sqrt{\frac{E}{m_{\bar{q}}}}$ .

**NLL<sub>s+h</sub>+C** (red, dot-dashed): The pure Coulomb corrections, obtained by using the trivial soft function  $W^{(0)} = \delta(\omega)$  and the resummed potential function (3.28) without bound state effects, are added to the NLL<sub>s+h</sub> approximation.

It can be seen that the soft-Coulomb interference effects, given by the difference of the NLL<sub>noBS</sub> and NLL<sub>s+h</sub>+C curves, are sizable, in particular for large squark masses. Most of this effect is due to the interference of the first Coulomb correction with the resummed soft corrections; for instance at the 14 TeV LHC the relative correction at  $m_{\bar{q}} = 2$  TeV in this approximation is  $\Delta K_{\text{NLL}} = 9.0\%$  as opposed to  $\Delta K_{\text{NLL}} = 9.7\%$  in the full NLL soft plus Coulomb resummation. The NLL<sub>s+h</sub> corrections are of a similar magnitude as the soft NLL corrections obtained in [17, 18, 20] from resummation in Mellin space. A quantitative comparison to these previous results will be performed below. The Coulomb corrections are larger than those observed in [18]. This can be traced to the choice of the Coulomb scale, which was taken to be  $\mu_C = \mu_f$  in that reference, while we use the smaller scale (4.25) required to sum all NLL terms, as discussed above.

In tables 2 and 3 we compare the NLL resummed results pertaining to  $p\bar{p}$  collisions at the Tevatron cms energy  $\sqrt{s} = 1.96$  TeV and  $pp$  collisions at LHC with  $\sqrt{s} = 7, 10$  and 14 TeV to the LO and NLO results obtained from PROSPINO. For the LO predictions we have used the MSTW2008LO set of PDFs, for the NLO and resummed predictions the MSTW2008NLO set. One observes a sizable reduction in the scale dependence for larger squark masses. This improvement can also be seen in figure 9. In the left-hand plots the scale dependence of the NLO cross section, the full NLL and the NLL<sub>s+h</sub> correction are plotted as a function of the squark mass for the Tevatron and the 14 TeV LHC. For the NLL results, the soft, hard, Coulomb scales and the factorization scale are varied and the uncertainties added in quadrature. Clearly, a significant reduction of the scale dependence requires the inclusion of soft-Coulomb interference. In the right-hand plots in figure 9 we plot the LO, NLO and NLL cross section as a function of the factorization scale for  $m_{\bar{q}} = 1$  TeV at the 14 TeV LHC and for  $m_{\bar{q}} = 400$  GeV at the Tevatron. One observes a stabilization of the result with respect to variations of the factorization scale in going from the NLO to the NLL approximation if the factorization scale is varied in the usual interval  $0.5m_{\bar{q}} \leq \mu_f \leq 2m_{\bar{q}}$ , even after taking the variation of the soft, hard and Coulomb scales (shown as the green band) into account.

In table 4 we compare to the NLL result of [20] obtained from threshold resummation in Mellin space. In that reference no Coulomb resummation was considered. In order to compare to their result we use the approximation NLL<sub>s+h</sub> defined above, but in addition set the hard scale to  $\mu_h = \mu_f$ . As can be seen from the comparison, this approximation, denoted by NLL<sub>s</sub>, is in good agreement with the result from [20] at the 14 TeV LHC, while the full NLL corrections including Coulomb effects are considerably larger at higher masses. At the Tevatron the NLL<sub>s</sub> approximation results in smaller corrections than the ones obtained in the Mellin space approach, while again the Coulomb corrections and



$\sigma(pp \rightarrow \tilde{q}\tilde{q})(\text{pb}), \sqrt{s} = 1.96 \text{ TeV}$				
$m_{\tilde{q}}[\text{GeV}]$	LO	NLO	NLL	$\Delta K_{\text{NLL}}$
200	$9.59^{+4.36}_{-2.76}$	$11.6^{+1.7}_{-1.8}$	$12.4^{+1.3}_{-0.9}$	6.9%
300	$5.44^{+2.64}_{-1.65} \times 10^{-1}$	$6.68^{+1.19}_{-1.16} \times 10^{-1}$	$7.41^{+0.84}_{-0.62} \times 10^{-1}$	10.9%
400	$3.44^{+1.80}_{-1.10} \times 10^{-2}$	$4.31^{+0.94}_{-0.85} \times 10^{-2}$	$5.06^{+0.64}_{-0.45} \times 10^{-2}$	17.3%
500	$1.87^{+1.06}_{-0.63} \times 10^{-3}$	$2.39^{+0.63}_{-0.53} \times 10^{-3}$	$3.04^{+0.41}_{-0.28} \times 10^{-3}$	27.3%
600	$6.93^{+4.27}_{-2.47} \times 10^{-5}$	$9.09^{+2.89}_{-2.25} \times 10^{-5}$	$1.30^{+0.19}_{-0.13} \times 10^{-4}$	43.4%

$\sigma(pp \rightarrow \tilde{q}\tilde{q})(\text{pb}), \sqrt{s} = 7 \text{ TeV}$				
$m_{\tilde{q}}[\text{GeV}]$	LO	NLO	NLL	$\Delta K_{\text{NLL}}$
200	$1.83^{+0.65}_{-0.44} \times 10^2$	$2.40^{+0.30}_{-0.31} \times 10^2$	$2.52^{+0.27}_{-0.08} \times 10^2$	5.0%
400	$4.47^{+1.66}_{-1.12}$	$5.58^{+0.69}_{-0.73}$	$5.95^{+0.51}_{-0.21}$	6.5%
600	$3.33^{+1.29}_{-0.86} \times 10^{-1}$	$4.01^{+0.53}_{-0.56} \times 10^{-1}$	$4.35^{+0.34}_{-0.17} \times 10^{-1}$	8.5%
800	$3.69^{+1.49}_{-0.99} \times 10^{-2}$	$4.32^{+0.63}_{-0.64} \times 10^{-2}$	$4.79^{+0.37}_{-0.20} \times 10^{-2}$	11.0%
1000	$4.92^{+2.05}_{-1.35} \times 10^{-3}$	$5.52^{+0.90}_{-0.88} \times 10^{-3}$	$6.30^{+0.50}_{-0.29} \times 10^{-3}$	14.1%
1200	$7.08^{+3.07}_{-2.0} \times 10^{-4}$	$7.53^{+1.35}_{-1.28} \times 10^{-4}$	$8.89^{+0.71}_{-0.43} \times 10^{-4}$	17.9%

$\sigma(pp \rightarrow \tilde{q}\tilde{q})(\text{pb}), \sqrt{s} = 10 \text{ TeV}$				
$m_{\tilde{q}}[\text{GeV}]$	LO	NLO	NLL	$\Delta K_{\text{NLL}}$
200	$4.32^{+1.4}_{-1.0} \times 10^2$	$5.73^{+0.70}_{-0.69} \times 10^2$	$5.97^{+0.66}_{-0.16} \times 10^2$	4.2%
400	$1.39^{+0.47}_{-0.33} \times 10^1$	$1.77^{+0.20}_{-0.21} \times 10^1$	$1.86^{+0.16}_{-0.06} \times 10^1$	5.1%
600	$1.41^{+0.50}_{-0.34}$	$1.75^{+0.20}_{-0.22}$	$1.86^{+0.14}_{-0.06}$	6.1%
800	$2.25^{+0.82}_{-0.56} \times 10^{-1}$	$2.72^{+0.33}_{-0.35} \times 10^{-1}$	$2.92^{+0.21}_{-0.11} \times 10^{-1}$	7.4%
1000	$4.48^{+1.68}_{-1.14} \times 10^{-2}$	$5.32^{+0.69}_{-0.72} \times 10^{-2}$	$5.79^{+0.42}_{-0.22} \times 10^{-2}$	8.9%
1200	$1.02^{+0.39}_{-0.26} \times 10^{-2}$	$1.18^{+0.17}_{-0.17} \times 10^{-2}$	$1.30^{+0.10}_{-0.05} \times 10^{-2}$	10.6%
1400	$2.48^{+0.98}_{-0.66} \times 10^{-3}$	$2.79^{+0.42}_{-0.42} \times 10^{-3}$	$3.15^{+0.23}_{-0.13} \times 10^{-3}$	12.7%

Table 2: Results for the squark-antisquark production cross section at the Tevatron and the LHC at  $\sqrt{s} = 7 \text{ TeV}$  and  $10 \text{ TeV}$  for  $m_{\tilde{g}} = 1.25m_{\tilde{q}}$  at leading order, next-to-leading order (NLO) and NLO plus resummed soft and Coulomb corrections (NLL). The error estimates of the LO and NLO results are obtained by varying the factorization scale in the interval  $m_{\tilde{q}}/2 \leq \mu_f \leq 2m_{\tilde{q}}$ , the error estimate of the NLL result is obtained by varying  $\mu_i \in \{\mu_f, \mu_h, \mu_s, \mu_C\}$  in the interval  $\tilde{\mu}_i/2 \leq \mu_i \leq \hat{2}\mu_i$  around the default values and adding the variations of the cross section in quadrature.

$m_{\tilde{q}}[\text{GeV}]$	$\sigma(pp \rightarrow \tilde{q}\tilde{q})(\text{pb}), \sqrt{s} = 14 \text{ TeV}$			$\Delta K_{\text{NLL}}$
	LO	NLO	NLL	
200	$0.91^{+0.27}_{-0.2} \times 10^3$	$1.21^{+0.14}_{-0.14} \times 10^3$	$1.25^{+0.15}_{-0.03} \times 10^3$	3.6%
400	$3.48^{+1.1}_{-0.78} \times 10^1$	$4.53^{+0.49}_{-0.51} \times 10^1$	$4.73^{+0.43}_{-0.13} \times 10^1$	4.2%
600	$4.27^{+1.39}_{-0.98}$	$5.43^{+0.57}_{-0.62}$	$5.69^{+0.45}_{-0.16}$	4.8%
800	$0.84^{+0.28}_{-0.2}$	$1.04^{+0.11}_{-0.12}$	$1.10^{+0.08}_{-0.03}$	5.5%
1000	$2.11^{+0.72}_{-0.5} \times 10^{-1}$	$2.58^{+0.29}_{-0.31} \times 10^{-1}$	$2.74^{+0.19}_{-0.09} \times 10^{-1}$	6.3%
1500	$1.15^{+0.41}_{-0.28} \times 10^{-2}$	$1.35^{+0.17}_{-0.18} \times 10^{-2}$	$1.47^{+0.10}_{-0.06} \times 10^{-2}$	8.8%
2000	$8.92^{+3.38}_{-2.3} \times 10^{-4}$	$9.97^{+1.43}_{-1.44} \times 10^{-4}$	$1.12^{+0.08}_{-0.05} \times 10^{-3}$	12.1%
2500	$7.84^{+3.16}_{-2.09} \times 10^{-5}$	$8.16^{+1.33}_{-1.29} \times 10^{-5}$	$9.49^{+0.69}_{-0.42} \times 10^{-5}$	16.3%
3000	$7.01^{+2.92}_{-1.94} \times 10^{-6}$	$6.54^{+1.21}_{-1.12} \times 10^{-6}$	$7.96^{+0.60}_{-0.37} \times 10^{-6}$	21.7%

Table 3: Results for the leading order, fixed-order NLO and resummed soft + Coulomb corrections (NLL) to squark-antisquark production at the LHC at  $\sqrt{s} = 14 \text{ TeV}$ , setup as in table 2.

$m_{\tilde{q}}[\text{GeV}]$	$\sigma(pp \rightarrow \tilde{q}\tilde{q})(\text{pb}), \sqrt{s} = 14 \text{ TeV}$			
	NLO	NLL <sub>Mellin</sub> (ref. [20])	NLL <sub>s</sub>	NLL
200	$1.3 \times 10^3$	$1.31 \times 10^3$ (1%)	$1.31 \times 10^3$ (1%)	$1.34 \times 10^3$ (3.4%)
500	$1.6 \times 10^1$	$1.61 \times 10^1$ (1.2%)	$1.62 \times 10^1$ (1.3%)	$1.67 \times 10^1$ (4.2%)
1000	$2.89 \times 10^{-1}$	$2.93 \times 10^{-1}$ (1.7%)	$2.94 \times 10^{-1}$ (1.7%)	$3.06 \times 10^{-1}$ (5.8%)
2000	$1.11 \times 10^{-3}$	$1.14 \times 10^{-3}$ (3.4%)	$1.14 \times 10^{-3}$ (3.1%)	$1.24 \times 10^{-3}$ (11%)
3000	$7.13 \times 10^{-6}$	$7.59 \times 10^{-6}$ (6.4)%	$7.54 \times 10^{-6}$ (5.8%)	$8.61 \times 10^{-6}$ (21%)

$m_{\tilde{q}}[\text{GeV}]$	$\sigma(p\bar{p} \rightarrow \tilde{q}\tilde{q})(\text{pb}), \sqrt{s} = 1.96 \text{ TeV}$			
	NLO	NLL <sub>Mellin</sub> (ref. [20])	NLL <sub>s</sub>	NLL
200	$1.29 \times 10^1$	$1.30 \times 10^1$ (1.6%)	$1.30 \times 10^1$ (1%)	$1.37 \times 10^1$ (6.5%)
300	$7.35 \times 10^{-1}$	$7.55 \times 10^{-1}$ (2.6%)	$7.47 \times 10^{-1}$ (1.5%)	$8.11 \times 10^{-1}$ (10%)
400	$4.70 \times 10^{-2}$	$4.91 \times 10^{-2}$ (4.5%)	$4.83 \times 10^{-2}$ (2.7%)	$5.48 \times 10^{-2}$ (17%)
500	$2.58 \times 10^{-3}$	$2.77 \times 10^{-3}$ (7.1%)	$2.70 \times 10^{-3}$ (4.6%)	$3.26 \times 10^{-3}$ (27%)
600	$9.79 \times 10^{-5}$	$10.9 \times 10^{-5}$ (11)%	$10.6 \times 10^{-5}$ (7.8%)	$13.9 \times 10^{-5}$ (42%)

Table 4: Comparison to the results of [20] for the LHC at 14 TeV (above) and the Tevatron (below) for  $m_{\tilde{g}} = m_{\tilde{q}}$ . In brackets we quote the corrections  $\Delta K_{\text{NLL}}$  relative to the NLO result.

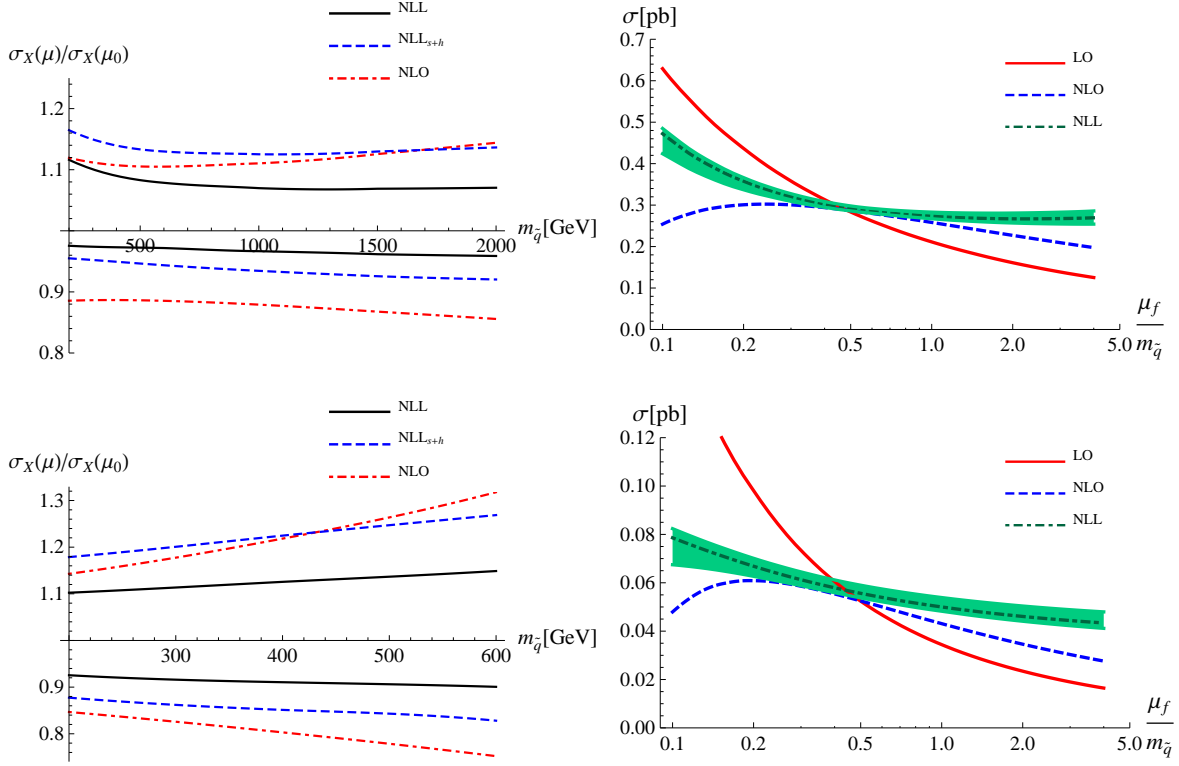


Figure 9: Left: Scale dependence of the NLO, NLL and  $\text{NLL}_{s+h}$  approximations at the LHC with  $\sqrt{s} = 14$  TeV (top) and the Tevatron with  $\sqrt{s} = 1.96$  TeV (bottom). The corrections are normalized to the value at the default scales. Right: Dependence of the LO, NLO and NLL result on the factorization scale, for  $m_{\bar{q}} = 1$  TeV at the 14 TeV LHC (top) and for  $m_{\bar{q}} = 400$  GeV at the Tevatron (bottom). The green band indicates the uncertainty on the NLL result from the choice of the soft, hard and Coulomb scales.

mixed soft/gluon corrections are sizable (note that, due to statistical fluctuations, some of the NLO results from PROSPINO differ from the numbers quoted in [20] in the last digit).

## 5 Conclusion

The production of pairs of massive coloured particles is an integral part of hadron collider physics programmes, since such particles, the top quark for certain, may be produced in large numbers. Precise calculations of the production cross sections are hampered by potentially large quantum corrections originating from the suppression of soft gluon emission and the exchange of Coulomb gluons near the partonic production threshold, especially for large masses of the produced particles. The techniques for summing soft gluon effects to

all orders in perturbation theory have been available for some time, and have been used extensively to improve Drell-Yan production and related processes. Likewise, the summation of Coulomb effects is well established in the context of calculations of top quark pair production near threshold in  $e^+e^-$  collisions. But the interplay of both effects as relevant to hadronic pair production had not been studied to all orders up to now.

Joint soft-gluon and Coulomb resummation is a non-trivial issue, since the energy of soft gluons is of the same order as the kinetic energy of the heavy particles produced. Soft-gluon lines may therefore connect to the heavy-particle propagators in between the Coulomb ladders, as well as to the Coulomb gluons itself, impeding the standard factorization arguments that assume either no couplings to the final state, or to energetic particles. In this paper we employed a combination of soft-collinear and non-relativistic effective field theory techniques to show that, despite these apparent complications, soft gluons can be decoupled from the non-relativistic final state. Their effect is then contained in a more complicated soft function including two time-like Wilson lines for the final state particles, and in a convolution in energy of the soft function with the final state Coulomb function, since the latter depends on the energy but not the momentum taken away by the radiated gluons. Our main result is therefore a new factorization formula for the partonic cross section of heavy-particle pair production near threshold in hadron collisions given by (2.63), and the corresponding equation (2.93) for the invariant mass distribution, together with the resummation formula (3.48) for the partonic cross section.

The result is naturally formulated in momentum space. When expressed in Mellin moment space, the factorization is multiplicative in each separate colour channel, and given by the product of a hard, soft and Coulomb (or potential) function. This justifies previous treatments of Coulomb effects at the one-loop order and extends them to all orders. The resummation of Coulomb effects to all orders is in fact formally required even at the leading-logarithmic level, though numerically the two- and higher-loop Coulomb correction is rather small. Starting from the NNLL level the combined soft-gluon and Coulomb resummation might have involved subleading soft gluon couplings from the effective Lagrangians (beyond the standard eikonal approximation in the collinear sector), making the resummation much more difficult. We applied symmetry considerations to show that these couplings do not contribute at NNLL. A new effect at this order is, however, that the potential function acquires factorization-scale dependence that cancels with the hard function, resulting in additional threshold logarithms on top of the ones from soft gluon emission. Eq. (2.63) is thus valid at NNLL, but beyond that order further, more complicated soft functions are most likely required.

Factorization and resummation are largely model-independent. The details of the hard production mechanism enter only in the momentum-independent short-distance coefficients. We exemplified our theoretical approach by considering squark-antiquark production in  $pp$  and  $p\bar{p}$  collisions at LHC and Tevatron energies with NLL accuracy. We find that the effect of resummation on top of the fixed-order NLO cross section is around (12–27)% for squark masses that give cross sections at the femtobarn level, and increases with mass as expected. The scale uncertainty is considerably reduced after resummation suggesting a reduction of the remaining theoretical error from which experimental limits or determi-

nations of squark masses would benefit. We find resummation effects larger than previous estimates in the literature, since we normalize the Coulomb function at the scale  $M\beta$  to sum all NLL terms, and include the interference terms between soft gluon and Coulomb exchange, as well as squark-antisquark bound-state production in the total cross section. A more extensive phenomenological analysis of sparticle production covering all final states at the NNLL level is therefore of interest.

## Acknowledgements

We thank U. Langenfeld and S. Moch for providing interpolating functions of squark production cross sections for performing numerical checks, G. Watt for discussions on the MSTW PDFs, J.R. Andersen for computing advice, and S. Klein for helpful discussions. M.B. thanks the CERN theory group for its hospitality, while part of this work was done. The work of M.B. is supported in part by the DFG Sonderforschungsbereich/Transregio 9 ‘‘Computergestutzte Theoretische Teilchenphysik’’; the work of P.F. by the grant ‘‘Premio Morelli-Rotary 2009’’ of the Rotary Club Bergamo.

## A Relation of collinear matrix elements to PDFs

In this appendix we show that collinear matrix elements of the form  $\langle p|\phi_c(x)\phi_c(0)|p\rangle$  can be expressed in terms of the parton distribution functions (PDFs) and a polarization sum of the external wavefunctions, as stated in (2.52). We recall the operator definitions of the PDFs of quarks and gluons in full QCD [90]:

$$f_{q/N}(x_1, \mu) = \frac{1}{2\pi} \int dt e^{-ix_1 t \bar{n} \cdot P_1} \langle N | [\bar{\psi}(t\bar{n}) \frac{\vec{\eta}}{2} W_{\bar{n}}(t\bar{n}, 0) \psi(0) | N \rangle, \quad (\text{A.1})$$

$$f_{g/N}(x_1, \mu) = \frac{1}{2\pi x_1 (\bar{n} \cdot P_1)} \int dt e^{-ix_1 t \bar{n} \cdot P_1} \langle N | (\bar{n}_\mu F^{\mu\nu}(t\bar{n}) W_{\bar{n}}(\bar{n}t, 0) (\bar{n}^\rho F_{\nu\rho}(0)) | N \rangle, \quad (\text{A.2})$$

where  $\psi$  is the quark field in QCD,  $F_{\mu\nu}$  the full gluon field strength and an average over the physical polarization states is understood.  $W_{\bar{n}}(x_+, 0)$  denotes a Wilson line with the full gluon field  $\bar{n} \cdot A$  extending from 0 to  $x_+$ ,

$$W_{\bar{n}}(x_+, 0) = \text{P exp} \left[ ig_s \int_0^{x_+} dt \bar{n} \cdot A(\bar{n}t) \right]. \quad (\text{A.3})$$

The PDFs in SCET have been introduced in [62] and are collected in [91] in the SCET conventions used here. The purpose of the present discussion is to fix our conventions and identify all the numerical prefactors.

In order to relate the collinear matrix elements to the PDFs, we decompose the collinear and anticollinear matrix elements into a basis of spin structures  $\Gamma^i$ , so that (suppressing colour indices)

$$\langle p|\phi_{c;\beta}^\dagger \phi_{c;\alpha}|p\rangle = \sum_i \bar{\Gamma}_{\alpha\beta}^i \langle p|\phi_c^\dagger \Gamma^i \phi_c|p\rangle \quad (\text{A.4})$$

with  $\text{tr}[\bar{\Gamma}^i \Gamma^i] = 1$ . We now discuss the cases of quarks and gluons separately. For  $n$ -collinear quarks the fields are given by  $\phi_c = W_c^\dagger \xi_c$ . The identities  $\not{n} \xi_c = 0$  and  $(\not{n} \not{n} / 4) \xi_c = \xi_c$  satisfied by the collinear spinors imply [62] that the independent spin structures for the decomposition of a matrix element  $\langle p | \bar{\xi}_c \Gamma \xi_c | p \rangle$  can be taken as  $\Gamma^i \in \{\not{n}, \not{n} \gamma^5, \not{n} \gamma_\perp^\mu\}$ , up to normalization. Since we sum over the initial state parton spin, only the  $\not{n}$  term contributes. In colour space the product of  $\xi^\dagger$  and  $\xi$  decomposes into a singlet and an octet component but the sum over the initial state parton colours projects on the colour singlet. We therefore obtain for the collinear quark matrix element

$$\begin{aligned} & \langle p(P_1) | \phi_{c;k\beta}^{(0)\dagger}(z) \phi_{c;i\alpha}^{(0)}(0) | p(P_1) \rangle |_{\text{avg.}} \\ &= \frac{1}{2N_c} \delta_{ki} \left( \frac{\not{n}}{2} \gamma^0 \right)_{\alpha\beta} \langle p | [\bar{\xi}_c^{(0)} W_c^{(0)}](z) \frac{\not{n}}{2} [W_c^{(0)\dagger} \xi_c^{(0)}](0) | p \rangle |_{\text{avg.}} \\ &= N_{\alpha\beta}^q(P_1) \delta_{kj} \int_0^1 dx_1 e^{ix_1(z \cdot P_1)} f_{q/p}(x_1, \mu). \end{aligned} \quad (\text{A.5})$$

In the last step we have identified the quark PDF defined in terms of the SCET fields

$$f_{q/p}(x_1, \mu) = \frac{1}{2\pi} \int dt e^{-ix_1 t \bar{n} \cdot P_1} \langle p | [\bar{\xi}_c^{(0)} W_c^{(0)}](t \bar{n}) \frac{\not{n}}{2} [W_c^{(0)\dagger} \xi_c^{(0)}](0) | p \rangle |_{\text{avg.}}, \quad (\text{A.6})$$

which is consistent with the definition (2.52) in the main text, since for quarks the spin-dependent normalization factor, identified as a polarization sum of collinear quark spinors with momentum  $P_1^\mu = (\bar{n} \cdot P_1) / 2n^\mu$ ,

$$N_{\alpha\beta}^q(P_1) = \frac{\bar{n} \cdot P_1}{2N_c} \left( \frac{\not{n}}{2} \gamma^0 \right)_{\alpha\beta} = \frac{1}{2N_c} \sum_\lambda u_\alpha^\lambda(P_1) u_\beta^{\lambda*}(P_1), \quad (\text{A.7})$$

satisfies  $N^q(x_1 P_1) = x_1 N^q(P_1)$ . (The factor  $\gamma^0$  arises because of the definition of the conjugate quark and antiquark fields as discussed below (2.25).) Eq. (A.6) is of the same form as the PDF in full QCD (A.1) for external quark states, apart from the fact that the collinear quarks and Wilson lines appear instead of the full QCD fields. Since we are considering external massless on-shell partons with vanishing transverse momentum, the collinear region is the only one contributing to the PDFs. As the SCET Lagrangian for a single collinear direction is equivalent to full QCD [59], one can replace the collinear fields in (A.6) by the full QCD fields and identify the PDF with (A.1). For a matrix element with collinear antiquarks we obtain an analogous expression with the antiquark PDF

$$f_{\bar{q}/p}(x_1, \mu) = \frac{1}{2\pi} \int dt e^{-ix_1 t \bar{n} \cdot P_1} \langle p | \text{tr} \left\{ \frac{\not{n}}{2} [W_c^{(0)\dagger} \xi_c^{(0)}](t \bar{n}) [\bar{\xi}_c^{(0)} W_c^{(0)}](0) \right\} | p \rangle |_{\text{spin avg.}} \quad (\text{A.8})$$

and the normalization factor

$$N_{\alpha\beta}^{\bar{q}}(P_1) = \frac{\bar{n} \cdot P_1}{2N_c} \left( \gamma^0 \frac{\not{n}}{2} \right)_{\beta\alpha} = \frac{1}{2N_c} \sum_\lambda \bar{u}_\beta^{\lambda*}(P_1) \bar{u}_\alpha^\lambda(P_1). \quad (\text{A.9})$$

For the matrix element of  $n$ -collinear gluons, the only available transverse symmetric tensor is  $g_{\mu\nu}^\perp$  so that [62, 91]

$$\begin{aligned} \langle p | \mathcal{A}_{c;k\mu}^\perp(z_+) \mathcal{A}_{c;i\nu}^\perp(0) | p \rangle |_{\text{avg.}} &= \frac{1}{2(N_c^2 - 1)} g_{\mu\nu}^\perp \delta_{ki} \langle p | \mathcal{A}_{c;j}^{\perp\mu}(z_+) \mathcal{A}_{c;j\mu}^\perp(0) | p \rangle |_{\text{avg.}} \\ &= N_{\mu\nu}^g(P_1) \delta_{ki} \int_0^1 \frac{dx_1}{x_1} f_{g/p}(x_1, \mu) e^{ix_1(z \cdot P_1)} \end{aligned} \quad (\text{A.10})$$

with the gluon PDF in SCET

$$f_{g/p}(x_1, \mu) = -\frac{x_1(\bar{n} \cdot P_1)}{2\pi} \int dt e^{-ix_1 t \bar{n} \cdot P_1} \langle p | \mathcal{A}_c^{\perp\mu}(t\bar{n}) \mathcal{A}_{c,\mu}^\perp(0) | p \rangle |_{\text{avg.}}, \quad (\text{A.11})$$

which is consistent with the definition (2.52) in the main text. The normalization factor is

$$N_{\mu\nu}^g(P_1) = \frac{-g_{\mu\nu}^\perp}{2(N_c^2 - 1)} = \frac{1}{2(N_c^2 - 1)} \sum_\lambda \epsilon_\mu^\lambda(P_1) \epsilon_\nu^{\lambda*}(P_1). \quad (\text{A.12})$$

For the last identity we use the polarization sum of the gluon polarization vectors

$$\sum_\lambda \epsilon_\mu^\lambda(P_1) \epsilon_\nu^{\lambda*}(P_1) = -g_{\mu\nu} + \frac{q^\mu P_1^\nu + P_1^\mu q^\nu}{P_1 \cdot q} = -g_{\mu\nu} + \frac{q^\mu n^\nu + n^\mu q^\nu}{n \cdot q} \quad (\text{A.13})$$

and choose the arbitrary light-like vector  $q$  proportional to  $\bar{n}$ .

The equivalence of the SCET and QCD definitions of the gluon PDF is established most easily in light-cone gauge  $\bar{n} \cdot A = 0$ . In this gauge the SCET gluon operators (2.26) reduce to the collinear gluon fields:  $\mathcal{A}_c^\perp = A_c^\perp$ , while the QCD definition (A.2) becomes:

$$f_{g/p}(x_1, \mu) = -\frac{1}{2\pi x_1 (\bar{n} \cdot P_1)} \int dt e^{-ix_1 t \bar{n} \cdot P_1} \langle p | (\bar{n} \cdot \partial A^\nu(t\bar{n})) (\bar{n} \cdot \partial A_\nu(0)) | p \rangle |_{\text{avg.}}. \quad (\text{A.14})$$

Upon integration by parts and Fourier transformation one sees that this agrees with the SCET definition.

## B Coulomb potential for gluinos and squarks

Here we collect the coefficients  $D_{R_\alpha}$  of the Coulomb potential relevant for the production of coloured SUSY particles defined by the relation (3.20). This relation can be solved for arbitrary representations in terms of the quadratic Casimir operators of the representations of the two heavy particles and the final state system

$$D_{R_\alpha} = \frac{1}{2}(C_{R_\alpha} - C_R - C_{R'}), \quad (\text{B.1})$$

as can be deduced from the generator of the product representation  $\mathbf{T}^{(R \otimes R')} = \mathbf{T}^{(R)} \otimes \mathbf{1}^{(R')} + \mathbf{1}^{(R)} \otimes \mathbf{T}^{(R')}$  and by projecting the identity

$$\mathbf{T}^{(R)b} \otimes \mathbf{T}^{(R')b} = \frac{1}{2} \left[ \mathbf{T}^{(R \otimes R')b} \mathbf{T}^{(R \otimes R')b} - (C_R + C_{R'}) \mathbf{1}^{(R)} \otimes \mathbf{1}^{(R')} \right] \quad (\text{B.2})$$

on the irreducible representation. The explicit results for gluino pair production are long known [92] while all the remaining cases have recently been collected in [93]. We provide these results here for completeness. Note that our different sign convention implies that negative values of  $D_{R_\alpha}$  correspond to an attractive Coulomb force, positive values to a repulsive one.

*Squark-antisquark production.* The coefficients for squark-antisquark production have been quoted already in (3.23):

$$D_1 = -C_F = -\frac{N_C^2 - 1}{2N_C} = -\frac{4}{3}, \quad D_8 = \frac{C_A}{2} - C_F = \frac{1}{2N_C} = \frac{1}{6}. \quad (\text{B.3})$$

*Squark-squark production.* In squark-squark production  $qq \rightarrow \tilde{q}\tilde{q}$  the final state system is either in the  $\bar{3}$  or 6 representation and the coefficients of the Coulomb potential are

$$D_{\bar{3}} = -\frac{1}{2} \left( 1 + \frac{1}{N_C} \right) = -\frac{2}{3}, \quad D_6 = \frac{1}{2} \left( 1 - \frac{1}{N_C} \right) = \frac{1}{3}. \quad (\text{B.4})$$

*Gluino-squark production.* For gluino-squark production  $qg \rightarrow \tilde{q}\tilde{g}$  the final-state representations appear in the decomposition  $3 \otimes 8 = 3 + \bar{6} + 15$ . The coefficients read

$$D_3 = -\frac{N_c}{2} = -\frac{3}{2}, \quad D_{\bar{6}} = -\frac{1}{2}, \quad D_{15} = +\frac{1}{2}. \quad (\text{B.5})$$

*Gluino-pair production.* For gluino pair production the final state representations appear in the decomposition  $8 \otimes 8 = 1 \oplus 8_s \oplus 8_a \oplus 10 \oplus \bar{10} \oplus 27$  with the coefficients of the Coulomb potential:

$$D_1 = -3, \quad D_{8_s} = D_{8_a} = -\frac{3}{2}, \quad (\text{B.6})$$

$$D_{10} = 0, \quad D_{27} = 1. \quad (\text{B.7})$$

Note that only the singlet and octet states can be produced from a quark-antiquark initial state while all the states appear in gluon fusion.

## C Evolution functions

For convenience we quote here the explicit expressions of the resummation functions  $S$ ,  $a_i^V$  and  $a_\Gamma$  given in (3.42) up to NLL. The expressions for the corresponding functions for



the Drell-Yan process up to N<sup>3</sup>LL order have been given in [33]. Up to NLL the relevant expressions read

$$S(\mu_h, \mu_s) = \frac{\Gamma_{\text{cusp}}^{(0),r} + \Gamma_{\text{cusp}}^{(0),r'}}{8\beta_0^2} \left[ \frac{4\pi}{\alpha_s(\mu_h)} \left( 1 - \frac{\alpha_s(\mu_h)}{\alpha_s(\mu_s)} - \ln \frac{\alpha_s(\mu_s)}{\alpha_s(\mu_h)} \right) + \left( \frac{\Gamma_{\text{cusp}}^{(1),r} + \Gamma_{\text{cusp}}^{(1),r'}}{\Gamma_{\text{cusp}}^{(0),r} + \Gamma_{\text{cusp}}^{(0),r'}} - \frac{\beta_1}{\beta_0} \right) \left( 1 - \frac{\alpha_s(\mu_s)}{\alpha_s(\mu_h)} + \ln \frac{\alpha_s(\mu_s)}{\alpha_s(\mu_h)} \right) + \frac{\beta_1}{2\beta_0} \ln^2 \frac{\alpha_s(\mu_s)}{\alpha_s(\mu_h)} \right], \quad (\text{C.1})$$

$$a_\Gamma(\mu_h, \mu) = \frac{\Gamma_{\text{cusp}}^{(0),r} + \Gamma_{\text{cusp}}^{(0),r'}}{4\beta_0} \ln \frac{\alpha_s(\mu)}{\alpha_s(\mu_h)}, \quad (\text{C.2})$$

$$a_i^V(\mu_h, \mu) = \frac{\gamma_i^{(0),V}}{2\beta_0} \ln \frac{\alpha_s(\mu)}{\alpha_s(\mu_h)}. \quad (\text{C.3})$$

and an analogous expression for  $a^{\psi,r}$ . Here we have introduced the perturbative expansions of the beta function and the anomalous dimensions:

$$\beta(\alpha_s) = -2\alpha_s \sum_{n=0} \beta_n \left( \frac{\alpha_s}{4\pi} \right)^{n+1}, \quad (\text{C.4})$$

$$\gamma(\alpha_s) = \sum_{n=0} \gamma^{(n)} \left( \frac{\alpha_s}{4\pi} \right)^{n+1}, \quad (\text{C.5})$$

with

$$\beta_0 = \frac{11}{3}C_A - \frac{2}{3}n_f, \quad \beta_1 = \frac{34}{3}C_A^2 - \frac{10}{3}C_A n_f - 2C_F n_f. \quad (\text{C.6})$$

Explicit expressions for the anomalous dimensions required in the present work can be found, e.g. in [37].

## D Fixed-order expansions

The expression for the resummed cross section (3.48) can be expanded to a fixed order  $\alpha_s^n$  in the strong coupling, providing an approximation to the full  $\mathcal{O}(\alpha_s^n)$  QCD calculation. According to the counting (2.7), the expansion of the NLL resummed cross section to order  $\alpha_s$  compared to the leading order cross section is accurate up to terms of the order  $\alpha_s \times \beta^0$ . This approximation to the NLO cross section is obtained from (3.53) by expanding the evolution function  $U_i$  to  $\mathcal{O}(\alpha_s)$ , performing the convolution of the leading order Coulomb-Green function for arbitrary  $\eta$ , identifying  $\eta = 2a_\Gamma^{R\alpha}(\mu_s, \mu_f)$  and expanding up to  $\mathcal{O}(\alpha_s)$ . Inserting the explicit results for the one-loop cusp and soft anomalous dimensions, the result reads

$$f_{pp'(i)}^{\text{NLL}(1)} = -\frac{2\pi^2 D_{R\alpha}}{\beta} + (C_r + C_{r'}) \left[ 4 \left( \ln^2 \left( \frac{8E}{\mu_f} \right) - \ln^2 \left( \frac{8E}{\mu_s} \right) \right) + \ln^2 \left( \frac{4M^2}{\mu_h^2} \right) - \ln^2 \left( \frac{4M^2}{\mu_f^2} \right) \right] - 4(C_{R\alpha} + 4(C_r + C_{r'})) \ln \left( \frac{\mu_s}{\mu_f} \right)$$

$$+ 2(\gamma^{\phi,r(0)} + \gamma^{\phi,r'(0)} + 2C_{R_\alpha} - 2\beta_0) \ln\left(\frac{\mu_h}{\mu_f}\right) + \mathcal{O}(1). \quad (\text{D.1})$$

We have introduced the expansion of the cross section in the strong coupling

$$\hat{\sigma}_{pp'}^{(i)}(\beta, \mu_f) = \hat{\sigma}_{pp'}^{(0,i)} \left\{ 1 + \frac{\alpha_s(\mu_f)}{4\pi} f_{pp'}^{(1)} + \left(\frac{\alpha_s(\mu_f)}{4\pi}\right)^2 f_{pp'}^{(2)} + \mathcal{O}(\alpha_s^3) \right\}. \quad (\text{D.2})$$

The term involving  $2\beta_0$  in the last line of (D.1) appears, since we express  $\hat{\sigma}_{pp'}^{(0,i)} \propto \alpha_s^2$  in terms of the strong coupling at scale  $\mu_f$ , while in the factorization formula the hard function involves the scale  $\mu_h$ . The expansion (D.1) is used in (3.55) to match the NLL resummed prediction for squark-antisquark production to the fixed-order NLO calculation. At the order considered here, one can further approximate  $E = M\beta^2 + \mathcal{O}(\beta^4)$  to write the result in a more familiar form.

The NLL approximation to the NLO cross section (D.1) can be improved to include in addition all terms of order  $\alpha_s \times \beta^0$  by inserting the Laplace transform of the one-loop soft function (3.9) as well as the hard function in (3.48). Performing the derivatives with respect to  $\eta$  and expanding to  $\mathcal{O}(\alpha_s)$  afterwards we obtain for the NLO corrections to the cross section in the colour-channel  $i$  [45]:

$$\begin{aligned} f_{pp'}^{(1)} = & -\frac{2\pi^2 D_{R_\alpha}}{\beta} + 4(C_r + C_{r'}) \left[ \ln^2\left(\frac{8E}{\mu_f}\right) + 8 - \frac{11\pi^2}{24} \right] \\ & - 4(C_{R_\alpha} + 4(C_r + C_{r'})) \ln\left(\frac{8E}{\mu_f}\right) + 12C_{R_\alpha} + h_i^{(1)}(\mu_f) + \mathcal{O}(\beta). \end{aligned} \quad (\text{D.3})$$

We note that the dependence on the soft scale has canceled between the one-loop soft function and the expansion of the evolution function. Similarly the evolution equation (3.33) implies that the dependence on the hard scale cancels between  $h_i^{(1)}(\mu_h) \equiv H_i^{(1)}(\mu_h)/H_i^{(0)}$  and the evolution function. This can also be checked explicitly for the case of top-pair production where the one-loop hard functions can be obtained from [80]. In contrast, the NLL result (D.1) contains residual dependence on the soft and hard scale that is formally of higher order if the scales are chosen of the order  $\mu_s \sim E \sim M\beta^2$  and  $\mu_h \sim 2M$ . We observe that the  $\ln 8$  constant terms in the NLO result (D.3) can be reproduced exactly with  $\mu_s = 8E$ .

Expanding the NNLL resummed cross section in the same way results in an approximation to the NNLO cross sections  $f_{pp}^{(2)}$  that is accurate up to terms  $\alpha_s^2\beta^0$ . The results for the production of heavy particles of arbitrary spin and colour and the application to top-pair production have already been presented in [45] and will not be repeated here.

## References

- [1] G. Sterman, *Nucl. Phys.* **B281** (1987) 310.

- [2] S. Catani and L. Trentadue, *Nucl. Phys.* **B327** (1989) 323.
- [3] E. Laenen, J. Smith, and W. L. van Neerven, *Nucl. Phys.* **B369** (1992) 543–599.
- [4] E. L. Berger and H. Contopanagos, *Phys. Rev.* **D54** (1996) 3085–3113, [arXiv:hep-ph/9603326](#).
- [5] S. Catani, M. L. Mangano, P. Nason, and L. Trentadue, *Nucl. Phys.* **B478** (1996) 273–310, [arXiv:hep-ph/9604351](#).
- [6] N. Kidonakis and G. Sterman, *Phys. Lett.* **B387** (1996) 867–874.
- [7] N. Kidonakis and G. Sterman, *Nucl. Phys.* **B505** (1997) 321–348, [arXiv:hep-ph/9705234](#).
- [8] N. Kidonakis, G. Oderda, and G. Sterman, *Nucl. Phys.* **B531** (1998) 365–402, [arXiv:hep-ph/9803241](#).
- [9] R. Bonciani, S. Catani, M. L. Mangano, and P. Nason, *Phys. Lett.* **B575** (2003) 268–278, [arXiv:hep-ph/0307035](#).
- [10] S. Catani, M. L. Mangano, P. Nason, and L. Trentadue, *Phys. Lett.* **B378** (1996) 329–336, [arXiv:hep-ph/9602208](#).
- [11] R. Bonciani, S. Catani, M. L. Mangano, and P. Nason, *Nucl. Phys.* **B529** (1998) 424–450, [arXiv:hep-ph/9801375](#).
- [12] N. Kidonakis, E. Laenen, S. Moch, and R. Vogt, *Phys. Rev.* **D64** (2001) 114001, [arXiv:hep-ph/0105041](#).
- [13] M. Cacciari, S. Frixione, M. L. Mangano, P. Nason, and G. Ridolfi, *JHEP* **04** (2004) 068, [arXiv:hep-ph/0303085](#).
- [14] S. Moch and P. Uwer, *Phys. Rev.* **D78** (2008) 034003, [arXiv:0804.1476 \[hep-ph\]](#).
- [15] M. Cacciari, S. Frixione, M. L. Mangano, P. Nason, and G. Ridolfi, *JHEP* **09** (2008) 127, [arXiv:0804.2800 \[hep-ph\]](#).
- [16] N. Kidonakis and R. Vogt, *Phys. Rev.* **D78** (2008) 074005, [arXiv:0805.3844 \[hep-ph\]](#).
- [17] A. Kulesza and L. Motyka, *Phys. Rev. Lett.* **102** (2009) 111802, [arXiv:0807.2405 \[hep-ph\]](#).
- [18] A. Kulesza and L. Motyka, *Phys. Rev.* **D80** (2009) 095004, [arXiv:0905.4749 \[hep-ph\]](#).
- [19] U. Langenfeld and S.-O. Moch, *Phys. Lett.* **B675** (2009) 210–221, [arXiv:0901.0802 \[hep-ph\]](#).

- [20] W. Beenakker *et al.*, *JHEP* **12** (2009) 041, arXiv:0909.4418 [hep-ph].
- [21] A. Idilbi, C. Kim, and T. Mehen, *Phys. Rev.* **D79** (2009) 114016, arXiv:0903.3668 [hep-ph].
- [22] A. Idilbi, C. Kim, and T. Mehen, arXiv:1007.0865 [hep-ph].
- [23] V. S. Fadin, V. A. Khoze, and T. Sjostrand, *Z. Phys.* **C48** (1990) 613–622.
- [24] K. Hagiwara, Y. Sumino, and H. Yokoya, *Phys. Lett.* **B666** (2008) 71–76, arXiv:0804.1014 [hep-ph].
- [25] Y. Kiyo, J. H. Kühn, S. Moch, M. Steinhauser, and P. Uwer, *Eur. Phys. J.* **C60** (2009) 375–386, arXiv:0812.0919 [hep-ph].
- [26] K. Hagiwara and H. Yokoya, *JHEP* **10** (2009) 049, arXiv:0909.3204 [hep-ph].
- [27] H. Contopanagos, E. Laenen, and G. Sterman, *Nucl. Phys.* **B484** (1997) 303–330, arXiv:hep-ph/9604313.
- [28] G. P. Korchemsky and G. Marchesini, *Nucl. Phys.* **B406** (1993) 225–258, hep-ph/9210281.
- [29] G. P. Korchemsky and G. Marchesini, *Phys. Lett.* **B313** (1993) 433–440.
- [30] A. V. Manohar, *Phys. Rev.* **D68** (2003) 114019, hep-ph/0309176.
- [31] T. Becher and M. Neubert, *Phys. Rev. Lett.* **97** (2006) 082001, hep-ph/0605050.
- [32] T. Becher, M. Neubert, and B. D. Pecjak, *JHEP* **01** (2007) 076, hep-ph/0607228.
- [33] T. Becher, M. Neubert, and G. Xu, *JHEP* **07** (2008) 030, arXiv:0710.0680 [hep-ph].
- [34] V. Ahrens, T. Becher, M. Neubert, and L. L. Yang, *Phys. Rev.* **D79** (2009) 033013, arXiv:0808.3008 [hep-ph].
- [35] V. Ahrens, T. Becher, M. Neubert, and L. L. Yang, *Eur. Phys. J.* **C62** (2009) 333–353, arXiv:0809.4283 [hep-ph].
- [36] V. Ahrens, A. Ferroglia, M. Neubert, B. D. Pecjak, and L. L. Yang, arXiv:1003.5827 [hep-ph].
- [37] M. Beneke, P. Falgari, and C. Schwinn, *Nucl. Phys.* **B828** (2010) 69–101, arXiv:0907.1443 [hep-ph].
- [38] T. Becher and M. Neubert, *Phys. Rev.* **D79** (2009) 125004, arXiv:0904.1021 [hep-ph].

- [39] N. Kidonakis, *Phys. Rev. Lett.* **102** (2009) 232003, arXiv:0903.2561 [hep-ph].
- [40] G. P. Korchemsky and A. V. Radyushkin, *Phys. Lett.* **B279** (1992) 359–366, arXiv:hep-ph/9203222.
- [41] M. Czakon, A. Mitov, and G. Sterman, *Phys. Rev.* **D80** (2009) 074017, arXiv:0907.1790 [hep-ph].
- [42] A. Ferroglia, M. Neubert, B. D. Pecjak, and L. L. Yang, *Phys. Rev. Lett.* **103** (2009) 201601, arXiv:0907.4791 [hep-ph].
- [43] A. Ferroglia, M. Neubert, B. D. Pecjak, and L. L. Yang, *JHEP* **11** (2009) 062, arXiv:0908.3676 [hep-ph].
- [44] A. Mitov, G. Sterman, and I. Sung, arXiv:1005.4646 [hep-ph].
- [45] M. Beneke, M. Czakon, P. Falgari, A. Mitov, and C. Schwinn, *Phys. Lett.* **B690** (2010) 483–490, arXiv:0911.5166 [hep-ph].
- [46] M. Beneke, A. P. Chapovsky, A. Signer, and G. Zanderighi, *Phys. Rev. Lett.* **93** (2004) 011602, arXiv:hep-ph/0312331.
- [47] M. Beneke, A. P. Chapovsky, A. Signer, and G. Zanderighi, *Nucl. Phys.* **B686** (2004) 205–247, arXiv:hep-ph/0401002.
- [48] M. Beneke, N. Kauer, A. Signer, and G. Zanderighi, *Nucl. Phys. Proc. Suppl.* **152** (2006) 162–167, arXiv:hep-ph/0411008.
- [49] M. Beneke, P. Falgari, C. Schwinn, A. Signer, and G. Zanderighi, *Nucl. Phys.* **B792** (2008) 89–135, arXiv:0707.0773 [hep-ph].
- [50] M. Beneke, P. Falgari, and C. Schwinn, *PoS (EPS-HEP 2009)* (2009) 319, arXiv:0909.3488 [hep-ph].
- [51] M. Beneke, P. Falgari, and C. Schwinn, *PoS (RADCOR2009)* (2010) 012, arXiv:1001.4627 [hep-ph].
- [52] H. Baer, V. Barger, A. Lessa, and X. Tata, *JHEP* **09** (2009) 063, arXiv:0907.1922 [hep-ph].
- [53] H. Baer, V. Barger, A. Lessa, and X. Tata, *JHEP* **06** (2010) 102, arXiv:1004.3594 [hep-ph].
- [54] **D0 collaboration** Collaboration, V. M. Abazov *et al.*, *Phys. Lett.* **B660** (2008) 449–457, arXiv:0712.3805 [hep-ex].
- [55] **CDF collaboration** Collaboration, T. Aaltonen *et al.*, *Phys. Rev. Lett.* **102** (2009) 121801, arXiv:0811.2512 [hep-ex].

- [56] V. Ahrens, A. Ferroglia, M. Neubert, B. D. Pecjak, and L. L. Yang, *Phys. Lett.* **B687** (2010) 331–337, [arXiv:0912.3375 \[hep-ph\]](#).
- [57] C. W. Bauer, S. Fleming, D. Pirjol, and I. W. Stewart, *Phys. Rev.* **D63** (2001) 114020, [hep-ph/0011336](#).
- [58] C. W. Bauer, D. Pirjol, and I. W. Stewart, *Phys. Rev.* **D65** (2002) 054022, [hep-ph/0109045](#).
- [59] M. Beneke, A. P. Chapovsky, M. Diehl, and T. Feldmann, *Nucl. Phys.* **B643** (2002) 431–476, [hep-ph/0206152](#).
- [60] M. Beneke and T. Feldmann, *Phys. Lett.* **B553** (2003) 267–276, [arXiv:hep-ph/0211358](#).
- [61] S. Actis, M. Beneke, P. Falgari, and C. Schwinn, *Nucl. Phys.* **B807** (2009) 1–32, [arXiv:0807.0102 \[hep-ph\]](#).
- [62] C. W. Bauer, S. Fleming, D. Pirjol, I. Z. Rothstein, and I. W. Stewart, *Phys. Rev.* **D66** (2002) 014017, [hep-ph/0202088](#).
- [63] M. Beneke, P. Falgari, and C. Schwinn, *PoS (RADCOR2009)* (2010) 011, [arXiv:1001.4621 \[hep-ph\]](#).
- [64] P. Falgari, *W-pair production near threshold in unstable-particle effective theory*. PhD thesis, RWTH Aachen University, 2008.
- [65] T. Becher, R. J. Hill, B. O. Lange, and M. Neubert, *Phys. Rev.* **D69** (2004) 034013, [hep-ph/0309227](#).
- [66] M. Beneke and V. A. Smirnov, *Nucl. Phys.* **B522** (1998) 321–344, [arXiv:hep-ph/9711391](#).
- [67] A. Pineda and J. Soto, *Nucl. Phys. Proc. Suppl.* **64** (1998) 428–432, [arXiv:hep-ph/9707481](#).
- [68] M. Beneke, [arXiv:hep-ph/9806429](#).
- [69] N. Brambilla, A. Pineda, J. Soto, and A. Vairo, *Nucl. Phys.* **B566** (2000) 275, [arXiv:hep-ph/9907240](#).
- [70] M. Beneke, [arXiv:hep-ph/9911490](#). Proceedings of the 8th International Symposium on Heavy Flavor Physics (Heavy Flavours 8), Southampton, England, 25-29 Jul 1999.
- [71] P. Labelle, *Phys. Rev.* **D58** (1998) 093013, [arXiv:hep-ph/9608491](#).

- [72] B. Grinstein and I. Z. Rothstein, *Phys. Rev.* **D57** (1998) 78–82, [arXiv:hep-ph/9703298](#).
- [73] R. J. Hill and M. Neubert, *Nucl. Phys.* **B657** (2003) 229–256, [arXiv:hep-ph/0211018](#).
- [74] C. M. Arnesen, J. Kundu, and I. W. Stewart, *Phys. Rev.* **D72** (2005) 114002, [arXiv:hep-ph/0508214](#).
- [75] M. B. Voloshin, *Nucl. Phys.* **B154** (1979) 365.
- [76] M. Beneke, A. Signer, and V. A. Smirnov, *Phys. Lett.* **B454** (1999) 137–146, [arXiv:hep-ph/9903260](#).
- [77] V. S. Fadin and V. A. Khoze, *JETP Lett.* **46** (1987) 525–529.
- [78] A. H. Hoang *et al.*, *Eur. Phys. J. direct* **C2** (2000) 1, [arXiv:hep-ph/0001286](#).
- [79] P. Artoisenet, F. Maltoni, and T. Stelzer, *JHEP* **02** (2008) 102, [arXiv:0712.2770](#) [hep-ph].
- [80] M. Czakon and A. Mitov, *Phys. Lett.* **B680** (2009) 154–158, [arXiv:0812.0353](#) [hep-ph].
- [81] N. Brambilla, A. Pineda, J. Soto, and A. Vairo, *Rev. Mod. Phys.* **77** (2005) 1423, [arXiv:hep-ph/0410047](#).
- [82] E. H. Wichmann and C.-H. Woo, *Journal of Mathematical Physics* **2** (1961) no. 2, 178–180. <http://link.aip.org/link/?JMP/2/178/1>.
- [83] A. H. Hoang, A. V. Manohar, I. W. Stewart, and T. Teubner, *Phys. Rev.* **D65** (2002) 014014, [arXiv:hep-ph/0107144](#).
- [84] A. Pineda and A. Signer, *Nucl. Phys.* **B762** (2007) 67–94, [arXiv:hep-ph/0607239](#).
- [85] W. Beenakker, R. Höpker, M. Spira, and P. M. Zerwas, *Nucl. Phys.* **B492** (1997) 51–103, [arXiv:hep-ph/9610490](#).
- [86] I. I. Y. Bigi, V. S. Fadin, and V. A. Khoze, *Nucl. Phys.* **B377** (1992) 461–479.
- [87] W. Beenakker *et al.*, [arXiv:1006.4771](#) [hep-ph].
- [88] A. D. Martin, W. J. Stirling, R. S. Thorne, and G. Watt, *Eur. Phys. J.* **C63** (2009) 189–285, [arXiv:0901.0002](#) [hep-ph].
- [89] P. M. Nadolsky *et al.*, *Phys. Rev.* **D78** (2008) 013004, [arXiv:0802.0007](#) [hep-ph].
- [90] J. C. Collins and D. E. Soper, *Nucl. Phys.* **B194** (1982) 445.

- [91] T. Becher and M. D. Schwartz, *JHEP* **02** (2010) 040, [arXiv:0911.0681](#) [hep-ph].
- [92] J. T. Goldman and H. Haber, *Physica* **15D** (1985) 181–196.
- [93] Y. Kats and M. D. Schwartz, *JHEP* **04** (2010) 016, [arXiv:0912.0526](#) [hep-ph].